

Master Thesis

Inland water levels from Sentinel-6: How can SAR altimetry improve the height estimation of rivers and lakes?

Author:

Deepankar Kumar

MSc. Earth Oriented Space Science and Engineering (2019-2022)

Technical University of Munich

Supervisors:

Prof. Dr.-Ing. habil. Florian Seitz

Prof. Dr.-Ing. Denise Dettmering

Dipl.-Inf. (FH) Christian Schwatke

Erklärung der Urheberschaft

Ich, Deepankar Kumar (MTK 03723157), erkläre hiermit an Eides statt, dass ich die vorliegende Arbeit ohne Hilfe Dritter und ohne Benutzung anderer als der angegebenen Hilfsmittel angefertigt habe; die aus fremden Quellen direkt oder indirekt übernommenen Gedanken sind als solche kenntlich gemacht. Die Arbeit wurde bisher in gleicher oder ähnlicher Form in keiner anderen Prüfungsbehörde vorgelegt und auch noch nicht veröffentlicht.

Munich, 16/11/2022



Ort , Datum

Unterschrift

Acknowledgement

This master thesis project was a great learning experience for me. Working on the project helped me to get practical exposure to radar and SAR altimetry and its advantages in global water monitoring. Indeed, without the valuable help of my supervisors and colleagues, my understanding of the subject would have remained cursory. Having said, there is still and will remain a lot for me to learn in this research field.

Henceforth, I would like thank my supervisor, Christian Schwatke for guiding me throughout the methodology part and helping me through any problems faced and Dr. Denise Dettmering for support in making sure the whole process moves smoothly . I'd also like to thank Dr. Florian Seitz for proving me an opportunity to write my Master thesis at DGFI-TUM.

Lastly but not the least, I would like thank my family and parents who always remember me in their prayers and provided additional moral and emotional support during this process.

Abstract

The global monitoring of our lakes and rivers is important to maintain hydrological balance and sustain human life. Many altimetry missions have been launched till date most of them operating in the Classic Low Resolution Mode and some in SAR mode. One such mission have been Jason series of satellite which have provided global altimetry data in LRM over a decade. With the last satellite getting deactivated in March this year, the Copernicus Sentinel-6a MF mission was launched in November 2020 with an objective to continue the services provided by the Jason series of satellites. The new mission operates on an innovative interleaved mode allowing the processing of both SAR and LRM data acquisition in parallel.

Over the past two decades, satellite altimetry have shown its capability in regularly monitor and provide repeatable results of the global hydrological cycle of inland water bodies. Many researches have tried to assess the quality of results provided by SAR altimetry over these water bodies by employing various techniques. In this thesis, we try to evaluate the measurements provided by the newly launched Sentinel-6 satellite and validate its objective of the continuity of services for Jason-3 mission.

The water level time series for Sentinel-6HR, Sentinel-6LR and Jason-3 satellites are generated over many inland water bodies in the United States. Initially, we investigate the measurement principle, retracking algorithm, outlier rejection algorithms and areas to be investigated thoroughly and then using the Improved Threshold Retracker with the determined optimum threshold, we generate the water level time series for all those areas. Both Great Lakes and many smaller lakes in US are investigated in this study and the quality of data provided by both SAR and LRM is checked with respect to the in-situ data. Consequently, the performance is also compared mission wise by comparing the offsets in the height values.

Our investigation show that the Sentinel-6HR retracked data has provided very high quality results with RMSE lying in the range of 3cm to 10cm for both Great lakes and the smaller lakes. In smaller lakes, the LRM missions along with Sentinel-6HR unretacked mission provided an RMSE of 10 to 30 cm for smaller lakes. We also examined the optimum threshold value that must be used for the improved Threshold Retracker. Furthermore, we assessed the capability of Sentinel-6 MF mission in monitoring global oceans and large lakes along with smaller water bodies for a long time.

Contents

Acknowledgement	4
Abstract.....	5
List of Figures	9
List of Tables	12
1. Introduction	13
1.1. Motivation.....	13
1.2. Monitoring Hydrological cycle using satellite altimetry	15
1.3. Objectives.....	17
1.4. Outline of the thesis.....	18
2. Satellite altimetry measurement.....	19
2.1. Measurement principle.....	19
2.1.1. Water level Height	20
2.1.2. Corrections in range.....	21
2.2. Waveform Construction and Retracking.....	23
2.3. Challenges of Inland altimetry	25
2.3.1. Hooking effect.....	25
2.3.2. Insufficient Spatial and Temporal resolution.....	26
2.3.3. Monitoring over Sea Ice surfaces.....	26
2.4. Waveform Retracking	27
2.4.1. Improved Threshold Retracker	28
2.5. Delay-Doppler/SAR Altimetry vs Classic Low Resolution Mode Altimeter	29
3. Satellite altimetry missions.....	31
3.1. Jason-3	31
3.2. Sentinel-6a and its comparison with previous SAR missions.....	32
4. Areas of Study & methodologies	34
4.1. Areas of study and data acquisition.....	34
4.2. Methodology flow.....	44
4.2.1. Determination of the Optimum threshold.....	45
4.2.2. Water level generation	46
4.3. Outlier Rejection	47
4.4. Performance parameters.....	48
5. Experiments and Results.....	49
5.1. Lake Erie	49
5.2. Lake Michigan	53
5.3. Lake Ontario.....	56

5.4.	Lake Huron	60
5.5.	Lake Superior	63
5.6.	Lake of Woods.....	66
5.7.	Lake Winnebago.....	70
5.8.	Lake Richland Chambers	74
5.9.	Lake Toledo Bend.....	77
5.10.	Lake O.H. Ivie.....	80
5.11.	Lake Sam Rayburn.....	84
5.12.	Lake Sidney Lanier.....	87
5.13.	Lake Ray Roberts.....	90
5.14.	Lake Tawakoni.....	93
5.15.	Lake Champlain	96
5.16.	Optimum threshold distribution.....	99
5.17.	Offset validation.....	102
5.	Summary, Conclusion and future work	105
5.1.	Summary and Conclusion	105
5.2.	Future Work.....	107
	References	108

List of Figures

Figure 1.1 : Available stations (updated in March 2017) with discharge data according to the Global Runoff Data Centre (GRDC) database (http://www.bafg.de/GRDC) for different years from 1970–2013. [Tourian et al., 2017].....	14
Figure 1.2 : Periods of operation of satellite altimetry missions [Credits: DGFI-TUM Open Altimeter Database (OpenADB)]	15
Figure 2.1 : Schematic of the basic principle of Satellite altimetry [Credit: Aviso Altimetry].....	19
Figure 2.2: Schematic of the correction parameters for Satellite radar altimetry [Credits: altimetry.info]	21
Figure 2.3: The schematic of waveform construction [CNES].....	23
Figure 2.4: Schematic altimeter mean return waveform over ocean surface [Deng, 2003]	24
Figure 2.5: Schematic of the Hooking effect resulting in measurement of a slant height in along-track direction [Boergens et al., 2016]	25
Figure 2.6: Complex multi-peaked waveform derived from Sentinel-6HR mission over the Richland Chambers lake.....	27
Figure 2.7: Comparison between conventional radar altimeter (left) and Delay Doppler/SAR (right) altimetry [Credits: R.K. Raney, John Hopkins University Applied Physics Laboratory].....	30
Figure 2.8: Step by step process of formation of waveform in delay Doppler SAR altimetry [Credits: R.K. Raney, John Hopkins University Applied Physics Laboratory]	30
Figure 3.1: Jason-3 satellite and instruments on board [Credits: Aviso Altimetry]	31
Figure 3.2: The evolution of the satellite altimeter chronograms [Donlon et al., 2021].....	32
Figure 4.1: Map of Lake Erie along with Sentinel-6a pass over it [Credits: DGFI pass locator]	34
Figure 4.2: Map of Lake Michigan along with Sentinel-6a pass over it [Credits: DGFI pass locator] ...	35
Figure 4.3: Map of Lake Ontario along with Sentinel-6a pass over it [Credits: DGFI pass locator]	36
Figure 4.4: Map of Lake Huron along with Sentinel-6a pass over it [Credits: DGFI pass locator]	36
Figure 4.5: Map of Lake Superior along with Sentinel-6a pass over it [Credits: DGFI pass locator]	37
Figure 4.6: Map of Richland Chambers Reservoir along with Sentinel-6a pass over it [Credits: DGFI.38	
Figure 4.7: Map of Toledo Bend Reservoir along with Sentinel-6a pass over it [Credits: DGFI pass locator].....	38
Figure 4.8: Map of the Lake of Woods along with Jason-3 pass over it [Credits: DGFI pass locator] ..	39
Figure 4.9: Map of the Lake Winnebago along with Jason-3 pass over it [Credits: DGFI pass locator]40	
Figure 4.10: Map of the O.H. Ivie Lake along with Jason-3 pass over it [Credits: DGFI pass locator] ..	40
Figure 4.11: Map of the Sam Rayburn Reservoir along with Jason-3 pass over it [Credits: DGFI pass locator].....	41
Figure 4.12: Map of the Lake Sidney Lanier along with Sentinel-6a pass over it [Credits: DGFI pass locator].....	42
Figure 4.13: Map of Ray Roberts Lake along with Sentinel-6a pass over it [Credits: DGFI pass locator]	42
Figure 4.14: Map of Lake Champlain along with Jason-3 pass over it [Credits: DGFI pass locator]	43
Figure 4.15: Map of Lake Tawakoni along with Sentinel-6a pass over it [Credits: DGFI pass locator].44	
Figure 4.16: Flowchart explaining the methodology for determining the optimum threshold for the Retracker for each mission	45
Figure 4.17: Flowchart for generating water level time series for all mission	46
Figure 5.1: Plots for variation in RMSE, R2, offset and number of points for Lake Erie	49

Figure 5.2: Return waveforms for Lake Erie and the position of the retracking gate. (a) Jason-3 mission with threshold of 14%, (b) Sentinel-6aLR mission with threshold of 43%, (c) Sentinel-6aHR mission with threshold of 80%.....	50
Figure 5.3: Water level time series for Lake Erie in the overlapping period of operation	51
Figure 5.4: Plots for variation in RMSE, R2, offset and number of points for Lake Michigan	53
Figure 5.5: Return waveforms for Lake Michigan and the position of the retracking gate. (a) Jason-3 mission with threshold of 10%, (b) Sentinel-6aLR mission with threshold of 10%, (c) Sentinel-6aHR mission with threshold of 88%.....	54
Figure 5.6: Water level time series for Lake Michigan in the overlapping period of operation.....	55
Figure 5.7: Plots for variation in RMSE, R2, offset and number of points for Lake Ontario	56
Figure 5.8: Return waveforms for Lake Ontario and the position of the retracking gate. (a) Jason-3 mission with threshold of 10%, (b) Sentinel-6aLR mission with threshold of 45%, (c) Sentinel-6aHR mission with threshold of 79%.....	57
Figure 5.9: Water level time series for Lake Ontario in the overlapping period of operation	58
Figure 5.10: Plots for variation in RMSE, R2, offset and number of points for Lake Huron	60
Figure 5.11: Return waveforms for Lake Huron and the position of the retracking gate. (a) Jason-3 mission with threshold of 25%, (b) Sentinel-6aLR mission with threshold of 15%, (c) Sentinel-6aHR mission with threshold of 83%.....	61
Figure 5.12: Water level time series for Lake Huron in the overlapping period of operation	62
Figure 5.13: Plots for variation in RMSE, R2, offset and number of points for Lake Superior	63
Figure 5.14: Return waveforms for Lake Superior and the position of the retracking gate. (a) Jason-3 mission with threshold of 45%, (b) Sentinel-6aLR mission with threshold of 55%, (c) Sentinel-6aHR mission with threshold of 83%.....	64
Figure 5.15: Water level time series for Lake Superior in the overlapping period of operation.....	65
Figure 5.16: Plots for variation in RMSE, R2, offset and number of points for Lake Woods	66
Figure 5.17: Return waveforms for Lake of Woods and the position of the retracking gate. (a) Jason-3 mission with threshold of 8%, (b) Sentinel-6aLR mission with threshold of 12%, (c) Sentinel-6aHR mission with threshold of 50%.....	67
Figure 5.18: Water level time series for Lake Woods in the overlapping period of operation	68
Figure 5.19: Plots for variation in RMSE, R2, offset and number of points for Lake Winnebago.....	70
Figure 5.20: Return waveforms for Lake Winnebago and the position of the retracking gate. (a) Jason-3 mission with threshold of 15%, (b) Sentinel-6aLR mission with threshold of 10%, (c) Sentinel-6aHR mission with threshold of 40%	71
Figure 5.21: Water level time series for Lake Winnebago in the overlapping period of operation	72
Figure 5.22: Plots for variation in RMSE, R2, offset and number of points for Lake Richland Chambers	74
Figure 5.23: Return waveforms for Lake of Woods and the position of the retracking gate. (a) Jason-3 mission with threshold of 4%, (b) Sentinel-6aLR mission with threshold of 4%, (c) Sentinel-6aHR mission with threshold of 59%.....	75
Figure 5.24: Water level time series for Lake Richland Chambers in the overlapping period of operation.....	76
Figure 5.25: Plots for variation in RMSE, R2, offset and number of points for Toledo Bend Reservoir	77
Figure 5.26: Return waveforms for Lake Toledo Bend and the position of the retracking gate. (a) Jason-3 mission with threshold of 10%, (b) Sentinel-6aLR mission with threshold of 10%, (c) Sentinel-6aHR mission with threshold of 50%	78
Figure 5.27: Water level time series for Toledo Bend Reservoir in the overlapping period of operation	79
Figure 5.28: Plots for variation in RMSE, R2, offset and number of points for Lake O.H. Ivie.....	80

Figure 5.29: Return waveforms for Lake O.H. Ivie and the position of the retracking gate. (a) Jason-3 mission with threshold of 18%, (b) Sentinel-6aLR mission with threshold of 18%, (c) Sentinel-6aHR mission with threshold of 15%.....	81
Figure 5.30: Presence of small islands along the satellite track leading to errors in the range estimation	81
Figure 5.31: Water level time series for Lake O.H. Ivie in the overlapping period of operation.....	82
Figure 5.32: Plots for variation in RMSE, R2, offset and number of points for Sam Rayburn Reservoir	84
Figure 5.33: Return waveforms for Lake Sam Rayburn and the position of the retracking gate. (a) Jason-3 mission with threshold of 5%, (b) Sentinel-6aLR mission with threshold of 5%, (c) Sentinel-6aHR mission with threshold of 45%	85
Figure 5.34: Water level time series for Sam Rayburn Reservoir in the overlapping period of operation.....	86
Figure 5.35: Plots for variation in RMSE, R2, offset and number of points for Lake Sidney Lanier.....	87
Figure 5.36: Return waveforms for Lake Sidney Lanier and the position of the retracking gate. (a) Jason-3 mission with threshold of 5%, (b) Sentinel-6aLR mission with threshold of 5%, (c) Sentinel-6aHR mission with threshold of 45%	88
Figure 5.37: Water level time series for Lake Sidney Lanier in the overlapping period of operation ..	89
Figure 5.38: Plots for variation in RMSE, R2, offset and number of points for Lake Ray Roberts.....	90
Figure 5.39: Return waveforms for Lake Sidney Lanier and the position of the retracking gate. (a) Jason-3 mission with threshold of 10%, (b) Sentinel-6aLR mission with threshold of 5%, (c) Sentinel-6aHR mission with threshold of 40%	91
Figure 5.40: Water level time series for Lake Ray Roberts in the overlapping period of operation ...	92
Figure 5.41: Plots for variation in RMSE, R2, offset and number of points for Lake Tawakoni.....	93
Figure 5.42: Return waveforms for Lake Tawakoni and the position of the retracking gate. (a) Jason-3 mission with threshold of 20%, (b) Sentinel-6aLR mission with threshold of 5%, (c) Sentinel-6aHR mission with threshold of 45%.....	94
Figure 5.43: Water level time series for Lake Tawakoni in the overlapping period of operation	95
Figure 5.44: Plots for variation in RMSE, R2, offset and number of points for Lake Champlain	96
Figure 5.45: Return waveforms for Lake Champlain and the position of the retracking gate. (a) Jason-3 mission with threshold of 17%, (b) Sentinel-6aLR mission with threshold of 18%, (c) Sentinel-6aHR mission with threshold of 15%.....	97
Figure 5.46: Water level time series for Lake Champlain in the overlapping period of operation	98
Figure 5.47: Histogram to find the optimum threshold for retracking using the Jason-3 mission.....	99
Figure 5.48: Histogram to find the optimum threshold for retracking using the Sentinel-6aLR mission	100
Figure 5.49: Histogram to find the optimum threshold for retracking using the Sentinel-6aHR mission	100
Figure 5.50: Histogram to validate offset for Sentinel-6aHR retracked and Jason-3 retracked missions	102
Figure 5.51: Histogram to validate offset for Sentinel-6aLR retracked and Jason-3 retracked missions	103
Figure 5.52: Histogram to validate offset for Sentinel-6aHR retracked and Sentinel-6aLR retracked missions.....	104

List of Tables

Table 5.1: Optimum threshold values and number of points for Lake Erie.....	50
Table 5.2: Performance analysis of Lake Erie	52
Table 5.3: Optimum threshold values and number of points for Lake Michigan.....	54
Table 5.4: Performance analysis of Lake Michigan.....	55
Table 5.5: Optimum threshold values and number of points for Lake Ontario	57
Table 5.6: Performance analysis of Lake Ontario	59
Table 5.7: Optimum threshold values and number of points for Lake Huron.....	61
Table 5.8: Performance analysis of Lake Huron.....	62
Table 5.9: Optimum threshold values and number of points for Lake Superior.....	64
Table 5.10: Performance analysis of Lake Superior.....	65
Table 5.11: Optimum threshold values and number of points for Lake Woods	67
Table 5.12: Performance analysis of Lake Woods	69
Table 5.13: Optimum threshold values and number of points for Lake Winnebago	71
Table 5.14: Performance analysis of Lake Woods	73
Table 5.15: Optimum threshold values and number of points for Lake Richland Chambers.....	75
Table 5.16: Performance analysis of Lake Richland Chambers.....	76
Table 5.17: Optimum threshold values and number of points for Toledo Bend Reservoir.....	78
Table 5.18: Performance analysis of Toledo Bend Reservoir	79
Table 5.19: Optimum threshold values and number of points for Lake O.H. Ivie	82
Table 5.20: Performance analysis of Lake O.H. Ivie	83
Table 5.21: Optimum threshold values and number of points for Sam Rayburn Reservoir.....	85
Table 5.22: Performance analysis of Sam Rayburn Reservoir	86
Table 5.23: Optimum threshold values and number of points for Lake Sidney Lanier	88
Table 5.24: Performance analysis of Lake Sidney Lanier	89
Table 5.25: Optimum threshold values and number of points for Lake Ray Roberts	91
Table 5.26: Performance analysis of Lake Ray Roberts	92
Table 5.27: Optimum threshold values and number of points for Lake Tawakoni	94
Table 5.28: Performance analysis of Lake Tawakoni	95
Table 5.29: Optimum threshold values and number of points for Lake Champlain.....	97
Table 5.30: Performance analysis of Lake Champlain.....	98

1. Introduction

1.1. Motivation

Water is the most valuable natural resource available to sustain life on this planet. It is not just a primary need for living creatures but has a lot of industrial and economic applications. Out of approximately 1.4 billion cubic kilometers of water on this planet which covers almost 71% of the Earth's surface, only 2.5% is freshwater and 97.5% is salt water. In liquid form, only 0.3% of this fresh water is available to human beings on the earth's surface through lakes, rivers and reservoirs [Gleick 1993] [Eakins & Sharman 2010]. Due to increasing demand, this natural resource is facing the threat of non-renewability [Kim et al., 2008]. Therefore, measuring and understanding the quantity of surface water moving through landscapes is critical for water resources management, flood management, agriculture irrigation and aquatic ecological applications [Coe & Birkett, 2004].

Inland water bodies like lakes, rivers, reservoirs, creeks and streams are of vital importance to human beings. The freshwater obtained from inland water bodies have a multitude of uses and values like economic uses, recreational uses, aesthetic values, cultural values, educational uses, scientific values and ecological values, but all bodies are subjected to human impacts which have caused loss or degradation of these uses and values [Williams, 2002]. Floods and droughts are extreme hydrological natural disasters that reflect the probability of decades of outcomes of anthropogenic climate change [Cooley, 2006] [Peterson et al., 2008]. As a result, not just the human costs, these hydrological disasters harm wildlife by causing downing, disease proliferation and habitat destruction as well as cause sedimentation and erosion of the riverbanks. Thus, they impact the fertility of the soil, fresh water supply and transportation of goods. Therefore, continuous monitoring of these surface water bodies with precise measurements is of utmost necessity to avoid any possible hydrological disasters and management of water resources.

To maintain the global hydrological cycle as well as sustain human life, monitoring the amount and the availability of terrestrial water is necessary. Chander et al., 2014 identified three major problems due to which the measurement of the temporal variation of water levels in lakes, rivers and reservoirs becomes necessary. Those reasons are (a) Many developing countries have insufficient networks of hydrological gauging stations especially in the remote and high-flow locations (b) Hydrological models, which are widely used by water managers as a decision support tool for both real-time and long-term applications such as optimal management of reservoir releases, water allocation in drought conditions etc., face problem of initialization and calibration (c) flood forecasting systems are developed to predict flooding events based on the real-time observations of water levels. Since, flooding after rainstorms or typhoons can seriously damage property, routine monitoring of river surface changes is critical for disaster risk management as well as for hydrological and climatological research. Therefore, monitoring becomes important

To serve this purpose, a network of gauging stations has been installed around the world in the previous decades with the objective of continuously monitoring the surface bodies by measuring the discharge and the water levels of a stream. Traditionally, water volume has been quantified by measuring discharge at gauging stations by recording the elevation of water and converting water height to volume per unit time using a stage-discharge rating curve. River discharge is one of the most accurately measured components of the hydrological cycle, but access to the river discharge is typically limited [Hagemann & Dümenil, 1998] [Dingman, 2001] [Fekete & Vörösmarty, 2007]. This could be attributed due to many reasons. The monitoring network is sparse in large part of the globe and there is no mechanism in place to collect and distribute river discharge data globally on a real-time basis [Fekete & Vörösmarty, 2007]. Moreover, the implementation, availability and maintenance of the gauge network vary from region to region often depending on national policies. Especially, gauge stations are vulnerable during flood seasons and other extreme circumstances [Biancamaria et al., 2010]. Moreover, where and when in-situ gauge time series are accessible, they still suffer from the gaps in recording data, disunity in processing and quality regulation [Harvey and Grabs, 2003].

As a result, there has a widespread loss of hydrological monitoring networks been observed in the last 10-15 years in both developed and developing countries causing a great level of concern in the scientific community that seeks to manage water resources and detect the impact of global change on the hydrological cycle [Lanfear & Hirsch, 1999]. Statistically, the total area monitored decreased by 67% from 1986 through 1999 [Shiklomanov et al., 2011]. Figure 1.1 depicts the gauging stations spread spatially around the world and the decrease in the number through the years from 1970 to 2013.

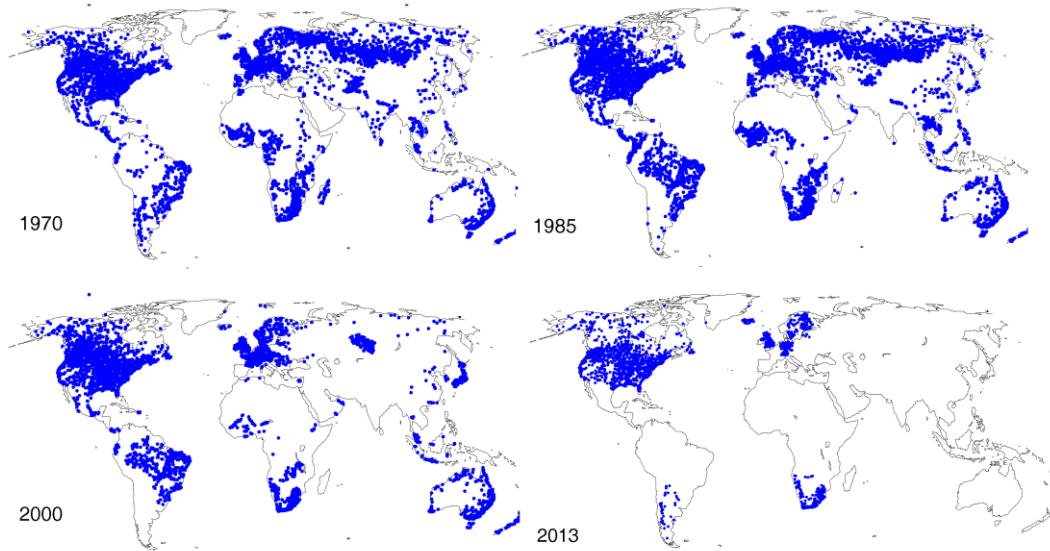


Figure 1.1 : Available stations (updated in March 2017) with discharge data according to the Global Runoff Data Centre (GRDC) database (<http://www.bafg.de/GRDC>) for different years from 1970–2013. [Tourian et al., 2017]

1.2. Monitoring Hydrological cycle using satellite altimetry

The continuous and widespread monitoring capabilities of various satellites launched till date has provided an excellent alternative to measure the water level height. Although, satellite altimeters were designed and optimized for operating over ocean initially [Berry et al. 2005], since decades of studies, altimetry missions also provide an opportunity to monitor inland hydrological cycles [Calmant & Seyler 2006]. Over the past two decades, major advancements in radar systems and data processing methodologies have been observed, leading to satellite altimetry being used as a tool for repeatable monitoring of the hydrological cycle and inland water bodies [Crétaux and Birkett, 2006]. As a result, an increase in the measurement accuracy of the radar techniques has provided an opportunity for the researchers to explore its potential for the inland water bodies as well.

The analysis and interpretation of satellite radar altimeter data obtained over inland water was pioneered using data from the SEASAT mission [Berry, 2006]. Although the mission life was short, it provided a valuable first look at echoes from inland water, with a precision that allowed meaningful measurements to be made over a small number of large lake targets, wet-lands and rivers [Rapley et al., 1987] [Berry, 2006]. The figure 1.2 below depicts the status of the missions launched till date. Currently, there are 8 active missions which continuously provide altimetry data with a repetition rate of 10 to 35 days.

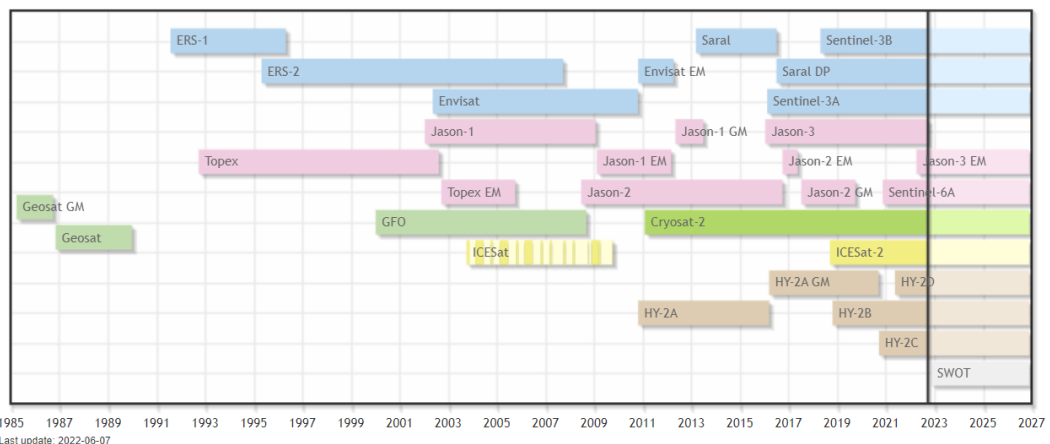


Figure 1.2 : Periods of operation of satellite altimetry missions [Credits: DGFI-TUM Open Altimeter Database (OpenADB)]

Numerous researchers and scientists have explored the potential of satellite altimetry, radar altimetry in particular over various continental water bodies and has proved its high effectiveness and better accuracies over these regions. With development in these missions, many studies have provided a comprehensive evaluation of the performance of the past and current radar altimetry missions according to their acquisition (Low Resolution Mode or Synthetic Aperture Radar), acquisition

CHAPTER 1: INTRODUCTION

frequencies (Ku, Ka, S, single, dual etc), use of retrackers (brown, OCOG, ICE-2, Threshold, Beta etc) and size of the target areas (oceans, lakes, rivers, reservoirs etc.).

Berry et al., 2005 explored the capabilities multiple missions over the Amazon River basin. They compared the measurements received from ERS-2, ENVISAT and TOPEX mission with datasets derived from the gauge networks and calculated the Pearson coefficient of the TOPEX, ERS-2 and Envisat satellites to be 0.91, 0.93 and 0.98 respectively. Chander el al., 2014 used the water level information derived from SARAL satellite over the Ukai Dam reservoir in India. They compared the measurements obtained using six different retrackers (OCOG, ICE-2, Brown, Threshold, Beta and a New Improved retracker) and compared the results with the in-situ tide-gauge dataset. The New Improved Retracker displayed best results with the RMSE value within the range of 8 cm. Schwatke et al., 2015 introduced a new approach to generate the water level time series for multiple altimetry missions. The new method is based on incorporating Kalman filter on the datasets and the use of an extended outlier rejection procedure. The results were accurate yielding RMS difference between 4 and 36 cm for lakes and 8 and 114 cm for rivers.

Since 1985, several radar altimetry missions have been launched like ERS-2, ENVISAT, Jason-1/2/3, SARAL operate on classic Low-Resolution Mode – LRM of acquisition whereas missions like Sentinel-3A and 3B, Cryosat-2 and recently launched Sentinel-6a MF operate in SAR mode (Sentinel-6a MF satellite operates in both LRM and SAR mode in parallel). When comparing the quality of results achieved from these classic LRM missions with high resolution SAR missions, Lan Vu et al., 2018 studied the measurements obtained by the LRM radar altimetry missions Jason-2 & Jason-3 and compared the results with measurements from Higher Resolution SAR altimeter from Sentinel-3A over the French Atlantic coast. Sentinel-3A exhibited better results with correlation coefficient of 98% and RMSE value of 0.15 m as compared to 95% and 0.30m values each for Jason-2 and Jason-3. Frappart et al., 2021 evaluated the quality of water level retrievals from high precision radar altimetry missions launched after 1995 like ERS-2, ENVISAT, Jason-1/2/3, SARAL (operating in LRM), SENTINEL-3A and 3-B (operating in SAR mode) over eight lakes in Switzerland. The study showed that with the SAR acquisition mode on SENTINEL-3A and -3B mission outperformed the classical LRM of other missions with RMSE generally lower than 7cm and correlation coefficient higher than 85% in most of the times when compared with in-situ gauge records. Nielsen et al., 2015 validated the high-resolution data in SAR acquisition mode acquired from the CryoSat-2 altimetry satellite with the LRM ENVISAT satellite and the in-situ gauge datasets available from 5 lakes (3 in Denmark, 1 in the USA and 1 in Sweden). They found an improved precision with CryoSAT-2 SAR altimetry with RMS values less than 8cm.

Although numerous studies have been conducted in comparing the accuracy of data acquired from the LRM and SAR altimetry missions, the research done on Sentinel-6a Michael Freilich mission is very limited. The newly launched satellite operates on an innovative interleaved mode which allows data processing in SAR and LRM parallelly. The satellite is the continuation to the decades of services provided by the Jason series of satellites in the areas of topological analysis of our oceans and currently flies in tandem with Jason-3 satellite. This leads to a plethora of potential areas of studies that could be conducted in understanding the performance and the potential of the mission in providing high quality data over various target regions specifically inland water bodies.

1.3. Objectives

The aim of this thesis is to explore the potential of the Sentinel-6a MF satellite in providing water level time series for inland water bodies as a continuation of the Jason-3 satellite. The Sentinel-6a satellite was launched in November 2020 and flies in tandem with Jason-3 satellite, thus following the same path and period of revisit. Since the Sentinel-6a MF satellite uses an innovative interleaved mode (LRM and SAR data processing in parallel), the intention of the study will be to compare the water level time series generated since its launch with the time series generated by Jason-3 mission (operating in LRM) since 2016 and validate its objective of continuation of services of Jason series of satellites. The results would then be compared with the measurements from the in-situ network of gauging stations datasets available for various continental water bodies in the United States. The following points summarise the tasks for the thesis:

- Select the satellite radar altimetry mission path and data available for the area of interest and generate an initial water level time series.
- Apply various corrections and the Improved Threshold Retracking algorithm.
- Remove the outliers using an outlier rejection algorithm.
- Generate water-levels for all thresholds of the retrackers to determine the best threshold based on certain performance parameters.
- Generate water level time series for all targets based on the optimum threshold values for each mission in the overlapping period of operations to visualise the quality.
- Compare the quality of the results with in situ datasets as well as to each satellite using certain metrics.

The above tasks will help to answer the following questions for this thesis:

- What is the measuring principle of the Sentinel-6 MF mission and how does it differ from the classic Low Resolution Mode altimetry missions?
- What is the best threshold to use during the retracking process to obtain results with high quality for different target areas and different missions and modes of acquisition?
- What is the quality of measurements from the Jason-3 and Sentinel-6a missions on inland water bodies when compared to the in-situ data from the gauging stations?
- Since, Sentinel-6a and Jason-3 missions fly in tandem, how does the Sentinel-6a mission perform with respect to Jason-3 mission when investigating the inland water bodies like rivers and lakes which are of much smaller size?
- Assessment of the validity of the objective of the Sentinel-6a mission as the continuity of services provided by the Jason series of satellite.

1.4. Outline of the thesis

The structure of the thesis will be aligned with achieving the objectives and carrying out the tasks outlined above. Chapter 2 will give a detailed explanation of the principles and processes in Satellite radar altimetry. The concept and difference in LRM and SAR mode is also explained. Chapter 3 will give a brief idea about the Satellite missions and their characteristics. The difference in the measurement technique of open and closed burst mode of SAR altimetry will also be discussed. The areas of interest as well as overall description of the methodology will be discussed in Chapter 4. In Chapter 5, we will discuss results obtained while carrying out the above mentioned tasks of thesis. These results would include the variation and determination of quality in time series with changing thresholds along with validating the consistency of the intermission offsets. And based on the best threshold, the generated water level time series will be shown for each target area and the quality will be analysed based on certain performance parameters. The intermission offset as well as the trend s of thresholds would be checked too. The final chapter will include conclusion along with the recommendations and directions for the future work.

2. Satellite altimetry measurement

Satellite altimeters are nadir pointing active microwave instruments, whose principal aim is to calculate as accurately as possible the two-way travel time of short pulses reflected from the Earth's surface. The reflected signal forms a waveform which represents the time evolution of the reflected power as the radar pulse hits the surface. In addition to measuring the range, this waveform provides information on the nature and properties of the reflecting surface [Vignudelli et al., 2011]. The following section describes in detail the measurement principle, waveform construction and characteristics, how the range is calculated, and various techniques and challenges faced when targeting the continental water bodies.

2.1. Measurement principle

The altimeter instrument which is an isotropic antenna transmits a short pulse of microwave radiation with known power towards the sea surface. The part of the signal is returned to the altimeter where the travel time is measured accurately. The precise measurement of the travel time helps in determining a one-way range R which is described in Figure 2.1 below.

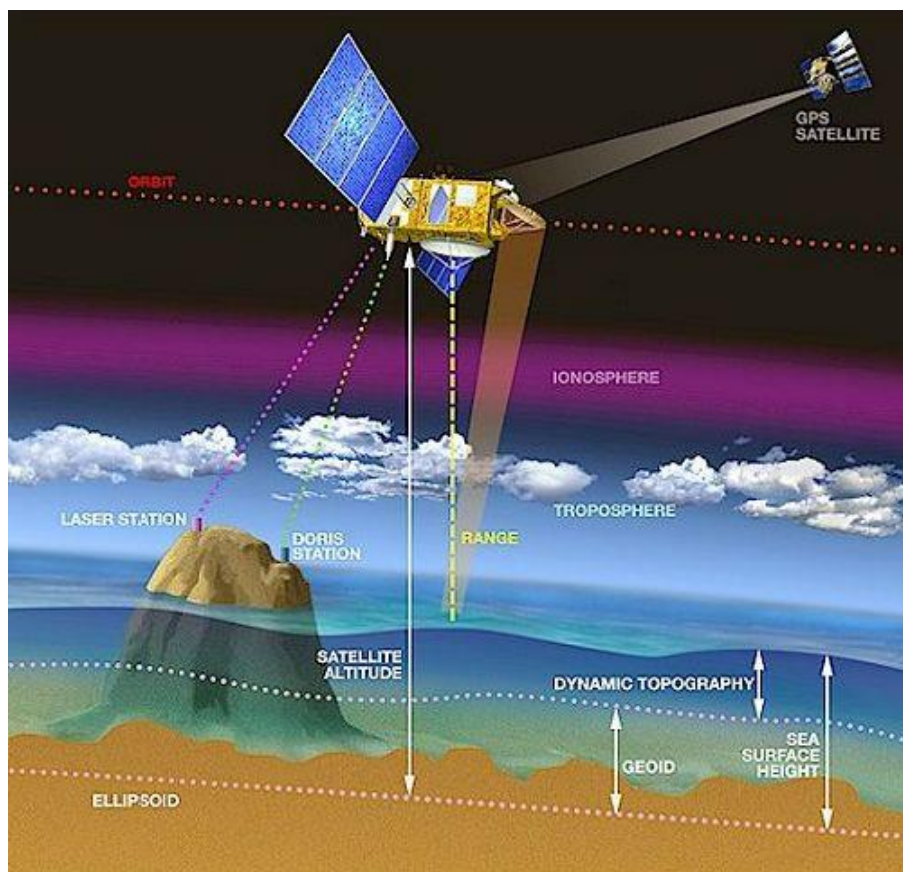


Figure 2.1 : Schematic of the basic principle of Satellite altimetry [Credit: Aviso Altimetry]

Although the range is corrupted by external influences, the ideal range R_{ideal} is calculated using the following Equation 2.1:

$$R_{ideal} = \frac{1}{2}ct$$

.... (Equation 2.1)

The observed range is computed by measuring the travel time t of the signal which is calculated by the on-board ultra-stable oscillator (USO) [Vignudelli et al., 2011]. However, there are a certain number of deviations in the measured value of the range which is expressed by the behaviour of the radar pulse through the atmosphere, corrections from the sea state and geophysical signals. As a result, these corrections ΔR must be added to the observed range to get a more accurate or corrected value $R_{corrected}$.

$$R_{corrected} = R_{obs} + \sum_i \Delta R_i$$

.. (Equation 2.2)

2.1.1. Water level Height

Global description of sea level and its variation with time to high accuracy is the ultimate derivative from a satellite altimeter's range measurement [Vignudelli et al., 2011]. As described in Figure 2.1, the Sea Surface Height (SSH) or the water level height (in case of inland altimetry) at a given instant is the distance calculated from water surface to the reference ellipsoid and is calculated using the following Equation 2.3:

$$h = H_{sat} - R_{corrected}$$

.... (Equation 2.3)

$$h = H_{sat} - \left(R_{obs} + \sum_i \Delta R_i \right)$$

.... (Equation 2.4)

H_{sat} is the height of the satellite measured from the reference ellipsoid. This is determined through Precise Orbit Determination (POD). POD helps in determining orbital parameters with high accuracy through observations received from on-board sensors and receivers such as Satellite Laser Ranging (SLR), Doppler Orbitography and Radiopositioning Integrated by Satellite (DORIS) and Global Positioning System (GPS). As it can be observed, the water level height accuracy is directly related to the accuracy of orbit determination. Fortunately, the radial orbit accuracy has improved from tens of meters on the first altimeters to about 1 cm on the most recent satellites [Bertiger et al. 2008].

The accuracy of the water level height is also directly linked with the accuracy of the corrections applied to the range calculations. During the propagation in vacuum, the radar pulse travels at the speed of light which remains unaffected during that part of the propagation. However, the presence of dry gases, water vapour and free electrons in the atmosphere reduces the speed of the radar pulse causing the observed range to become longer and the water level height to be too low as compared to the ideal condition [Vignudelli et al., 2011]. Further corrections are regarding instrumental errors

as well as the external geophysical adjustments. The following Figure 2.2 gives a brief overview of these corrections:

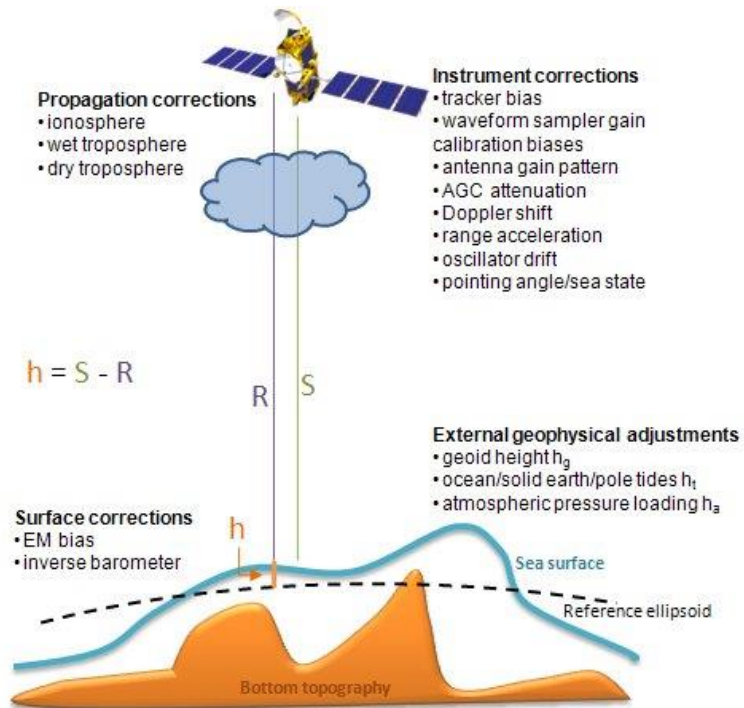


Figure 2.2: Schematic of the correction parameters for Satellite radar altimetry [Credits: altimetry.info]

2.1.2. Corrections in range

For inland water body applications, the following corrections in the observed range are required:

- Wet Troposphere ($h_{w trop}$)

Wet Troposphere Correction (WTC) is the correction in the path delay caused by the water vapour in the atmosphere. It is one of the major sources of error (10-20cm) in the calculation of the range and is difficult to model due to uncertainties caused in the model due to the high spatial and temporal variability of water vapour. The most used method for measuring this effect is the Microwave Radiometers (MWR) which calculates the radiation temperature to empirically determine the water vapour percentage in nadir direction. Since, any bias in the wet tropospheric correction directly impacts the sea level determination, therefore, MWR method provides the path delay with an accuracy of 1cm or better and is found in the recent altimetry missions [Eymard & Obligis, 2006]. When it comes to inland altimetry, this technique faces the problem of footprint size as radiometer footprint (approx. 50km) overlaps with land surfaces thus causing disturbances.

- Dry Troposphere ($h_{d trop}$)

Among all the corrections in the range, Dry Tropospheric Correction (DTC) formed due to refractions from dry atmospheric gases is by far the largest adjustment that must be applied to the range with the magnitude lying in the range 200-300 cm. In the units of cm, the DTC in the range can be computed using the Saastamoinen formula:

$$h_{dtrop} = -0.02277P_o(1 + 0.0026\cos 2\varphi)$$

.... (Equation 2.5)

Where, P_o is the Sea Level Pressure (SLP) and φ is the latitude. Since direction observations of SLP are infrequent and sparsely distributed, data from operational weather models lie European Centre for Medium-Range Weather Forecasts (ECMWF) and the U.S. National Centres for Environmental Predictions (NCEP). Therefore, the estimation of the DTC largely depends on the atmospheric pressure which is correlated to the station height.

- Ionosphere (h_{ionos})

Ionospheric corrections are another atmospheric-based delays caused in signal propagation which happen due to the presence of free electrons and ions in the atmosphere. The interaction caused between these charged particles and electromagnetic waves causes the waves to slow down by an amount proportional to the electron density in the ionosphere. In addition to depending on the electron density, the path delay also varies inversely with the frequency of the radar signal. Ionospheric corrections are not a major problem in higher frequency missions like SARAL AltiKa (which operates on single frequency Ka-band: 35.75 GHz altimetry) as compared to missions operating on lower frequencies like ENVISAT, TOPEX etc. Because of this, to accurately measure the delay caused by the Ionosphere in low frequency missions, dual frequency altimeters are used as they allow to measure the Total Electron Content (TEC) which directly impacts the path delay in the signal.

- Solid Earth and Pole Tides (h_{etide} and h_{ptide})

Tidal corrections are the measurements done to counter the effect of tidal forces occurring due to either gravitational forces of Sun and Moon or due to changes in the centrifugal forces in the Solid Earth on the altimetry measurements. Prominently, corrections due to ocean tides are the most significant corrections in measuring temporal sea surface height. This is followed by some smaller tides signals like Solid Earth and Polar tides.

Solid Earth tides occur due to the Earth's elastic response to the gravitational forces of Sun and Moon. The response is fast enough to be in equilibrium with the forces which results in the surface being parallel to the equipotential surface. The derived tidal elevation then becomes proportional to the tidal potential. The proportionality is determined using Love numbers and the corrections ranges up to $\pm 30\text{cm}$.

Polar tides are tide-like variations caused in water bodies due to the centrifugal forces occurring because of the variation of Earth's axis of rotation with respect to its geographical mean. The centrifugal potential periodically varies every 12 to 14 months causing temporal variations in the elevation of the ocean surface. The magnitude of the pole tide correction is approximately 2.5cm can be computed using Love numbers which is described in detail in Wahr (1985).

For the inland water altimetry applications, the water bodies are not affected by the ocean tides. As a result, they do not produce any errors when measuring the water surface elevation.

- Geoid height (h_{geoid})

When it comes to geophysical corrections, the corrections due to the height of the geoid are the most dominant for the determination of sea surface height. Spatially, the height varies in the range of -105m in the south of India to +85m northeast of New Guinea depending on the inhomogeneities in the density of Earth's interior and crust. For ocean applications, the sea

surface mimics the geoid so the discrepancies in the measured height can be ignored. But for the inland applications, the correction must be considered and can be determined using models like DNSC08MSS, EGM2008 etc.

As a result, the sea surface height is determined using the equation 2.6:

$$h = H_{sat} - R_{obs} - h_{geoid} - h_{wtrop} - h_{dtrop} - h_{ionos} - h_{etide} - h_{ptide}$$

... (Equation 2.6)

2.2. Waveform Construction and Retracking

A conventional radar altimeter emits a microwave spherical pulse towards the earth's surface in the nadir direction and measures the reflected echoes. The shape of the reflected signals which is known as the waveform represents the time evolution of the reflected power as the radar pulse hits the surface. Looking at Figure 2.3 below, as the wavefront reaches the water surface, it illuminates an area of the nearest water surface based on the antenna pattern. As it encounters the target area, a backscatter is received which essentially opens the receiving window of the waveform and the power will increase. The reflected signal intensity grows in a disc shape (also called the pulse limited circle or footprint) as the area of interaction between the pulse and surface increases till it reaches the point of maximum extension. Thereafter, a decay in the backscatter energy is observed and the shape of the interaction surface changes to an annulus with increasing diameter and constant area till the antenna pattern decays and mispoints. The diameter of the pulse-limited footprint lies in the range of 2 to 11 km depending on the significant wave height [Vignudelli et al., 2011]..

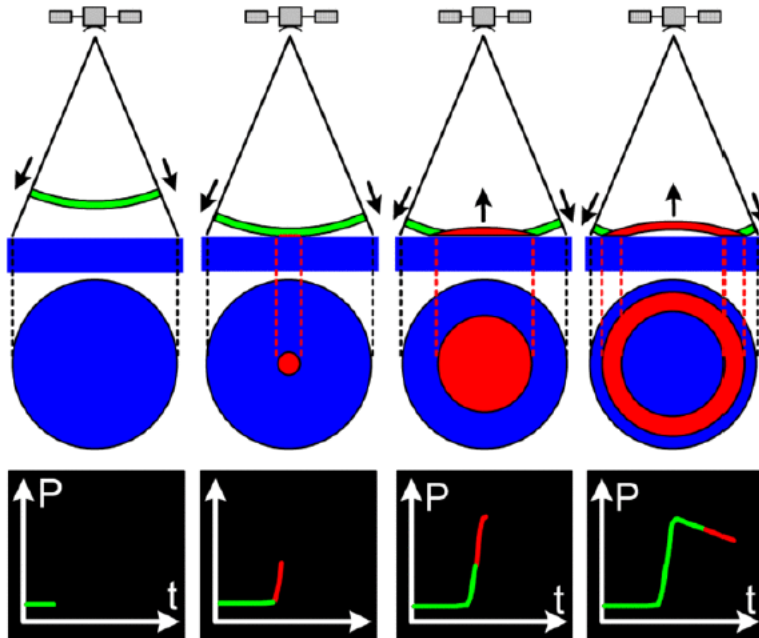


Figure 2.3: The schematic of waveform construction [CNES]

In the above figure, the waveform constructed using the received power is contaminated by noise from many sources. To mitigate the level of noise, the power from the waveforms is averaged and a

time series of mean waveform is constructed which broadly consists of three components: the thermal noise, the leading edge and the trailing edge as described in Figure 2.4 [Brown 1997] [Quarly et al., 2001] [Chelton et al., 2001] [Tourian 2012].

- The thermal noise:

This is a low-power bias (P_0) created in the received power before the first return of the signal due to internal noise in the altimetry instrument. This noise signal is received corresponding to the parasite reflection of the pulse in the ionosphere and atmosphere, in addition to the instrument electronic noise [Rsmorduc et al., 2018].

- The leading edge:

The leading edge is the main part of the waveform as it records the power of the return waveform from the scattering surface. The leading edge essentially provides the information on the range between the satellite and mean sea surface in the nadir direction as well as the sea wave height.

- The trailing edge:

The trailing edge reflects the return power from the scattering surface acquired from a decaying antenna pattern. It can be approximated by a straight line whose slope depends on the altimeter antenna pattern and the off-nadir angle [Chelton et al., 2001].

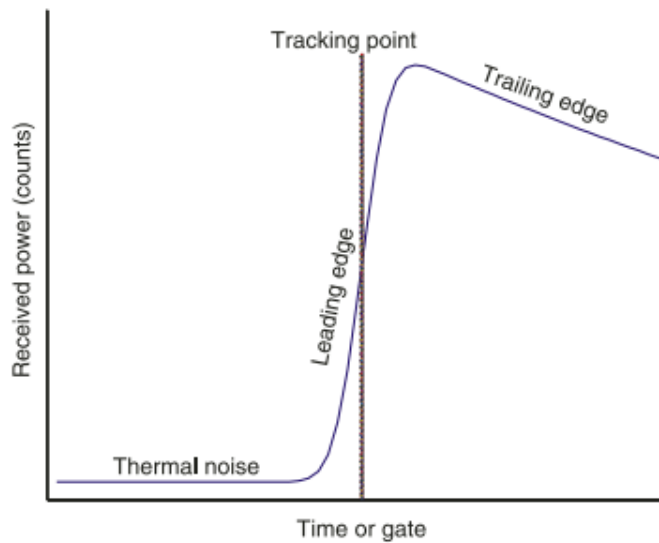


Figure 2.4: Schematic altimeter mean return waveform over ocean surface [Deng, 2003]

Over the ocean surface, the characteristic shape of the waveform can be described analytically using the Brown model [Brown, 1977]. The epoch at the mid height gives the time delay of the expected return of the radar pulse (estimated by the on-board tracking algorithm) and thus the time the radar pulse took to travel the satellite-surface distance (or ‘range’) and back again in the nadir direction [Rsmorduc et al., 2018]. The on-board Retracker continuously adjusts the tracking point so that the leading edge of the waveform remains stable at the fixed center of the range window [Deng, 2003]. The tracking gate is a pre-designed bin index of a waveform, which defines the initial range between the satellite and the surface at nadir [Wang, 2019].

2.3. Challenges of Inland altimetry

Over the inland water bodies, the magnitude and shape of the echoes (or waveforms) also contain information about the characteristics of the surface which caused the reflection. This results in a noisier and broader waveform which makes measuring the range much more difficult. The best results are obtained over the oceans, which are spatially homogeneous bodies, and have a surface which conforms to known statistics. Surfaces which are not homogeneous, which contain discontinuities or significant slopes, such as some land surfaces, make accurate interpretation more difficult.

Additionally, the challenges on the availability of satellite pass over the water body, frequency of instrument effecting the footprints. In case of lakes bordering Canada, in winters the lake freezes which results in noisy waveform and altimetry values.

2.3.1. Hooking effect

A satellite altimeter measures range in the nadir direction and consequently the target surface or the footprint location should be directly under the instrument. However, for the water bodies surrounded by a land surface, the altimetry pulses might illuminate the land area too which might contain a rough terrain or a vegetation cover. In that case, the water surface, which gives a stronger reflection, might result in an altimetry measurement in a slant direction even though the instrument is not nadir positioned over the water surface. This distortion in altimetry data in an off-nadir direction results in a parabolic shape (as described in the Figure 2.5) of the track-height profile which is called as the Hooking effect [Boergens et al., 2016].

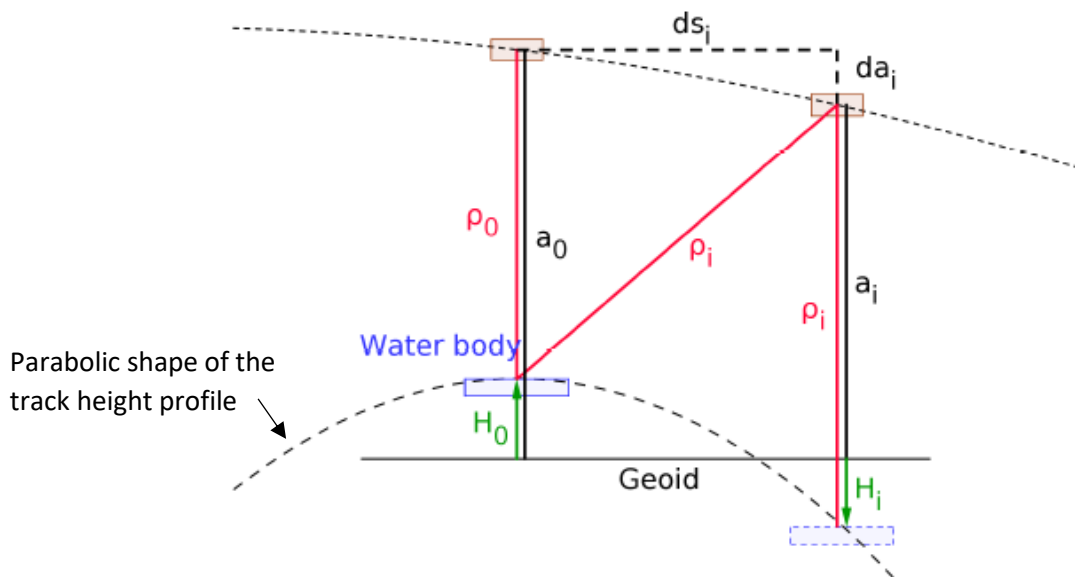


Figure 2.5: Schematic of the Hooking effect resulting in measurement of a slant height in along-track direction [Boergens et al., 2016]

In Figure 2.5, the satellite moves along the orbit calculating the slant range to the water body ρ_i and altitude a_i from the reference geoid. This results in a measurement of the range in nadir direction equivalent to the calculated slant range giving the water level height as $H_i = a_i - \rho_i$. However, the

actual range from the satellite is ρ_o and the altitude at the zenith of the water body is a_o . This should give the true height as $H_o = a_o - \rho_o$.

The hooking effect is generally observed in most land-water transition, but for larger lakes, this effect can be ignored as we have enough nadir measurements to retrieve a reliable water level height. But for smaller lakes (< 1km size), the altimeter can lose lock due to rapidly changing topography [Boergens et al., 2016]. In these cases, the hooking parabola must be analysed to obtain reliable water levels. Many methods have been used in the past for the analysis and mitigation of the error caused due to the parabola. Maillard et al., 2015 developed a new method by comparing the theoretical shape of the hooking parabola with the derived data profiles. Boergens et al., 2016 used the RANdom SAmples Consensus (RANSAC) algorithm along with the Mutli-Subwaveform Retracker (MSR) to detect useful measurements that are effected by the hooking effect. These studies were carried out using the classic LRM data, but for many modern missions like Cryosat-2, Sentinel-3 and Sentinel-6 which use the SAR altimetry data for measuring water level, the hooking effect doesn't pose much error and therefore does not require correction [Boergens et al., 2016].

2.3.2. Insufficient Spatial and Temporal resolution

Satellite altimetry missions are normally designed with a purpose of monitoring global oceanographic variations and can provide the coverage for 90% of the world's oceans within a few days cycle [Zhao 2018]. For inland water bodies, the coverage is very limited due to less spatial and temporal resolution. Missions like Jason series, Sentinel-6 , TOPEX have a 10 day repeat orbit but the consecutive ground tracks are 315 km apart leaving many target areas away from its footprint. On the other hand, Cryosat-2 ground track is 8km apart and has a more dense ground track but the 365 day repeat orbit limits the monitoring of daily and monthly variation leaving data gaps. Therefore, the constraints in spatial and temporal resolution of the mission results in the limitations in water level monitoring.

2.3.3. Monitoring over Sea Ice surfaces

Although, the target areas for this thesis are the lakes and reservoirs in the United States, many lakes specifically along the US-Canada border freeze during winters resulting into a layer of ice over it during that period. The presence of ice and mix of water and ice modifies the amplitude and the shape of the radar echo (waveform) acquired by the altimetry satellite affecting the height retrieval [Tseng et al., 2012]. Reflections from multiple surfaces results in multiple peaks in the waveform which results in misinterpretation of extracted water level height to be lesser than the gauge data.

2.4. Waveform Retracking

Apart from the discrepancies in the accuracy of estimation of the travel time, orbit positions and range corrections, the quality of the water height obtained from lakes and rivers is affected by a few more factors. Smith 1997 stated that the major difficulty in retrieving ranges over continental bodies results from variability in the shape of the returned waveform. Normally, the on-board retrackers are designed for a typical “ocean-type” waveforms which have long tail shape of the returned power. However, over the lakes and river bodies, the waveforms are more multi-peaked which result in an erroneous range estimation.

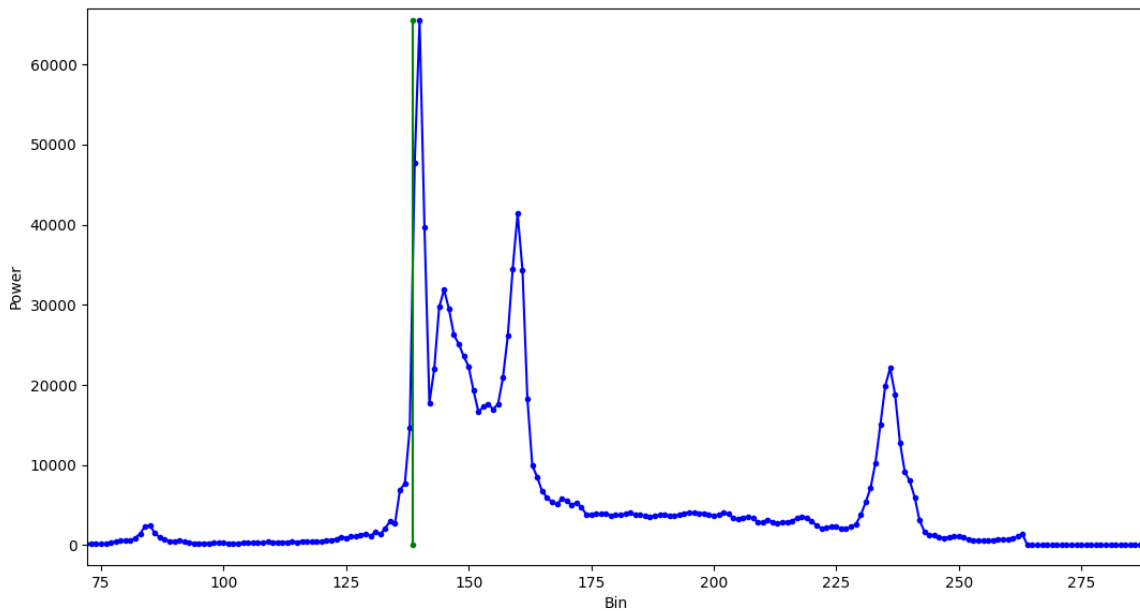


Figure 2.6: Complex multi-peaked waveform derived from Sentinel-6HR mission over the Richland Chambers lake

To rectify these errors over continental bodies, a post-processing procedure called retracking is applied over the standard altimetry data processing. This is done by estimating the offset of the actual tracking gate which is related to the mid-point on the leading edge from the designed tracking gate used by default on-board for satellite processing. This correction is then applied on the range calculated by the on-board retracking algorithm [Deng & Featherstone 2006]. The Improved threshold Retracker developed by Hwang et al., 2006 has been used in this study to retrieve water level height with great quality as it works very effectively in determining the center of the leading edge in complex waveforms.

2.4.1. Improved Threshold Retracker

The Retracker constructs sub-waveforms based on the detection of leading edge and determines the retracking gates of these waveforms. Then the best retracking gate is selected using the following steps [Hwang et al., 2006]:

- First, difference between the powers of every other two gates is computed. If half of that power is greater than a given value ε_1 , then it shows that the antenna begins to pick up the returning power.
- When this condition (half of the difference $> \varepsilon_1$), is satisfied, the difference between the power of every consecutive gate is calculated. If that difference is greater than another given value ε_2 , it indicates that the antenna continues to pick up the returning power and the corresponding gate and power are included in the first sub-waveform. Both ε_2 and ε_1 are determined empirically and the best values computed by Hwang et al., 2006 are: $\varepsilon_1 = 8$ and $\varepsilon_2 = 2$.
- The sub waveform is constructed including the four gates at the beginning and four at the end of the waveform.
- Using the selected samples in the sub-waveform, a retracking gate corresponding to this sub-waveform is determined using the following equations:

$$A = \sqrt{\frac{\sum_{i=1+n}^{60-n} y_i^4}{\sum_{i=1+n}^{60-n} y_i^2}}$$

.... (Equation 2.7)

$$y_N = \frac{1}{5} \sum_{i=1}^5 y_i$$

.... (Equation 2.8)

$$T_l = \alpha(A - y_N) + y_N$$

.... (Equation 2.9)

$$G_{thr}^r = G_{k-1} + \frac{T_l - y_{k-1}}{y_k - y_{k-1}} (G_k - G_{k-1})$$

.... (Equation 2.10)

Where,

A: Power amplitude of the sub-waveform,

y_i : Returning power picked up by the antenna for the i^{th} gate.

y_N : The average value of the first five powers

α : Threshold value

T_l : Threshold power

G_k : k^{th} gate of the sub-waveform whose value is greater than T_l

G_{thr}^r : Retracking gate

This process is repeated for the next sub-waveform and a new retracking gate is determined

- At the final step, the best retracking gate is determined by comparing the previous water level heights and the current water level height. The best retracking gate would yield the smallest difference in the current and previous water level height. If the gradient is higher, then in that case the previous tracking gate is selected.

The threshold α basically determines percentage of power that the sub-waveform must have which directly impacts the quality of the time measured and consequently the range. The selection of this threshold value changes depending upon the mission and its characteristics as well as the target area of investigation. After the application of this Retracker, the new improved retracked height of the water body can be determined by altering the Equation 2.6: eq 2.12

$$h = H_{sat} - R_{retracked} - h_{geoid} - h_{wtrop} - h_{dtrop} - h_{ionos} - h_{etide} - h_{ptide}$$

.... (Equation 2.11)

2.5. Delay-Doppler/SAR Altimetry vs Classic Low Resolution Mode Altimeter

In modern altimetry missions like Cryosat-2, Sentinel-3 and Sentinel-6, a Delay-Doppler mode of altimeter is used which is different than the conventional LRM radar altimeter found in most missions. A classic LRM pulse limited altimeter transmits and received pulses in a time sequence and the footprint changes gradually from a point to a disc to an annuli. The waveforms are incoherent and are averaged to reduce the speckle noise [Martin-Puig et al., 2008]. It has a lot of disadvantages including waste of radiated power and footprint dilation over rougher terrain which leads to less than optimal estimation of the surface height and roughness [Raney, 1998]. As compared to the conventional LRM altimetry, radar waves are emitted at a very higher rate of approximately 18,000 pulses per second as compared to 2000 in LRM. The much higher Pulse Repetition Frequency (PRF) allows the pulses to be constructed in bursts and the pulses within a burst to be correlated because the coherency allows for SAR processing [Sentinel Online].

The Delay Doppler SAR altimeter basically operates on exploiting the full Doppler bandwidth in the along-track direction of the signal to make the most efficient use of the power reflected from the surface. This results in higher spatial resolution in the along-track direction. The Figure 2.6 below depicts the difference in the footprint shape and size of both LRM and Delay-Doppler SAR mode of acquisition. The SAR altimeter “stares” at each resolved along-track cell as the radar passes overhead for as long as that particular cell is illuminated. Each cell is viewed over a larger fraction of the antenna beam than the pulse-limited thus more data is gathered which leads to substantial benefits [Rasmussen et al., 2018].

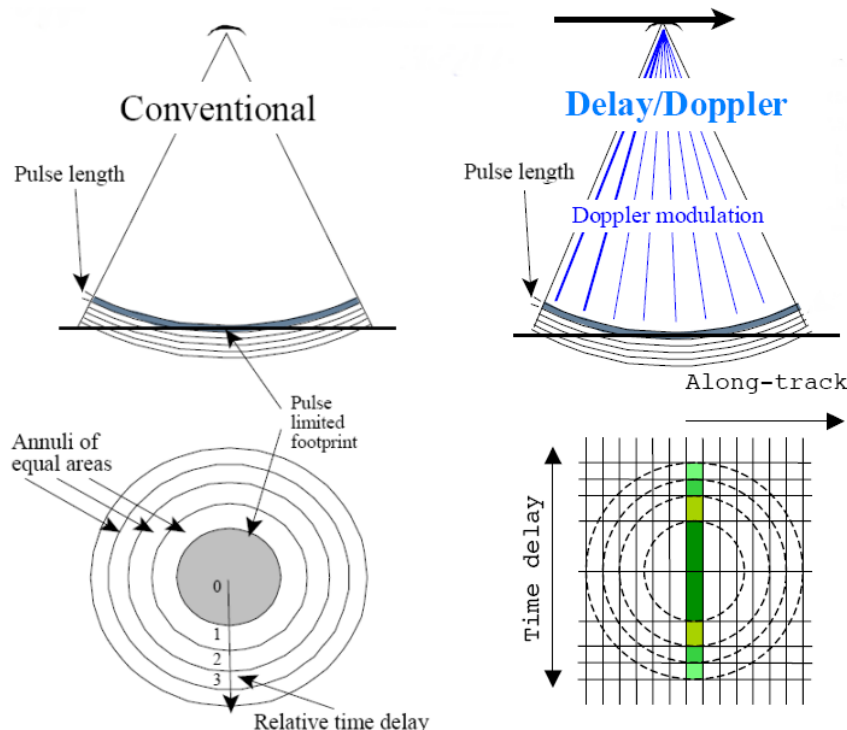


Figure 2.7: Comparison between conventional radar altimeter (left) and Delay Doppler/SAR (right) altimetry [Credits: R.K. Raney, John Hopkins University Applied Physics Laboratory]

Figure 2.8 below illustrates the process of waveform formation in delay Doppler altimetry. The red part on the footprint represents the LRM of acquisition and the red part on the footprint represents the SAR mode of acquisition. Before the signal reaches the target a slight offset in the power received is observed which is the thermal noise. As soon as the signal strikes the target, a sharp increase in the power received is observed as the footprint is no longer a disc but a narrow bin. The trailing edge of the waveform is more concave because of stacking of multiple beams over the footprint [Wu, 2021]

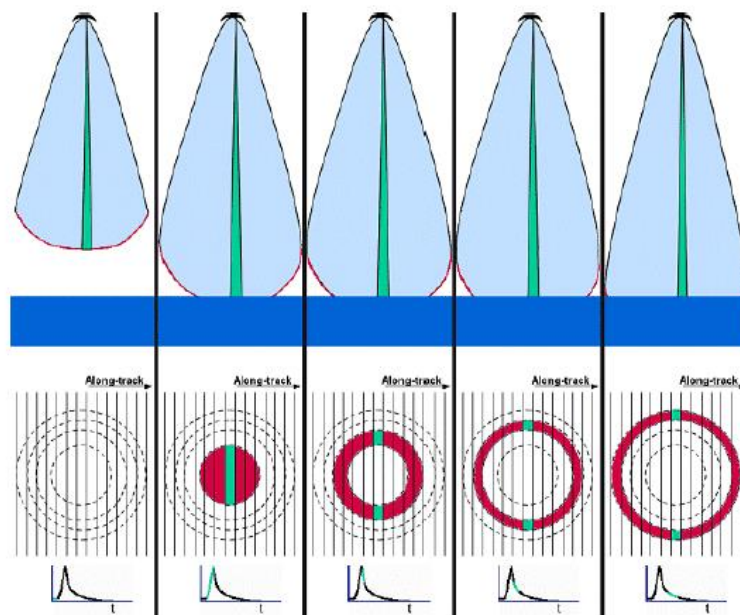


Figure 2.8: Step by step process of formation of waveform in delay Doppler SAR altimetry [Credits: R.K. Raney, John Hopkins University Applied Physics Laboratory]

3. Satellite altimetry missions

3.1. Jason-3

Jason-3 is an altimetry mission developed with a partnership of the EUMETSAT, NASA, CNES and NOAA to extend the services of the TOPEX/Poseidon and Jason-1 and 2 in the areas of topographic measurements of the ocean surface and climate change. The mission was launched on January 17, 2016 and orbits in a sun-synchronous orbit at an altitude of 1336 km and inclination of 66°. The mission produces global sea surface height (SSH) measurements every 10 days approximately with an accuracy of less than 4cm.

Jason-3 is a key mission in continuing the long term operations on oceanographic observations. It succeeded Jason-2 with increased advancements to its system and processing of data that it delivers. The primary instrument on-board Jason-3 is the Poseidon-3B which is a classic LRM radar altimeter and provides range measurements. It emits radar pulses in two frequencies: Ku band at 13.8 GHz and C band at 5.3 GHz. The dual frequency ensures range estimation with high accuracy in nadir direction and along track resolution of 30km. Apart from this, the mission carries other instruments like AMR radiometer which helps in measuring signal delay due to atmospheric water vapours as well as DORIS, Laser tracking and GPS receiver to compute the satellite orbit with high precision.

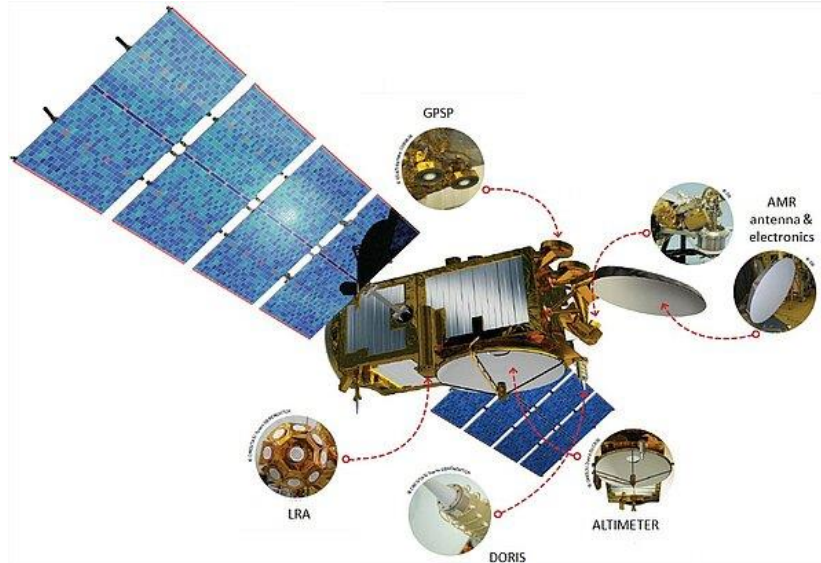


Figure 3.1: Jason-3 satellite and instruments on board [Credits: Aviso Altimetry]

3.2. Sentinel-6a and its comparison with previous SAR missions

The Copernicus Sentinel-6/Jason-CS mission was launched in November 2020 with an objective to provide the continuation of the decade long services in sea level measurement and sea state monitoring offered by the Jason satellites till the year 2030. The mission comprises of two identical satellites Sentinel-6a Michael Freilich launched in 2020 and Sentinel-6B to be launched in 2026 to fly in tandem. The mission is the result of international cooperation between ESA, EUMETSAT, EU, NOAA, CNES and NASA/JPL. It follows the same orbit as the ocean surface topographic missions since 1992 with orbit altitude of 1336 km and inclination of 66°.

The payload includes the POD instruments like DORIS, Laser tracking and GNSS receiver along with a microwave radiometer and the Poseidon-4 dual frequency (Ku and C) nadir pointing altimeter which allows an accuracy in centimetre range.

The primary payload is the Poseidon-4 dual frequency (C/Ku-band) nadir-pointing radar altimeter that uses an innovative interleaved mode. This enables radar data processing on two parallel chains the first provides synthetic aperture radar (SAR) processing in Ku-band to improve the received altimeter echoes through better along-track sampling and reduced measurement noise; the second provides a Low Resolution Mode that is fully backward-compatible with the historical reference altimetry measurements, allowing a complete inter-calibration between the state-of-the-art data and the historical record as well as ensuring that the introduction of SAR technologies into the reference does not introduce a bias into the historical records. [Donlon et al., 2021]. The interleaved mode works on an open burst configuration with a PRF of 9 kHz. This allows the rearrangement of the transmission and reception of pulses simultaneously to increase the number of measurements over a given target and thereby reduce the thermal and speckle noise. The Figure 3.2 shows the evolution of the altimeter chronograms highlighting the optimal use of available transmit and receive time when using the open burst measurement approach compared to the closed burst mode and the classic LRM measurements.

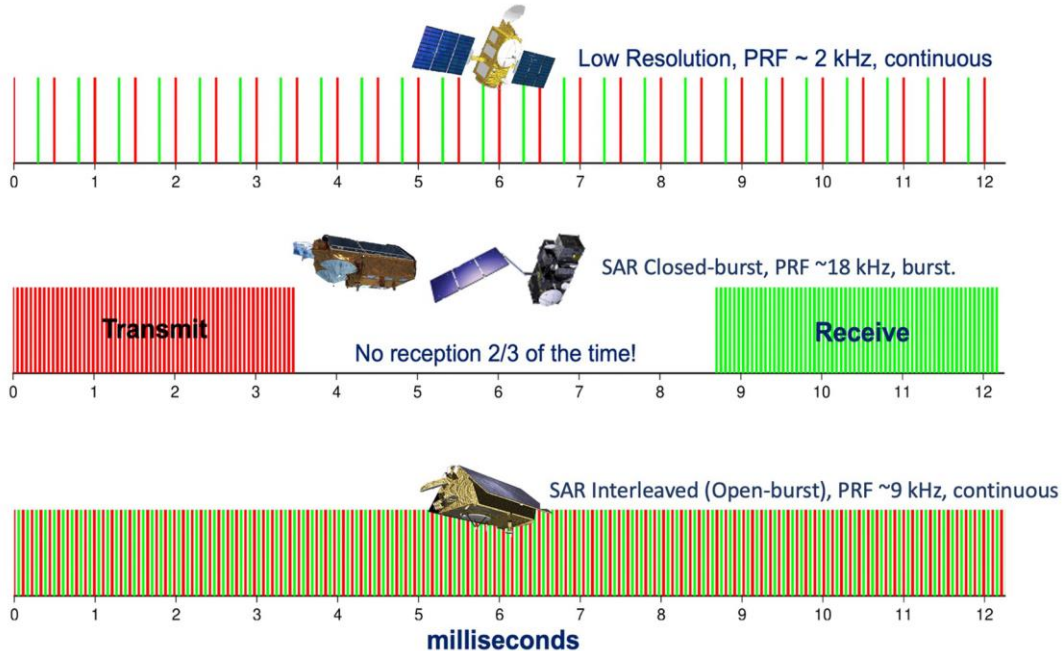


Figure 3.2: The evolution of the satellite altimeter chronograms [Donlon et al., 2021]

The application of the SAR interleaved mode has huge potential in analysing the inland water bodies due to a huge improvement in the long track resolution to 300 meters as compared to the along track resolution of 30 km in the classic LRM altimeter. Additionally, reduction in measurement noise due to increased number of radar looks has allowed to overcome the effects caused due to the presence of ‘unwanted’ objects in the footprint of the radar altimeter. Previously, a few SAR altimetry missions were launched to improve our estimation of water level height not just the oceans but many smaller water bodies like rivers and lakes.

The Copernicus Sentinel-3 SAR altimetry mission, in particular, was launched as a continuation of services provided by ENVISAT missions. The satellites (currently Sentinel-3a and Sentinel-3b) fly in tandem in an almost circular orbit at an inclination of 98.65° and a revisit rate of 27 days provides high resolution altimetry data along with other services. Apart from the traditional Closed-loop tracking mode, the on-board altimetry instrument (SRAL) can operate in Open-loop tracking mode as well which results in the benefit of precise positioning of the receiving window to allow an increase in time for which the altimeter hooks on the water surface. As a result, the mission provides a very good quality of measurements over lakes and rivers [Halicki & Niedzielski, 2022].

However, due to a lower revisit frequency (27 days), many temporal gaps occur in regular monitoring of those lakes and rivers. Based on this heritage, Sentinel-6a mission was designed and launched with an improved SAR altimeter and a higher revisit frequency. The basic difference between the Sentinel-3 and Sentinel-6 SAR altimetry is the inclusion of an interleaved mode of acquisition in Sentinel-6. As described before, the interleaved mode operates in SAR open-burst and LRM mode in parallel which applies the historical records in its measurements to get rid of any bias that might occur when measuring the water level height. This allows Sentinel-6 satellite to be capable enough to continuously monitor not just the oceans but the continental water bodies too with increased accuracy as compared to its predecessor missions.

In the following study, the water level retrieved from the high resolution SAR mode of Sentinel-6a (denoted as Sentinel-6a HR) is compared with the LRM data retrieved from Jason-3 as well as the Sentinel-6a (denoted as Sentinel-6a LR) using various performance parameters.

4. Areas of Study & methodologies

4.1. Areas of study and data acquisition

For this study, around 15 lakes and reservoirs in the country of United States were chosen because of an extensive network of gauge stations available which provide decades of water level data by minute, days, months and years. The target areas include the bigger lakes like the five great lakes along with smaller lakes spread throughout the country. Brief information on the acquisition of both in-situ and the satellite data has also been described

1. Lake Erie

Lake Erie is the fourth largest lake (by surface area) of the five Great Lakes in North America. It is situated at the USA-Canada border and has a surface area of 25,744 sq km. Mean surface elevation is 173m.

The in-situ data for Lake Erie was acquired from National Oceanic and Atmospheric Administration (NOAA) Tides and Currents website through the monitoring station Cleveland (OH) located at 41° 32.5 N and 81° 38.1 W with station ID: 9063063. For acquisition of the satellite data from the OpenADB on DGFI-TUM servers, the pass number for Jason-3 and Sentinel-6a is 193 between the latitudes of 48.48° and 42.7. Due to large size of the lake, retracking using the Improved Threshold Retracker takes a longer time for computation, therefore, for determining the optimum threshold, the latitude range is reduced to 41.9 to 42.2 degrees north.

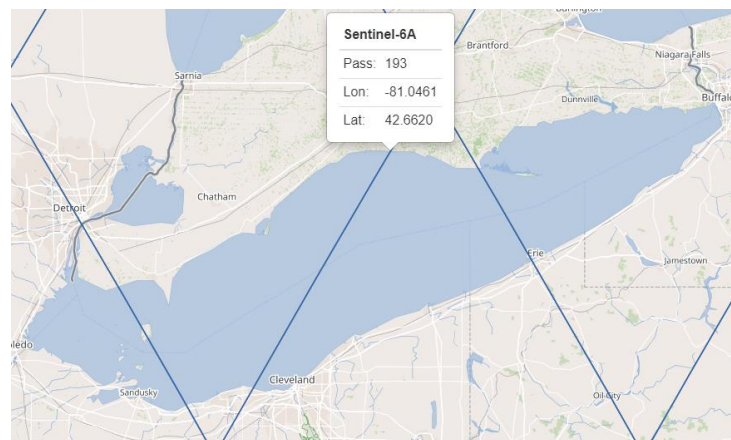


Figure 4.1: Map of Lake Erie along with Sentinel-6a pass over it [Credits: DGFI pass locator]

2. Lake Michigan

Lake Michigan is the second largest lake by volume and third largest by surface area of the five Great Lakes of North America. It is located in United States bordered by the states of Wisconsin, Illinois, Indiana and Michigan. Its surface area is 58,030 sq km and average surface water level is 176m.

The in-situ data for Lake Michigan was also acquired from National Oceanic and Atmospheric Administration (NOAA) Tides and Currents website through the monitoring station Calumet Harbor (IL) located at $41^{\circ} 43.8' N$ and $87^{\circ} 32.3' W$ with station ID: 9087044. The satellite data has been acquired through the OpenADB platform on the servers at DGFI-TUM using the pass number 041 for both missions within the latitudes 41.65 and 43.2 degrees north. Due to large size of the lake, retracking using the Improved Threshold Retracker takes a longer time for computation, therefore, for determining the optimum threshold, the latitude range is reduced to 42.4 to 42.6 degrees north.

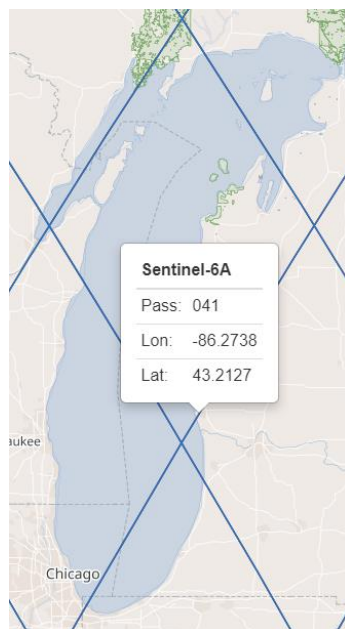


Figure 4.2: Map of Lake Michigan along with Sentinel-6a pass over it [Credits: DGFI pass locator]

3. Lake Ontario

Lake Ontario is one of the five Great Lakes of North America. It is surrounded by the Canadian province Ontario on the north, west and southwest direction and the state of New York on the south and east. Surface area wise, the lake covers a total surface area of 19,000 sq km and has an average surface water level of 74m.

The in-situ data for the Lake Ontario was acquired from the NOAA Tides and Currents website through the monitoring station Rochester (NY) located at $43^{\circ} 16.1' N$ and $77^{\circ} 37.5' W$ with station ID: 9052058. The satellite data has been acquired through the OpenADB platform on the servers at DGFI-TUM using the pass number 015 for both missions within the latitudes 43.3 and 43.87 degrees north. Due to large size of the lake, retracking using the Improved Threshold Retracker takes a longer time for computation, therefore, for determining the optimum threshold, the latitude range is reduced to 43.4 to 43.6 degrees north.

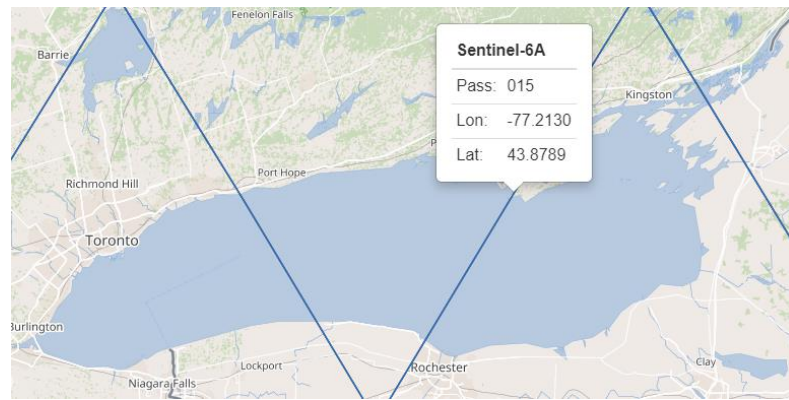


Figure 4.3: Map of Lake Ontario along with Sentinel-6a pass over it [Credits: DGFI pass locator]

4. Lake Huron

Lake Huron is one of the five Great Lakes of North America and is the third largest lake by surface area out of the Great Lakes. It is connected to Lake Michigan by a 8km wide gauge and has the same surface water elevation. It is bordered by the Canadian province Ontario in north and east direction as well by the US state Michigan in the southern and western direction. The surface area of the lake is 59,590 sq kms and the average surface water level is 176m.

The in-situ data for Lake Huron can be acquired from the NOAA Tides and Current website through the monitoring station Harbor Beach (MI) located at 43° 50.8 N and 82° 38.6 W with station ID: 9075014. The satellite data has been acquired through the OpenADB platform on the servers at DGFI-TUM using the pass number 117 for both missions within the latitudes 44 and 45.22 degrees north. Due to large size of the lake, retracking using the Improved Threshold Retracker takes a longer time for computation, therefore, for determining the optimum threshold, the latitude range is reduced to 44.9 to 45.1 degrees north.

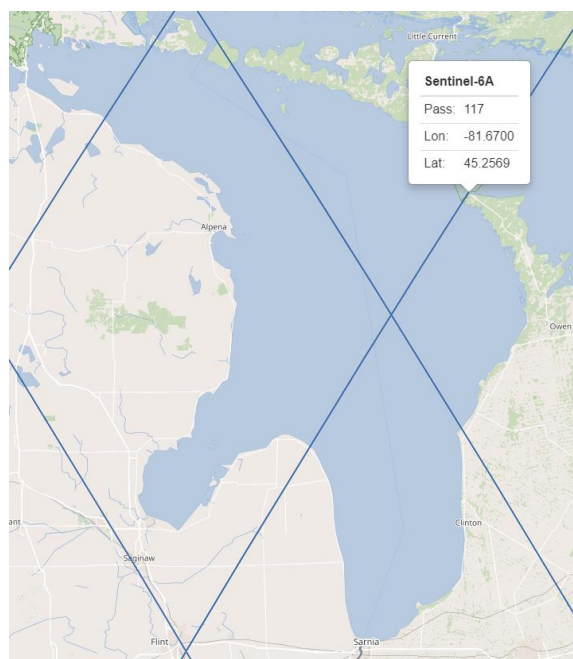


Figure 4.4: Map of Lake Huron along with Sentinel-6a pass over it [Credits: DGFI pass locator]

5. Lake Superior

Lake Superior is the largest freshwater lake in the world by surface area and third largest by volume. It is the northern most and western most of the Great Lakes in North America surrounded by the Ontario province in Canada to the north and the US states of Minnesota to the northwest, Wisconsin and Michigan to the south. The total surface area of the lake 82,000 km and the average surface water level is 183m.

The in-situ data for Lake Superior can be acquired from the NOAA Tides and Current website through the monitoring station Ontonagon (MI) located at 46° 52.5 N and 89° 19.4 W with station ID: 9099044. The satellite data has been acquired through the OpenADB platform on the servers at DGFI-TUM using the pass number 143 for both missions within the latitudes 47.45 and 48.8 degrees north. Due to large size of the lake, retracking using the Improved Threshold Retracker takes a longer time for computation, therefore, for determining the optimum threshold, the latitude range is reduced to 48.0 to 48.2 degrees north.

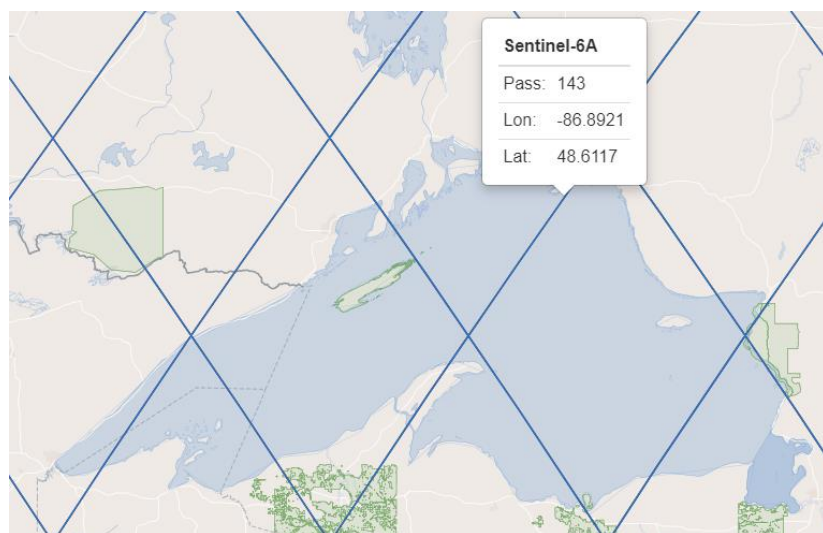


Figure 4.5: Map of Lake Superior along with Sentinel-6a pass over it [Credits: DGFI pass locator]

6. Richland Chambers Reservoir

Richland-Chambers Reservoir is the third largest inland reservoir by surface area and 8th largest reservoir by water volume and is formed by the impoundment of Richland Creek and Chambers Creek in Texas. The average surface water elevation is 96m and the total surface area is 167 sq kms.

The in-situ data for the Richland Chambers Reservoir can be acquired from the United States Geological Survey (USGS) website through the monitoring station Richland-Chambers Res nr Kerens (TX) located at 32°02'25" N and 96°12'23" W with station ID: USGS 08064550. The satellite data has been acquired through the OpenADB platform on the servers at DGFI-TUM using the pass number 052 for both missions within the latitudes 31.93 and 32 degrees.

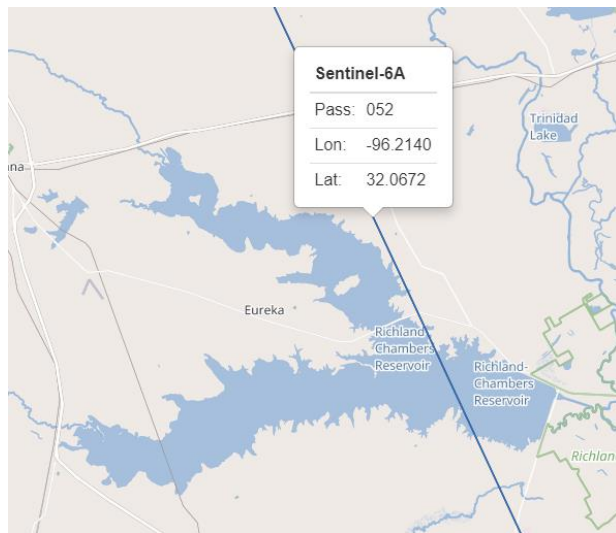


Figure 4.6: Map of Richland Chambers Reservoir along with Sentinel-6a pass over it [Credits: DGFI

7. Toledo Bend Reservoir

Toledo Bend Reservoir is a reservoir on the Sabine River located partially between Texas and Louisiana and has a total surface area of 749 sq kms. The average surface water height is 52 m above sea level.

The in-situ data for the Toledo Bend Reservoir was acquired from the USGS website with the nearest gauge station named Toledo Bend Res nr Negreet (LA) with the station id: USGS 312914093422701 and coordinates Latitude 31°29'14.39" & Longitude 93°42'27.11". The gauging station is located at a height of 167 feet (50.9m) above NAVD 1988 ([North American Vertical Datum](#)). The satellite data has been acquired through the OpenADB platform on the servers at DGFI-TUM using the pass number 041 for both missions within the latitudes 31.77 and 31.84 degrees.

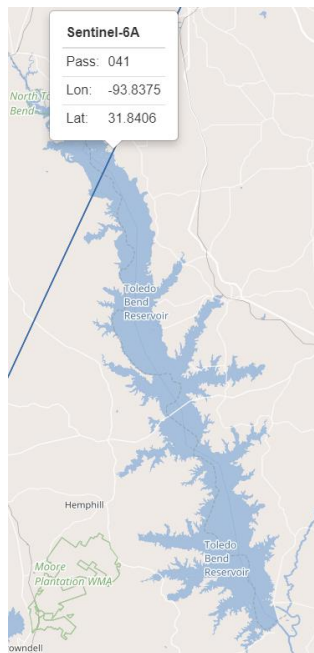


Figure 4.7: Map of Toledo Bend Reservoir along with Sentinel-6a pass over it [Credits: DGFI pass locator]

8. Lake of Woods

Lake of Woods is the sixth largest freshwater lake in the United States after the five Great Lakes. The lake is fed by the Rainy River. Shoal Lake, Kakagi Lake and other small river and it drains into the Winnipeg River and then into Winnipeg Lake. The lake freezes in winters causing inaccuracies in the estimation of water level. The total surface area is 4350 sq kms and the average surface water level height is 323 meters above sea level.

The in-situ data for the Lake of Woods has been acquired from the USGS website through the gauging station USGS 05140520 Lake of the Woods at Warroad (MN) which is located at the coordinates of Latitude 48°54'15", Longitude 95°18'57" and at a height of 1000 feet (304.8 m) above COE1912. The satellite data has been acquired through the OpenADB platform on the servers at DGFI-TUM using the pass number 178 for both missions within the latitudes 48.8 and 49.17 degrees. Due to a smaller size (as compared to the Great Lakes), lesser number of available data points and a very northern most location, the altimetry values over this lake gets corrupted due to ice formation during winters. So for a fair assessment of the quality of the altimetry datasets, measurements only during the summer months i.e. March to October, are analysed in the overlapping period of operation for both missions.

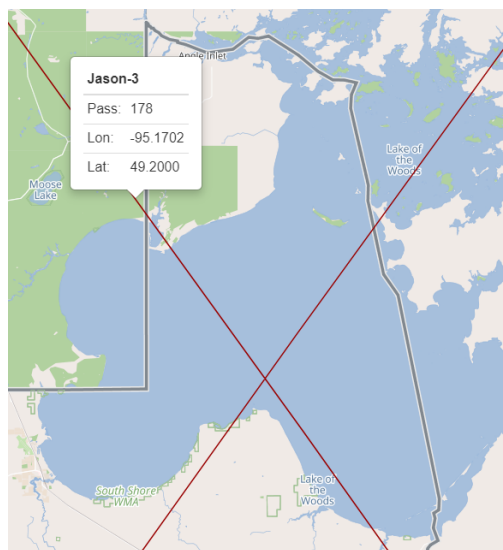


Figure 4.8: Map of the Lake of Woods along with Jason-3 pass over it [Credits: DGFI pass locator]

9. Lake Winnebago

Lake Winnebago is a very shallow freshwater lake located in the North Central United States. With a total surface area of 533.94 sq kms, it is the largest lake located entirely within one state of Wisconsin. The average surface water elevation is 227 m above sea level.

The in-situ data for the Lake Winnebago has been acquired from the USGS website through the gauging station USGS 04084255 Lake Winnebago near Stockbridge (WI) which is located at the coordinates of Latitude 44°04'14", Longitude 88°19'44" and at a height of 744 feet (226.771 m) above NAVD88. The satellite data has been acquired through the OpenADB platform on the servers at DGFI-TUM using the pass number 219 for both missions within the latitudes 43.94 and 44.17 degrees. The lake also freezes during winters, which result in noisy measurements. Therefore, the analyses only during the summer months i.e. March to October, are assessed.

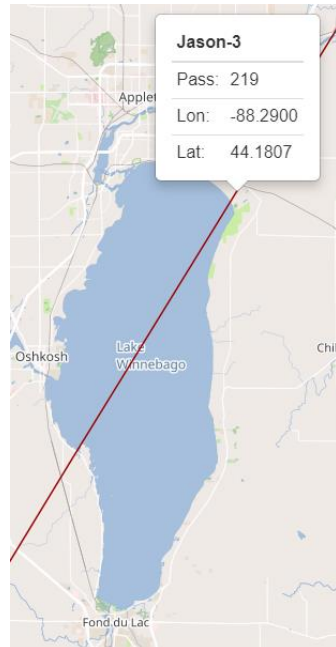


Figure 4.9: Map of the Lake Winnebago along with Jason-3 pass over it [Credits: DGFI pass locator]

10. Lake OH Ivie

O.H. Ivie Lake is a reservoir formed in 1990 by the construction of S.W. Freese Dam at the Concho-Coleman county line by Brown and Root located in Texas. The total surface area of the reservoir is 81 sq kms and average surface elevation above sea level 473m.

The in-situ data for O.H. Ivie Lake has been acquired from the official website of the Texas Water Development Board through the gauging station USGS 08136600 O. H. Ivie Res nr Voss (TX) which is located at the coordinates Latitude 31°30'00", Longitude 99°40'05". The satellite data has been acquired through the OpenADB platform on the servers at DGFI-TUM using the pass number 143 for both missions within the latitudes 31.49 and 31.55 degrees.



Figure 4.10: Map of the O.H. Ivie Lake along with Jason-3 pass over it [Credits: DGFI pass locator]

11. Sam Rayburn Reservoir

Sam Rayburn Reservoir is a reservoir located in the eastern part of Texas in USA and is fed by the Angelina River. The total surface area of the reservoir is 463 sq kms and the average surface water level is 49.5m.

The in-situ data for Sam Rayburn Reservoir has been acquired from the official website of the USGS through the gauging station USGS 08039300 Sam Rayburn Res nr Jasper (TX) which is located at the coordinates Latitude 31°03'38", Longitude 94°06'21". The satellite data has been acquired through the OpenADB platform on the servers at DGFI-TUM using the pass number 041 for both missions within the latitudes 31.1145 and 31.19 degrees.

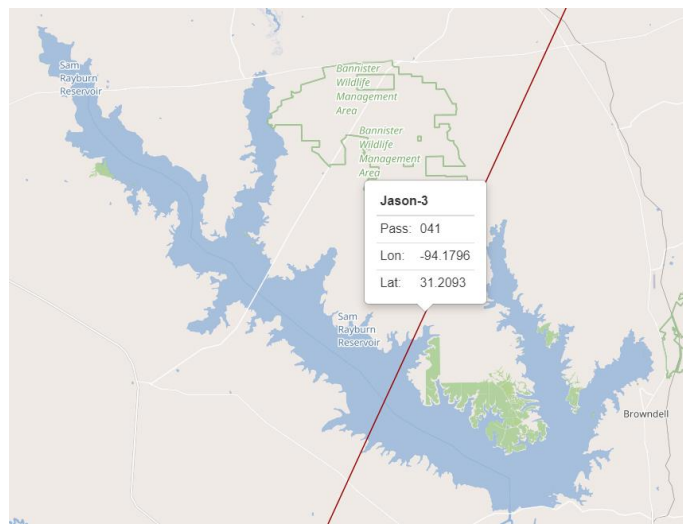


Figure 4.11: Map of the Sam Rayburn Reservoir along with Jason-3 pass over it [Credits: DGFI pass locator]

12. Lake Sidney Lanier

Lake Sidney Lanier is a reservoir situated in the northern part in the US state of Georgia. It is created in 1956 through the construction of Buford Dam on the Chattahoochee River and is also fed by Chestattee River. The total surface area of the lake is 150 sq km and the average surface water level is 326 m.

The in-situ data for Lake Sidney Lanier has been acquired from the official website of the USGS through the gauging station USGS 02334400 Lake Sidney Lanier near Buford (GA) which is located at the coordinates Latitude 34°09'45.8", Longitude 84°04'31.9". The satellite data has been acquired through the OpenADB platform on the servers at DGFI-TUM using the pass number 015 for both missions within the latitudes 34.15 and 34.3 degrees.



Figure 4.12: Map of the Lake Sidney Lanier along with Sentinel-6a pass over it [Credits: DGFI pass locator]

13. Ray Roberts Lake

The Ray Roberts Lake is an artificially lake built after the approval of construction by US Congress in 1945 and named after the local congressman Ray Roberts who supported its construction. The lake is situated in Texas and is filled by a tributary of the Trinity River. The total surface area of the lake is 119 sq km and the average surface water level is 192m above sea level.

The in-situ data for Ray Roberts Lake has been acquired from the official website of the Texas Water Development Board through the gauging station USGS 08051100 Ray Roberts Lk nr Pilot Point (TX) which is located at the coordinates Latitude 33°21'19", Longitude 97°02'59". The satellite data has been acquired through the OpenADB platform on the servers at DGFI-TUM using the pass number 052 for both missions within the latitudes 33.43 and 33.4455 degrees.

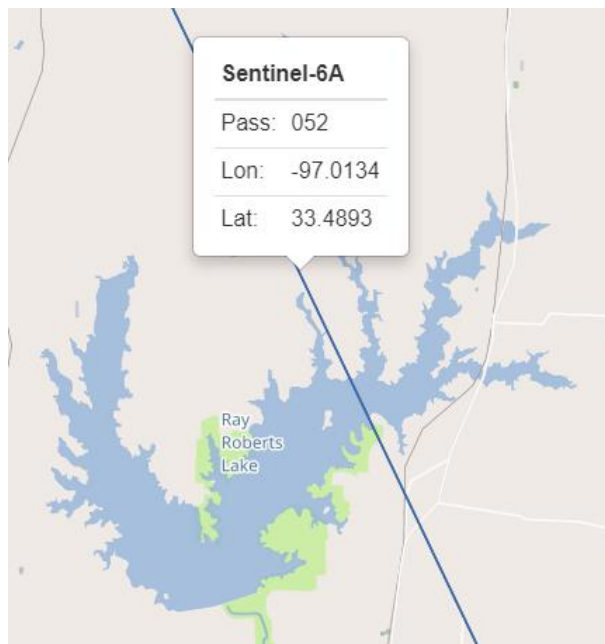


Figure 4.13: Map of Ray Roberts Lake along with Sentinel-6a pass over it [Credits: DGFI pass locator]

14. Lake Champlain

Lake Champlain is a natural freshwater lake located in Northern America. The lake is surrounded by the US states of New York and Vermont and extends till the Canadian province Quebec. The lake has a total surface area of 1331 sq kms and has an average surface water height of 29 to 30 meters.

The in-situ data for the Lake Champlain has been acquired from the USGS website through the gauging station located at the lake site USGS 04294500 Lake Champlain at Burlington (VT). The station is located at the coordinates Latitude 44°28'34", Longitude 73°13'19". The satellite data has been acquired through the OpenADB platform on DGFI-TUM servers using the pass number 126 for both missions in the latitude ranges of 44.22 and 44.246 degrees.

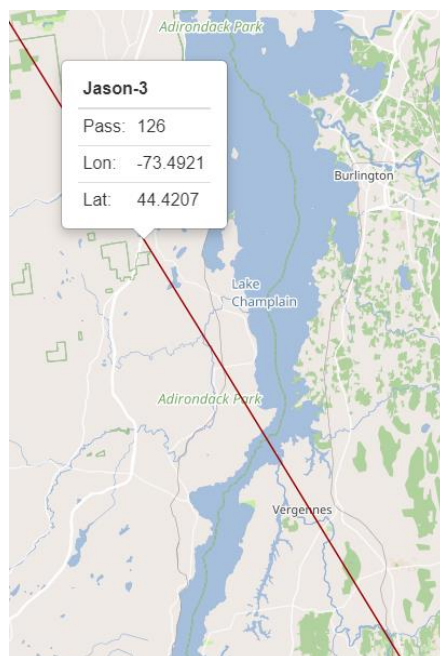


Figure 4.14: Map of Lake Champlain along with Jason-3 pass over it [Credits: DGFI pass locator]

15. Lake Tawakoni

Lake Tawakoni is a man-made reservoir constructed in 1960 with the Iron Bridge Dam and is located in the north eastern part of the US state of Texas. The total surface area of the reservoir is 153.29 sq kms and the average surface water level is 133.4 meters above sea level.

The in-situ data for the Lake Tawakoni has been acquired from the USGS website through the gauging station located at the lake site USGS 08017400 Lake Tawakoni nr Wills Point (TX). The station is located at the coordinates Latitude 32°48'31", Longitude 95°55'10". The satellite data has been acquired through the OpenADB platform on DGFI-TUM servers using the pass number 219 for both missions in the latitude ranges of 32.8460 and 32.93 degrees.

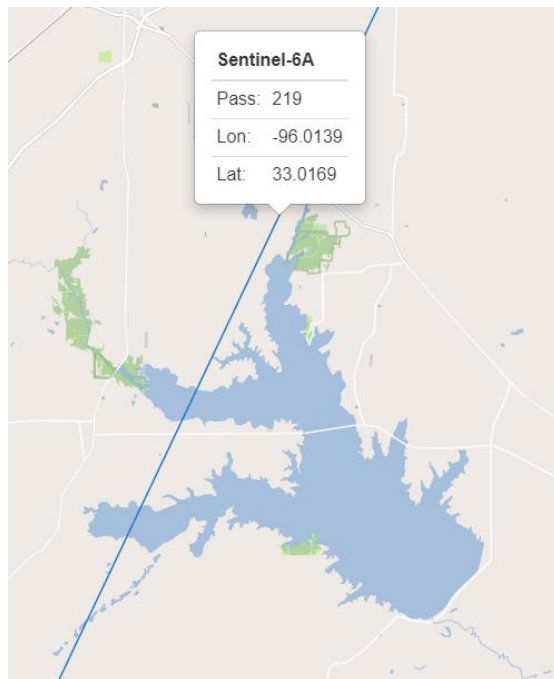


Figure 4.15: Map of Lake Tawakoni along with Sentinel-6a pass over it [Credits: DGFI pass locator]

4.2. Methodology flow

In this section, we discuss the methodology designed to reach the objectives and complete the tasks as described in the section 1.3. The quality of the data provided by the Sentinel-6a HR, Sentinel-6a LR and the Jason-3 missions will be assessed for the aforementioned areas of investigation by generating the respective time series for each lake. Although, the altimetry missions were initially designed for continuous monitoring of Topological variations in the ocean surface, the advancements in the radar system and data processing techniques have enabled an effective monitoring of continental water bodies as well. Even though these new technologies like closed and open burst SAR mode have shown prominence and potential specifically for inland water bodies, the inculcation of additional post processing retracking techniques have helped in getting a more refined result by mitigating the additional noise in the waveforms.

As explained in section 2.4, the Improved Threshold Retracker has been used in this study as a post processing strategy on the altimetry data to retrieved range values with high precision from a noisy waveform and improve our estimation of the water level heights. The Retracker works on a threshold value α which directly impacts the determination of the optimum tracking gate of the sub-waveform. This means that the selection of the optimum threshold directly impacts are measurements of range calculations and therefore affects the retrieved water level height. This selection may vary depending on the characteristics of the mission selected or the properties of the area of investigation and therefore a prior analysis is required to get the optimum value of the threshold.

Once, this analysis is completed and we have a best threshold value to be used for each mission and target area, water level time series in the overlapping periods of operation can be generated using the retracked heights for each area of investigation. To check the quality of the observations, certain performance metrics are analysed along with the intermission offsets in the height values to understand variations in our measurements.

Therefore, the methodology has been divided in two parts which are explained below:

4.2.1. Determination of the Optimum threshold

This step is a critical step as it helps to understand that at what threshold value, the returned waveform, which is already very noisy, will provide best the range of the satellite and consequently, the water level height. The procedure adopted to select the best threshold for each mission and area of investigation is described below:

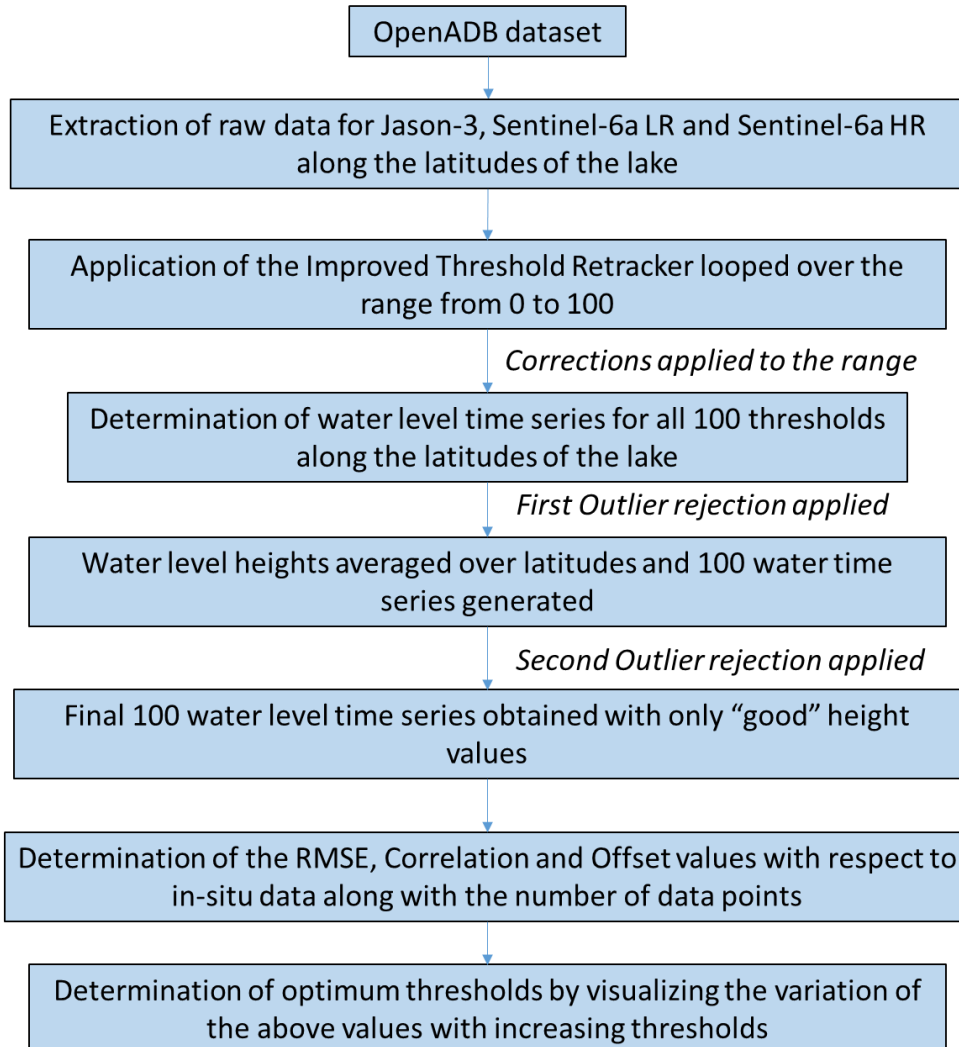


Figure 4.16: Flowchart explaining the methodology for determining the optimum threshold for the Retracker for each mission

Ideally, the optimum value of the threshold will have the least RMSE value and the highest correlation. In the later sections, after obtaining the optimum thresholds for each mission and each area of investigation, mission wise histograms will be plotted to visualise the occurrence of them for different lakes (different for larger and smaller lakes). The higher density of the occurrence of a particular threshold would give an idea for selecting that value and subsequently, generate water level time series for all aforementioned lakes. But for the generation of water level time series, the threshold values determined for each lake and mission would be used for further steps.

4.2.2. Water level generation

Once, an optimum threshold is selected for each investigated area and mission, water level time series are generated for each mission and target area. For the Great Lakes, since they are larger in size, there are enough measurements available in the nadir direction, therefore, water level heights are determined using both on-board Retracker of each mission and using the Improved Threshold Retracker. For smaller lakes, due to a larger footprint of the LRM missions (Jason-3 and Sentinel-6a LR), water level heights have been estimated using the Improved Threshold Retracker only. For the Sentinel-6aHR mission, due to a better along track resolution, the water levels have been determined using both On-board Retracker and the Improved Threshold Retracker. The procedure has been explained using the flowchart below:

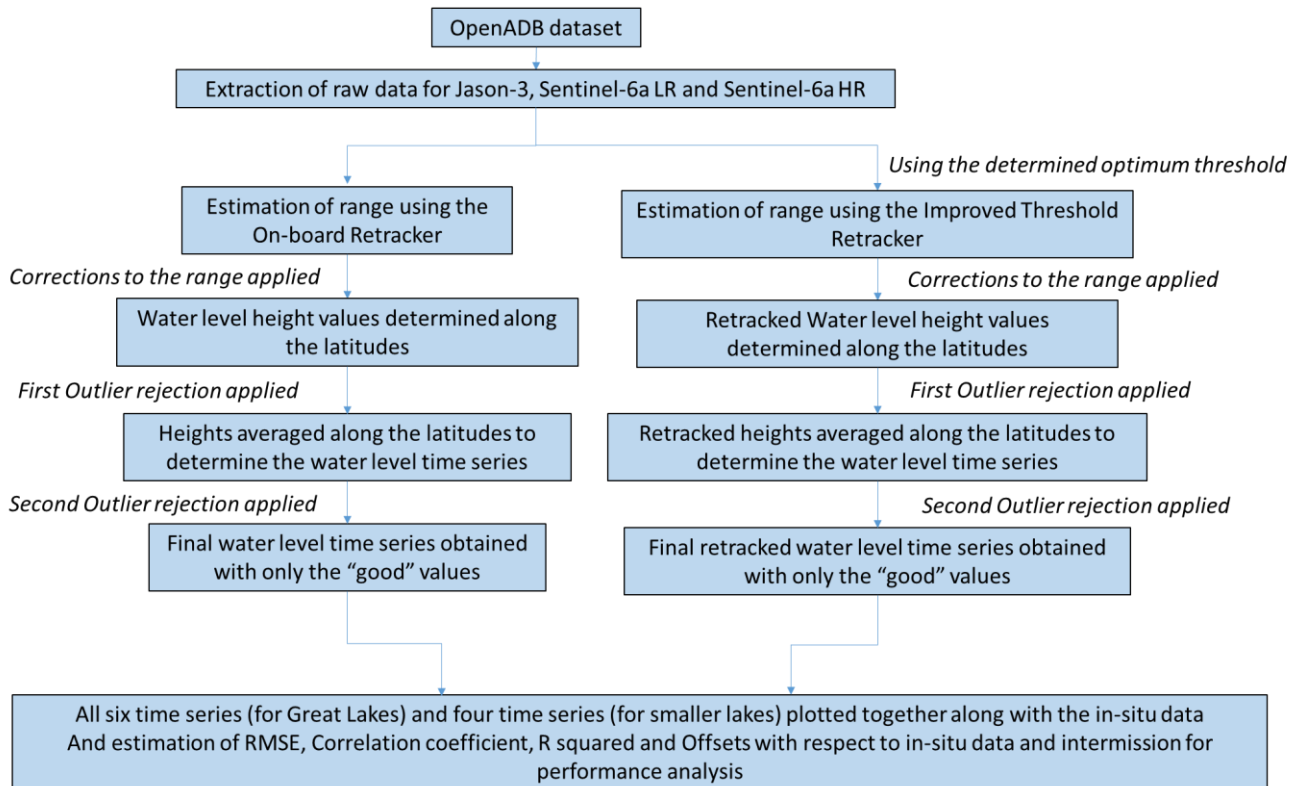


Figure 4.17: Flowchart for generating water level time series for all mission

Since, the launch of Sentinel-6MF satellite in November, 2020, the mission has been actively providing water level measurement since the end of December 2020. Jason-3 satellite on the other hand was operational and actively providing data from 2016 till March 2022 when it got discontinued. Therefore, the performance analysis of all the missions have been conducted in the overlapping period of operation which is December 2020 to March 2022. In some cases of smaller lakes especially like Lake of Woods, Lake Winnebago and Lake Champlain, which freeze over during winters, to avoid any discrepancies in the derived water level heights, the period of analysis is considered during the summer months only i.e. March 2021 to October 2021.

4.3. Outlier Rejection

As it can be noticed from the Figures 4.16 and 4.17, on a couple of stages, outlier rejection algorithms have been applied on the derived water level measurements. For the LRM measurement of Jason-3 and Sentinel-6aLR data is around 30km and for SAR measurement in Sentinel-6aHR the along-track resolution reduces to 300m. For larger lakes like the Great Lakes which are hundreds of kilometres in size, a lower resolution has a lower effect on the height measurements and more or less depict an idealized situation where each data point is not corrupted by any external influences. But for smaller lakes, these assumptions cannot be made due to the presence of certain external objects (like land, vegetation etc.) in the radar footprint leading to corrupted height values. Using a Retracker helps to some extent in predicting the range to some precision but for accurate assessment of the quality of measurements, certain ‘bad’ values must be removed. This is done using the outlier rejection algorithm which is described below.

- (i) Calculate the number of data points (n) and the standard deviation of the heights (h_{std})
- (ii) While the number of data points (n) and standard deviation (h_{std}) remain above or equal to a certain minimum values (N_{min} & $h_{std,min}$), the following outlier removal loop will run
- (iii) Calculate the difference between each height value (h) with the median height (h_{median}) which is the tolerance (r).

$$r = h - h_{median}$$

... (Equation 4.1)

- (iv) If the absolute value of tolerance (r) value is greater than a certain threshold value ($r_{threshold}$) then that height value gets rejected.
- (v) Again, calculate the number of data points (n) and the standard deviation of the heights (h_{std})
- (vi) The outliers will continue to get removed until the number of data points and standard deviation don't become less than the specified minimum values.

The threshold for tolerance, number of points and standard deviation varies for each mission and target area depending upon its resolution and size. For this study, the outliers were rejected in two stages: first along the latitudes for measurements derived for each cycle; second along the time series after averaging the clean values for each cycle. After several iterations we get water level time series with only ‘good’ height values.

4.4. Performance parameters

For the purpose of determining the quality of the water level time series with respect to the in-situ data available from various gauging stations, the following parameters were assessed:

- Root Mean Square Error (RMSE): It is used to measure the difference between the values predicted by the retrackers (h_i) and the ground truth data ($h_{i,true}$) by measuring the square-root of the mean of the square of the errors. N is the total number of data points.

$$RMSE = \sqrt{\frac{\sum_{i=1}^N (h_i - h_{i,true})^2}{N}}$$

.... (Equation 4.2)

- Correlation Coefficient and R-squared: the correlation coefficient is determined to measure the strength of relationship between two variables. If the correlation is positive then it means that the two variables move in the same direction and if it is negative then it means the two variables move in the opposite direction. It is measured on the scale of +1 to -1. If the correlation is 0, then the variables are not correlated at all. The formula for the Pearson correlation coefficient is:

$$corr = \frac{\sum_{i=1}^N (h_i - \bar{h})(h_{i,true} - \bar{h}_{true})}{\sqrt{\sum_{i=1}^N (h_i - \bar{h})^2} \sqrt{\sum_{i=1}^N (h_{i,true} - \bar{h}_{true})^2}}$$

... (Equation 4.3)

Where,

$corr$: Correlation coefficient,

h_i, \bar{h} : Derived height value and its mean,

$h_{i,true}, \bar{h}_{true}$: Ground truth data and its mean,

N : Number of samples.

R-squared is the square of the correlation coefficient. It measures the proportion of how much the variation in the derived height values is explained by the variation in the reference or the ground-truth data. R-squared values range from 0 to 1, 1 means that all movements of the derived height is explained by the movements in the in-situ data.

$$R^2 = (corr)^2$$

.... (Equation 4.4)

- Offset: the offsets of the inter-mission height values as well as with respect to in-situ data is also determined to validate whether it is consistent or not for all target areas. The value is basically the difference in the median values of the heights.

$$offset = h_i - h_{i,median}$$

.... (Equation 4.5)

5. Experiments and Results

In this chapter, we will discuss the results for the lakes as specified in section 4.1. For each lake, results in line with the flow of methodology (as described in section 4.2) would be shown and an analysis of those results would be carried out.

5.1. Lake Erie

For Lake Erie, the ground track of '193' was chosen along the latitudes of 41.9 to 42.1 degrees north for estimation of optimum thresholds based on height values determined for all 100 thresholds. After computing the RMSE, R2, offset with in-situ values as well number of available data points along the whole threshold spectrum, the following plot was obtained:

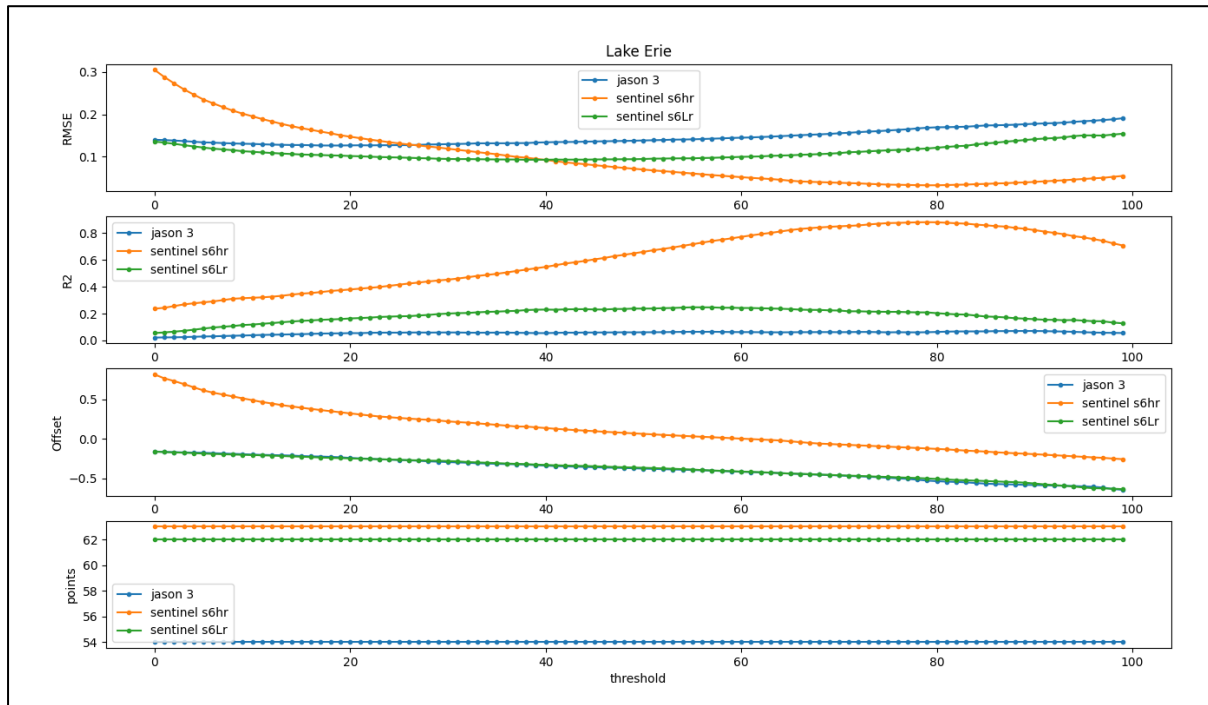


Figure 5.1: Plots for variation in RMSE, R2, offset and number of points for Lake Erie

For the outlier rejection algorithm for determination of the optimum threshold, as specified in the section 4.3, following upper and lower limits were used:

Number of minimum data points (N_{min}) = 30

Minimum standard deviation ($h_{std,min}$) = 0.05m

Tolerance ($r_{threshold}$) = 0.05m

As it can be observed from the above figure, a different behaviour which is somewhat opposite can be observed for the SAR and LRM missions. On one hand for the Sentinel-6aHR mission, the RMSE values reduce from 30 cm to 3 cm as the threshold increases with minima reaching at later part of threshold spectrum. But on the other hand the opposite trend can be observed for the LRM mission

CHAPTER 5: EXPERIMENTS AND RESULTS

whose RMSE values vary in 6 to 10 cm with minimum value reached at the earlier spectrum of the threshold values. To understand this behaviour in some more detail, let's have a look at the respective waveforms of these missions at the threshold values of 80% for Sentinel-6aHR, 14% for Jason-3 and 43% for Sentinel-6aLR.

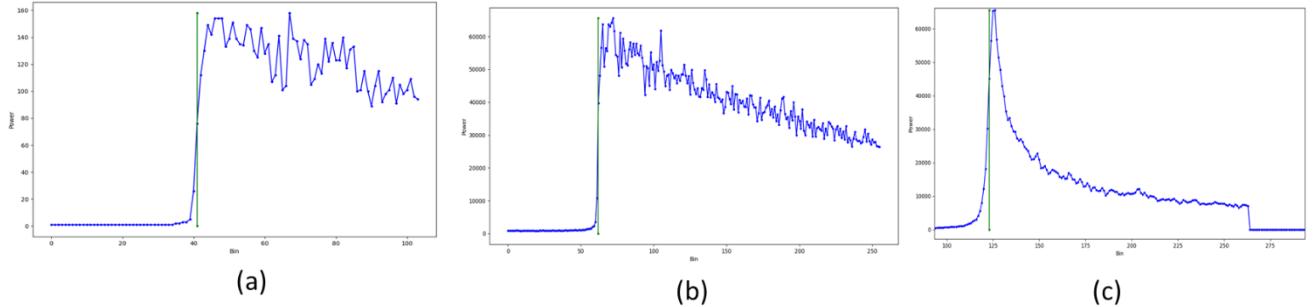


Figure 5.2: Return waveforms for Lake Erie and the position of the retracking gate. (a) Jason-3 mission with threshold of 14%, (b) Sentinel-6aLR mission with threshold of 43%, (c) Sentinel-6aHR mission with threshold of 80%

The Quasi-Brown type waveforms for the LRM missions (a) and (b) from the above figure 5.2 give a brief idea about the nature of the lake during the summer months. They both depict an “ocean-like” waveforms because of the rough surface and waves. Due to slightly noisy leading edge, the Improved Threshold Retracker yields the best position of the retracking gate in the earlier part of the threshold spectrum for Jason 3 and in the middle part for Sentinel-6aLR. From the waveforms, it can be seen that if the retracking gate moves towards right with increasing threshold, the error in the range estimation will increase, thereby, increasing the RMSE values as depicted in the figure 5.1.

Looking at the much smoother waveform returned from the High Resolution SAR mission (figure 5.2 (c)), the increased number of measurements due to the interleaved open burst mode of Sentinel-6aHR mission has resulted in less noisy and less peaky waveform. As a result, a higher threshold value of 80% for the Improved Threshold Retracker provides the best estimation of the range which reduces in accuracy if the threshold decreases.

So from observing the above waveforms, the result for the optimum thresholds for Lake Erie are:

Table 5.1: Optimum threshold values and number of points for Lake Erie

Mission	Optimum threshold	Number of Data Points
Jason-3	14%	54
Sentinel-6aHR	80%	63
Sentinel-6aLR	43%	62

Based on the above derived thresholds, the water level time series for Lake Erie is generated in the overlapping period of operation for all six missions (Jason-3, Jason-3 retracked, Sentinel-6aLR, Sentinel-6aLR retracked, Sentinel-6aHR, Sentinel-6aHR retracked) along with the in-situ data.

CHAPTER 5: EXPERIMENTS AND RESULTS

For the outlier rejection algorithm for determination of the time series, as specified in the section 4.3, following upper and lower limits were used:

Number of minimum data points (N_{min}) = 30

Minimum standard deviation ($h_{std,min}$) = 0.5m

Tolerance ($r_{threshold}$) = 0.5m

As it can be noticed, the limits for the outlier rejection for generation of time series are different to that of limits specified during evaluation of the optimum threshold. The reason is that the objective of the RMSE, R2 and offset plots are to analyze the behavior of the function with increasing thresholds. So for this reason, through experimentation, it could be understood that if the tolerance is smaller, many “good” values can be rejected which could lead in a higher RMSE and less correlation value. But due to this, the range of analysis of their behavior also increase (30cm to 3cm RMSE for SAR mission), which gives a nice overall idea for of their variation with increasing threshold. If the same tolerance is used for both optimum threshold and time series generation, the performance parameters improve for tolerance of 50cm but the range of analysis of RMSE reduces within 1cm which results in somewhat noisier plot making it difficult to analyze. As a result, one may notice a lower correlation and a higher RMSE values in the Figure 5.1 as compared to the values in Table 5.2 for all the missions. This change in tolerance limits have been done for all Great Lakes in this thesis.

So, using the outlier rejection for time series determination, the following water level time series for Lake Erie were obtained in the overlapping period of operation using the thresholds as mentioned in the table 5.1.

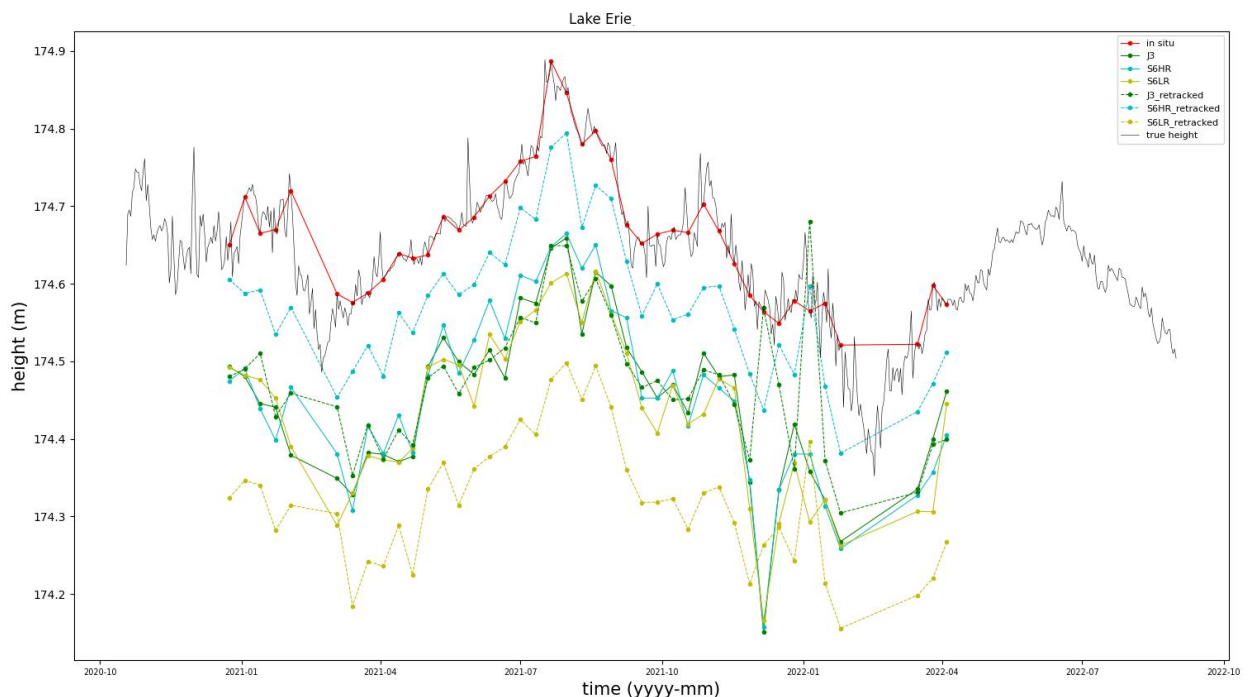


Figure 5.3: Water level time series for Lake Erie in the overlapping period of operation

Based on the water levels derived above, the following performance parameters were calculated:

Table 5.2: Performance analysis of Lake Erie

Mission	# data pts	corr coeff	RMSE (m)	R2	offset in situ (m)
Jason-3	44	86%	0.054	73.9%	-0.19
Sentinel-6a HR	44	90%	0.062	81%	-0.21
Sentinel-6a LR	44	87%	0.045	75.9%	-0.22
Jason-3 retracked	44	70%	0.079	50%	-0.19
Sentinel-6a HR retracked	44	92.5%	0.034	85%	-0.12
Sentinel-6a LR retracked	44	87.2%	0.062	76%	-0.34

From the table above, it can be observed that with both the on-board retracker and the use of Improved Threshold Retracker, the results show somewhat similar results. The RMSE values lie in the range of 3 to 8cm and the correlation coefficient stays above 85% except for Jason-3 retracked mission. This could be due to the availability of lower number of data points for the mission as correlation improves with more number of samples and in case of altimetry data it increases if the seasonal variation is included too. The absolute offset of the height values with respect to the insitu data remains in the range of 19 to 34cm. Since Lake Erie is big enough for the waveforms to depict an “ocean-like” behavior, the accurate assessment of advantages of the Sentinel-6a HR mission cannot be conclusively done. However, one may notice the slight reduction in quality when using the Improved threshold retracker on Lake Erie. To get a deeper idea on this hypothesis, we need to have a look at the other lakes as well.

5.2. Lake Michigan

The satellite data for Lake Michigan was acquired using the track ‘041’ in the latitude range of 42.4 to 42.6 degree north to obtain the water level time series for all hundred thresholds. The RMSE, R₂, offset with in-situ data and the number of data points have been plotted below.

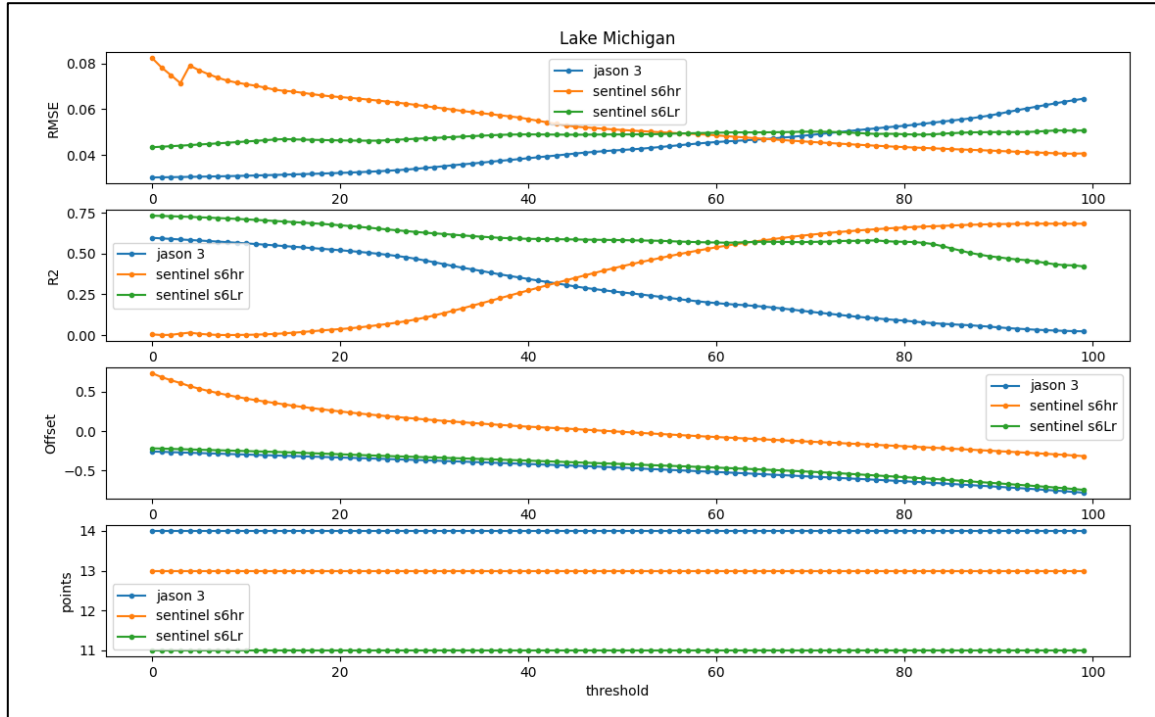


Figure 5.4: Plots for variation in RMSE, R₂, offset and number of points for Lake Michigan

For the outlier rejection algorithm for determination of the optimum threshold, as specified in the section 4.3, following upper and lower limits were used:

Number of minimum data points (N_{min}) = 30

Minimum standard deviation ($h_{std,min}$) = 0.05m

Tolerance ($r_{threshold}$) = 0.05m

Similar to Lake Erie, Lake Michigan also depicts similar behaviour of variation in the aforementioned parameters. For the high resolution SAR mission, the RMSE value reduces smoothly from 8cm to 4cm with a slight noise around the threshold of 5%. This gives an optimum threshold of 88% for the Sentinel-6aHR mission for Lake Michigan. For the LRM missions, similarly the trend is opposite with increasing RMSE from 4.2 cm to 4.4 cm in Sentinel-6aLR and 0.5cm to 6cm for Jason-3. Based on the trend, the optimum threshold for both the LRM missions seem to be around 10%. To understand this behavior, one needs to have a look at the waveforms returned from Lake Michigan. The returned waveforms for both Sentinel-6LR and Jason-3 are for the threshold of 10% and on the other for Sentinel-6HR it for 88%.

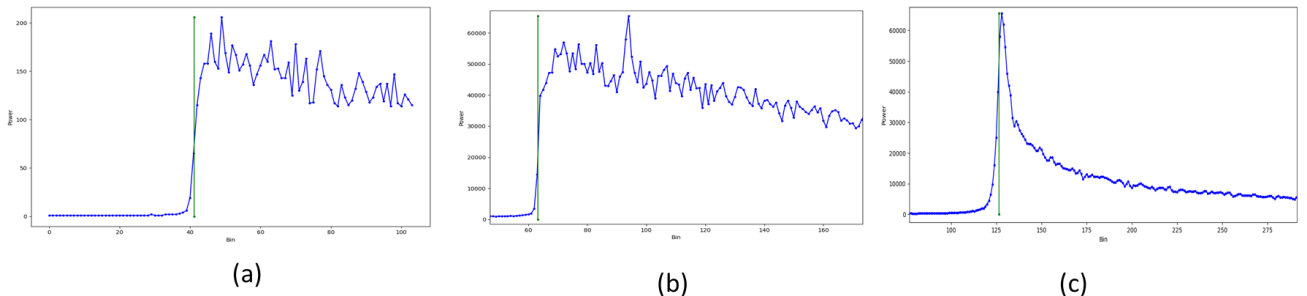


Figure 5.5: Return waveforms for Lake Michigan and the position of the retracking gate. (a) Jason-3 mission with threshold of 10%, (b) Sentinel-6aLR mission with threshold of 10%, (c) Sentinel-6aHR mission with threshold of 88%

As can be observed from Figure 5.5 above, Lake Michigan also depict similar “ocean-like” behavior for all three missions. The noisy trailing edge is an indication of rough lake surfaces due to waves. One small difference can be noticed for Sentinel-6aLR waveform in Figure 5.5 (b) is a shorter leading edge as compared to that in lake Erie. Due to this and a noisier trailing edge, the retracking gate for lake Michigan has shifted to an earlier part of the threshold spectrum for retrieving the best range for Sentinel-6aLR mission. Jason-3 returned waveform looks similar to that of Lake Erie, therefore has the same optimum threshold. If the retracker gate shifts towards right, error in the range estimation would be observed and thus increase the RMSE values.

For Sentinel-6aHR mission, the waveform is much smoother to that of lake Erie, as a result the retracking gate has shifted way more towards a higher part of the spectrum, giving the best threshold around 88%.

So from observing the above waveforms, the result for the optimum thresholds for Lake Michigan are:

Table 5.3: Optimum threshold values and number of points for Lake Michigan

Mission	Optimum threshold	Number of Data Points
Jason-3	10	14
Sentinel-6aHR	88	13
Sentinel-6aLR	10	11

Based on the above derived thresholds, the water level time series for Lake Michigan is generated in the overlapping period of operation for all six missions (Jason-3, Jason-3 retracked, Sentinel-6aLR, Sentinel-6aLR retracked, Sentinel-6aHR, Sentinel-6aHR retracked) along with the in-situ data.

For the outlier rejection algorithm for determination of the time series, as specified in the section 4.3, following upper and lower limits were used:

Number of minimum data points (N_{min}) = 30

Minimum standard deviation ($h_{std,min}$) = 0.5m

Tolerance ($r_{threshold}$) = 0.5m

So, using the outlier rejection for time series determination, the following water level time series for Lake Michigan were obtained in the overlapping period of operation using the thresholds as mentioned in the table 5.3.

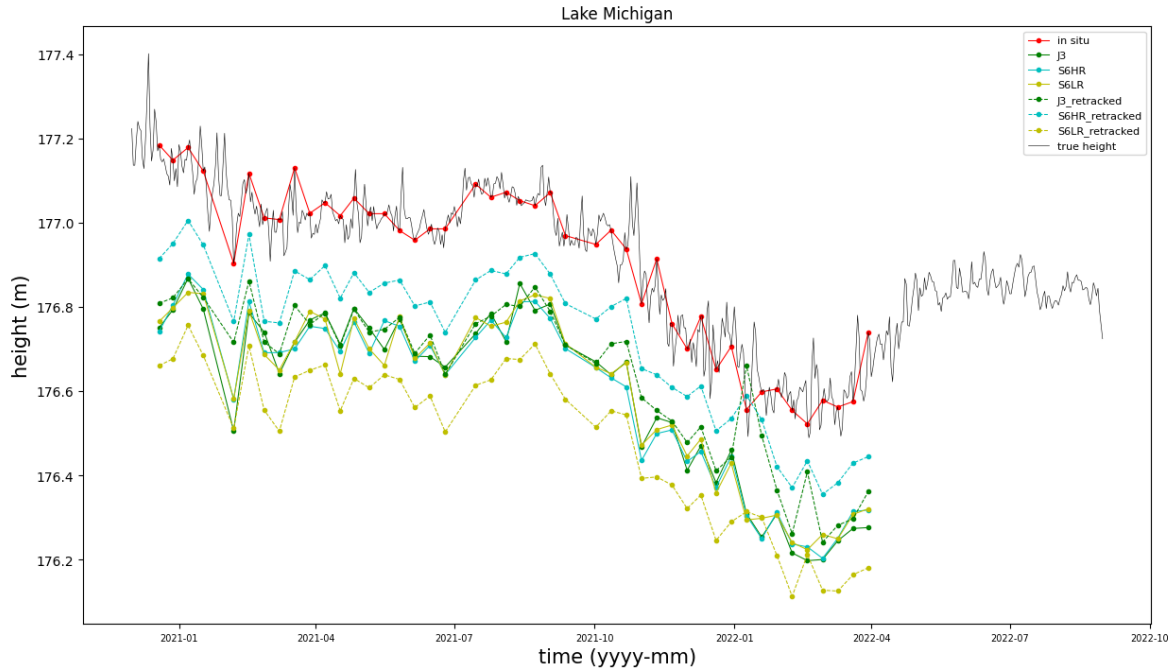


Figure 5.6: Water level time series for Lake Michigan in the overlapping period of operation

Based on the water levels derived above, the following performance parameters were calculated:

Table 5.4: Performance analysis of Lake Michigan

satellite	# data pts	corr coeff	RMSE (m)	R2	offset in situ (m)
Jason-3	48	96%	0.052	93%	-0.45
Sentinel-6a HR	48	96%	0.049	93.7%	-0.44
Sentinel-6a LR	48	92%	0.044	95%	-0.43
Jason-3 retracked	48	84%	0.077	84%	-0.29
Sentinel-6a HR retracked	48	97%	0.057	91%	-0.18
Sentinel-6a LR retracked	48	95%	0.059	91%	-0.38

By analyzing the performance parameters for Lake Michigan, it can be seen that all missions, both retracked with on-board retracker and retracked with Improved Threshold retracker show great results over the larger lakes. The RMSE varies in the range of 4 to 8cm and the correlation for all missions, except Jason-3 retracked stay above 90%. For Jason-3 retracked, similar to Lake Erie, the correlation coefficient is slightly less which is due to a lower number of data points and not inclusion of the seasonal variation through-out its period of operations. Alternatively, in case of Jason-3 which is not retracked using Improved Threshold Retracker, the correlation is quite good. This could be due to the reason that the on-board retracker is more compatible with “ocean-like” waveforms which extract range values based on the ideal Brown model. Again, since Lake Michigan is big enough for the waveforms to depict an “ocean-like” behavior, the accurate assessment of advantages of the Sentinel-6a HR mission cannot be conclusively done. Again just like in Lake Erie, although the difference in RMSE is small, untracked data has a slightly better performance than the retracked data.

5.3. Lake Ontario

The satellite data for Lake Ontario was acquired using the track '015 in the latitude range of 43.4 to 43.6 degree north to obtain the water level time series for all hundred thresholds. The RMSE, R₂, offset with in-situ data and the number of data points have been plotted below.

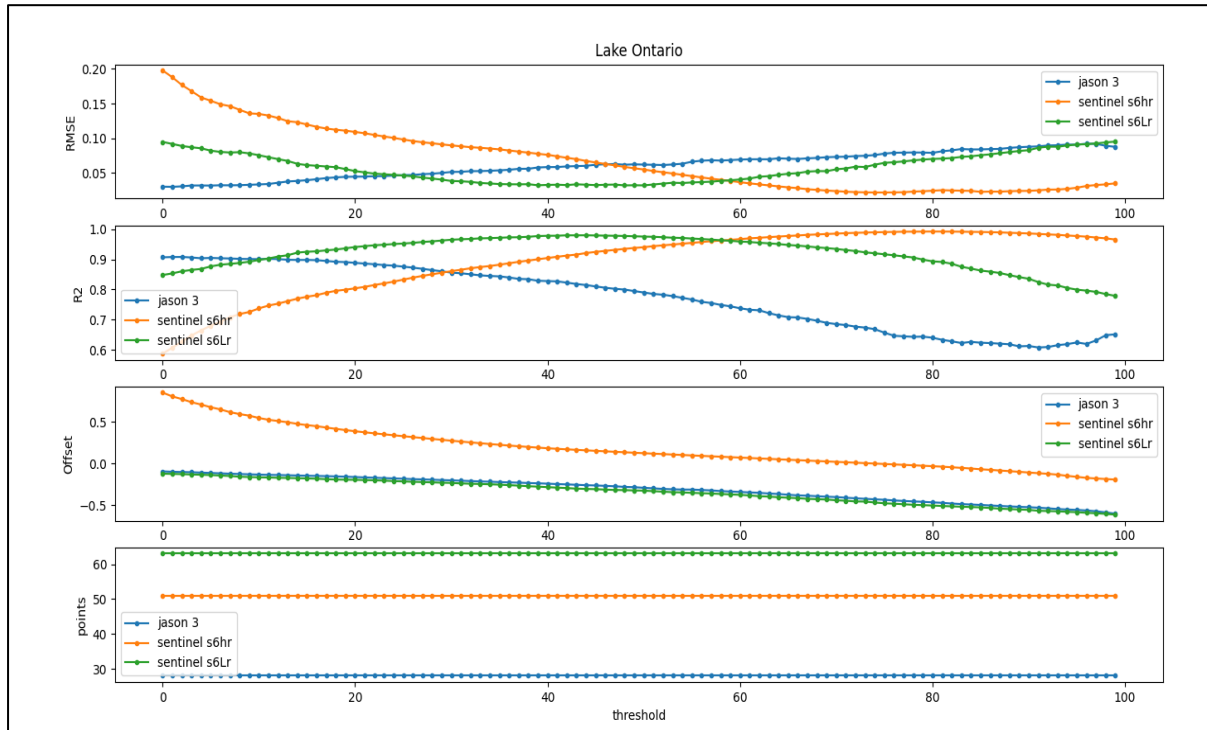


Figure 5.7: Plots for variation in RMSE, R₂, offset and number of points for Lake Ontario

For the outlier rejection algorithm for determination of the optimum threshold, as specified in the section 4.3, following upper and lower limits were used:

Number of minimum data points (N_{min}) = 30

Minimum standard deviation ($h_{std,min}$) = 0.05m

Tolerance ($r_{threshold}$) = 0.05m

As expected, Lake Ontario is one of the five Great Lakes and depicts a similar behavior in terms of the variation in RMSE and correlation as compared to the Lake Erie and Lake Michigan described above. The RMSE decreases from 20 cm to 2 cm and then increases slightly to 3cm when the high resolution SAR mission is considered. On the other hand, RMSE for Jason-3 increases from 2cm to 10cm with the minimum value lying in the earlier part of the threshold spectrum. For Sentinel-6aLR, a slight drop in RMSE is observed in the middle part of threshold range giving the minimum value of 4.5 cm around the threshold of 45%. Lake Ontario shows very similar behavior and optimum threshold values as compared to Lake Erie. Geographically, both lakes are neighbouring and have almost same size with Lake Erie being slightly larger in surface area as lake Ontario. This would become more clear after analysing the returned waveforms from Lake Ontario.

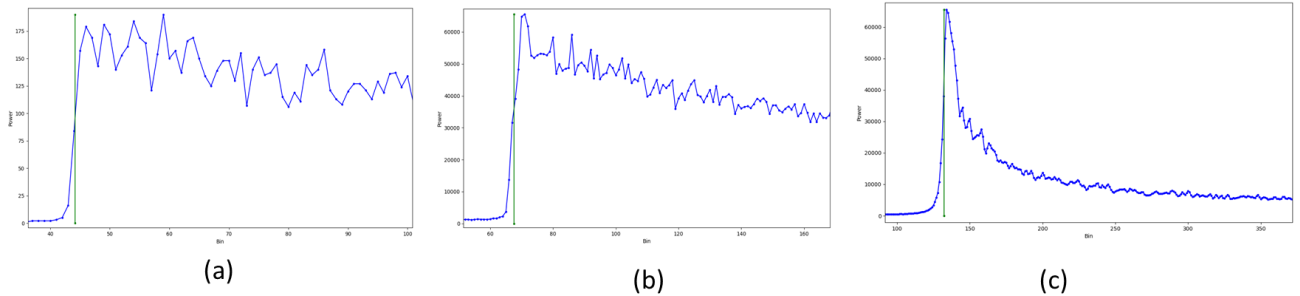


Figure 5.8: Return waveforms for Lake Ontario and the position of the retracking gate. (a) Jason-3 mission with threshold of 10%, (b) Sentinel-6aLR mission with threshold of 45%, (c) Sentinel-6aHR mission with threshold of 79%

As described in the above waveforms, all three missions depict an “ocean-like” behavior with Sentinel-6aHR showing a smooth trailing edge with reduced errors. For Sentinel-6a LR, the leading edge of the waveform is not as short as for Lake Michigan and returns somewhat similar waveform to that of Lake Erie and consequently, the retracking gate lies in the middle part of the threshold spectrum. This gives an interesting idea on the characteristic of the returned waveform based on the size, location and the characteristics of the lake.

Another interesting thing that can be noticed in the waveform for Sentinel-6aLR is that the leading edge is not exactly straight. Due to the windy atmosphere over the lake, the waves occur on the water surface which results in the change of slope of the leading edge. It has a slight change in slope in the middle and because of that the retracker could mark two leading edges while forming subwaveforms. For this, retraker needs to select just one overall leading edge based on the available waveform to retrieve the return signal time which is facilitated through the optimum selection of the threshold. A variation in the threshold either towards left or right will result in the retracker selecting either one of the leading edges resulting in an erroneous measurements. This is reflected perfectly in the decreasing and increasing nature of the Sentinel-6a mission along the threshold in the Figure 5.7, yeilding a perfect threshold at 45%.

So unlike Lake Erie, Lake Ontario has an optimum threshold in middle part of the spectrum because of the variation in the slope of the leading edge. In case of Lake Erie, the leading edge is longer thereby having the retracking bin positioned at the mid point of the leading edge at a threshold of 43%. Therefore, the earlier hypothesis of similarity in the size of lake is not correct as both lakes are large enough to have enough measurements in nadir direction for both LRM and SAR missions.

For the higher resolution Sentinel-6 mission, due to multiple looks by the instrument and lower along track resolution, the noise is reduced thereby resulting in a smooth leading edge. After applying retracking, one observe a smooth reduction in the RMSE values along the thresholds as depicted in Figure 5.7.

So from observing the above waveforms, the result for the optimum thresholds for Lake Ontario are:

Table 5.5: Optimum threshold values and number of points for Lake Ontario

Mission	Optimum threshold	Number of Data Points
Jason-3	10	25
Sentinel-6aHR	79	50
Sentinel-6aLR	45	64

CHAPTER 5: EXPERIMENTS AND RESULTS

Based on the above derived thresholds, the water level time series for Lake Ontario is generated in the overlapping period of operation for all six missions (Jason-3, Jason-3 retracked, Sentinel-6aLR, Sentinel-6LR retracked, Sentinel-6HR, Sentinel-6aHR retracked) along with the in-situ data.

For the outlier rejection algorithm for determination of the time series, as specified in the section 4.3, following upper and lower limits were used:

Number of minimum data points (N_{min}) = 30

Minimum standard deviation ($h_{std,min}$) = 0.5m

Tolerance ($r_{threshold}$) = 0.5m

So, using the outlier rejection for time series determination, the following water level time series for Lake Ontario were obtained in the overlapping period of operation using the thresholds as mentioned in the table 5.5.

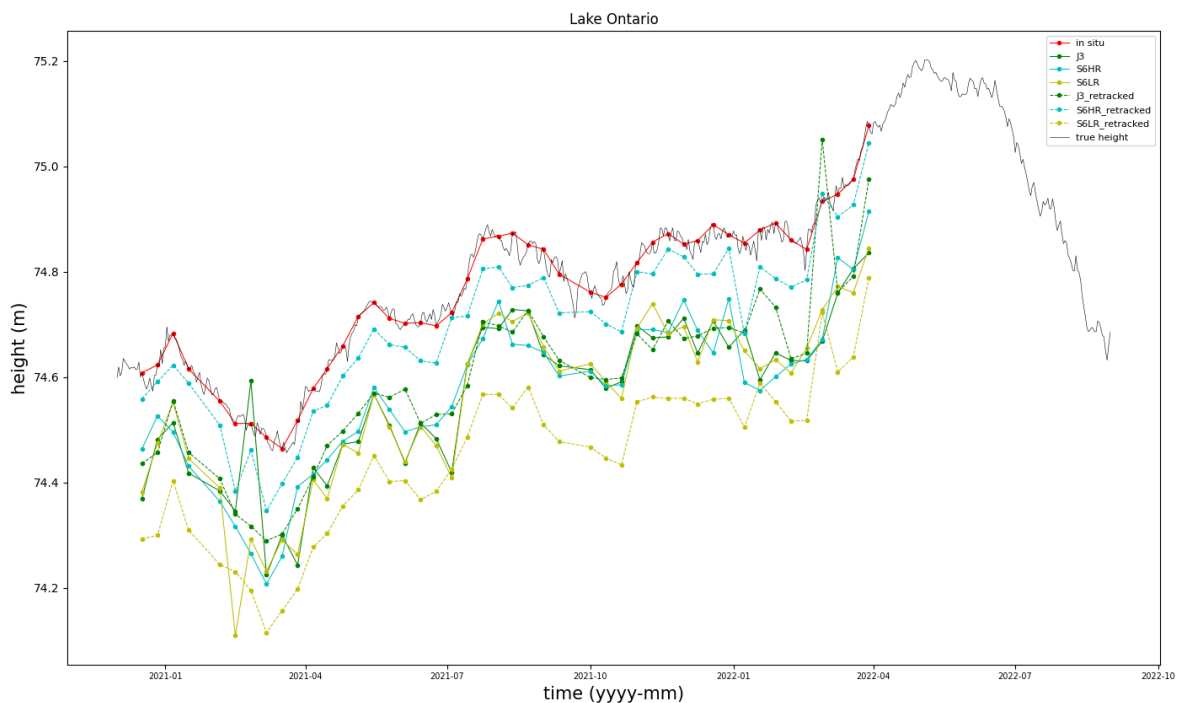


Figure 5.9: Water level time series for Lake Ontario in the overlapping period of operation

Based on the water levels derived above, the following performance parameters were calculated:

CHAPTER 5: EXPERIMENTS AND RESULTS

Table 5.6: Performance analysis of Lake Ontario

Mission	# data pts	corr coeff	RMSE (m)	R2	offset in situ (m)
Jason-3	46	95%	0.05	91%	-0.17
Sentinel-6a HR	46	94%	0.05	88%	-0.2
Sentinel-6a LR	46	94%	0.06	89%	-0.17
Jason-3 retracked	46	95%	0.052	91%	-0.13
Sentinel-6a HR retracked	46	97%	0.033	95%	-0.03
Sentinel-6a LR retracked	46	98%	0.0259	97%	-0.3

Looking at the values of the performance parameters above, it can be seen that all six missions perform very well over the common period of operation. The RMSE value lies in the range of 2 to 6cm and the correlation is above 94% in all cases. Unlike, for Lake Michigan and Lake Erie, in this case, a good correlation is observed for Jason-3 retracked as well. The absolute value of offsets from in-situ data lie in the range of 3 to 30cm. Again, since the lake is very large in size, this analysis does not conclusively assess the advantages of Sentinel-6aHR mission over the classic LRM missions.

5.4. Lake Huron

For Lake Huron, the ground track of ‘117’ was selected in the latitude range of 44.9 to 45.1 degree north to obtain the water level time series for all hundred thresholds. The RMSE, R2, offset with in-situ data and the number of data points have been plotted below.

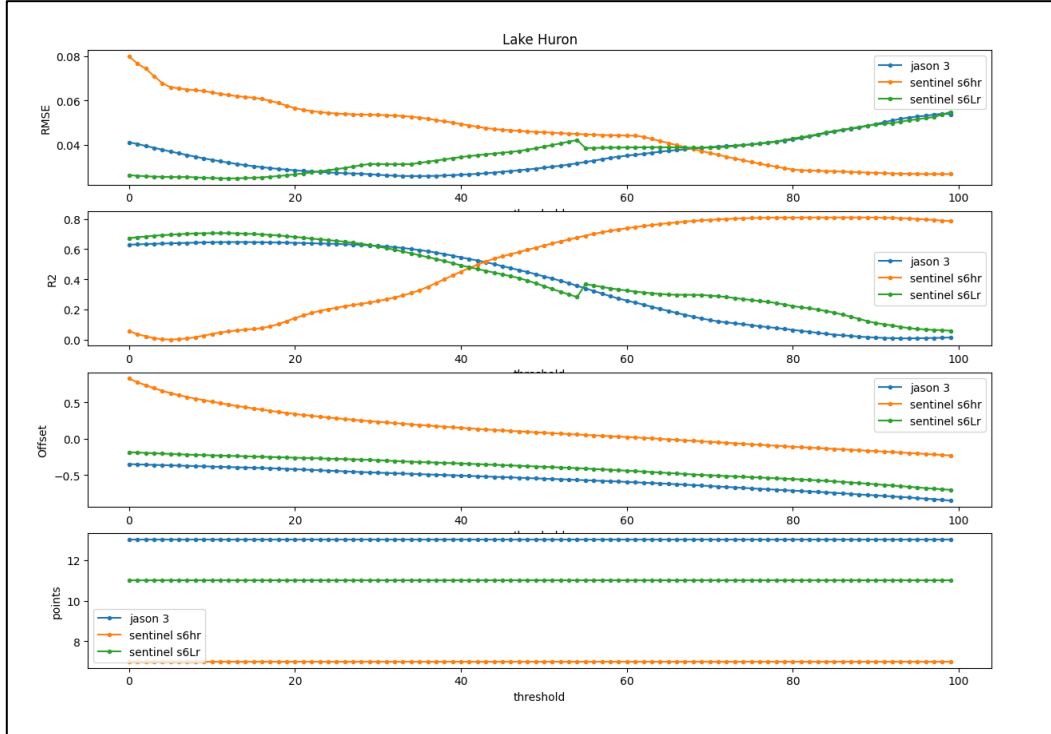


Figure 5.10: Plots for variation in RMSE, R2, offset and number of points for Lake Huron

For the outlier rejection algorithm for determination of the optimum threshold, as specified in the section 4.3, following upper and lower limits were used:

Number of minimum data points (N_{min}) = 30

Minimum standard deviation ($h_{std,min}$) = 0.05m

Tolerance ($r_{threshold}$) = 0.05m

Lake Huron is the third largest Lake of the five Great Lakes in America. As expected from previous cases, the Lake Huron shows similar behavior in the variation of the RMSE and correlation values. The RMSE for the Sentinel-6aHR mission reduces from 8cm to 1cm with minimum value lying in the later part of the threshold spectrum. And similar to Lake Michigan, the Sentinel-6aLR mission increases from 1cm to 5cm with increasing threshold with minimum value lying in the earlier part of the spectrum. However, in this case Jason-3 mission behaves in a slightly different way as compared to the earlier cases. The flow of RMSE for Jason-3 reduces to 1cm around the threshold of 25%. This threshold is slightly bigger for Jason-3 as compared to the previous cases where it was in much earlier part of the threshold spectrum. The reason behind this can be visualised by analysing the returned waveforms of the signals for all three missions.

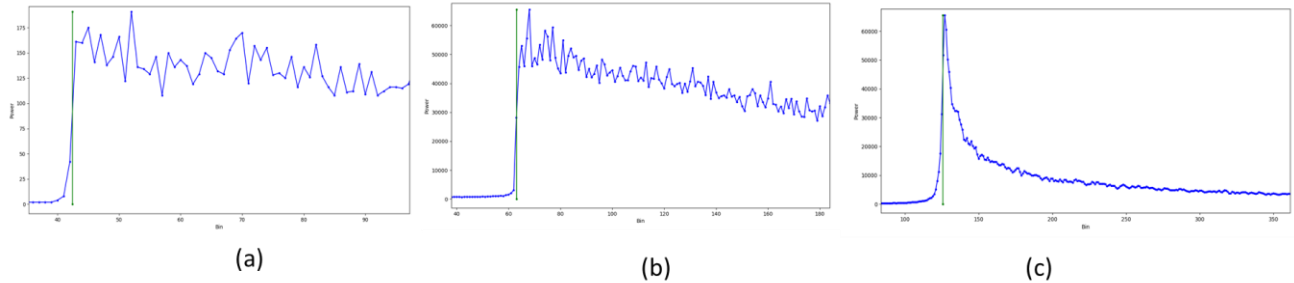


Figure 5.11: Return waveforms for Lake Huron and the position of the retracking gate. (a) Jason-3 mission with threshold of 25%, (b) Sentinel-6aLR mission with threshold of 15%, (c) Sentinel-6aHR mission with threshold of 83%

For the Sentinel-6aLR waveform, the leading edge is shorter in size just as in case of Lake Michigan. This results in the positioning of the retracking gate in the earlier part of the threshold spectrum just like in case of Lake Michigan. Sentinel-6aHR as usual displays a very smooth waveform with reduced noise and the retracking gate positioned at a higher threshold. However, the case of Jason-3 is a little different for this lake. Just like described for Lake Ontario for the mission Sentinel-6aLR, in this case Jason-3 has a slight change in slope in its leading edge which is located in the earlier bins. This explains the decreasing increasing nature of the RMSE value for Jason-3 and since the slope change occurs in smaller bins, the optimum threshold lies in the early to middle part of the threshold spectrum giving the optimum value as 25%.

So from observing the above waveforms, the result for the optimum thresholds for Lake Huron are:

Table 5.7: Optimum threshold values and number of points for Lake Huron

Mission	Optimum threshold	Number of Data Points
Jason-3	25	13
Sentinel-6aHR	83	7
Sentinel-6aLR	15	11

Based on the above derived thresholds, the water level time series for Lake Huron is generated in the overlapping period of operation for all six missions (Jason-3, Jason-3 retracked, Sentinel-6aLR, Sentinel-6aLR retracked, Sentinel-6aHR, Sentinel-6aHR retracked) along with the in-situ data.

For the outlier rejection algorithm for determination of the time series, as specified in the section 4.3, following upper and lower limits were used:

Number of minimum data points (N_{min}) = 30
 Minimum standard deviation ($h_{std,min}$) = 0.5m
 Tolerance ($r_{threshold}$) = 0.5m

So, using the outlier rejection for time series determination, the following water level time series for Lake Huron were obtained in the overlapping period of operation using the thresholds as mentioned in the table 5.7.

CHAPTER 5: EXPERIMENTS AND RESULTS

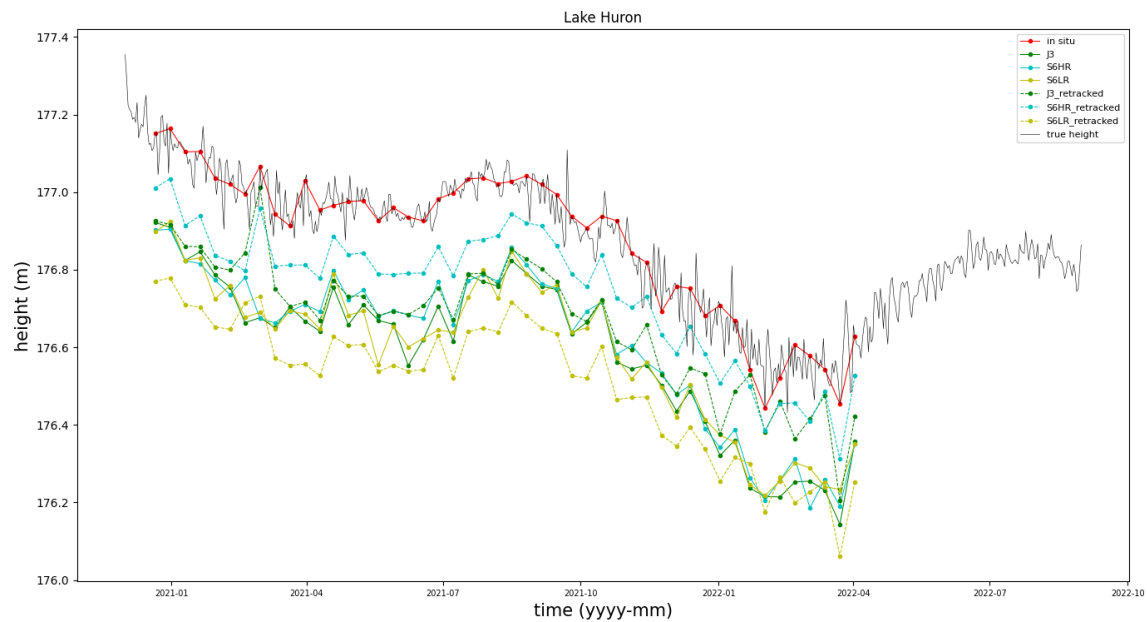


Figure 5.12: Water level time series for Lake Huron in the overlapping period of operation

Based on the water levels derived above, the following performance parameters were calculated:

Table 5.8: Performance analysis of Lake Huron

satellite	# data pts	corr coeff	RMSE (m)	R2	offset in situ (m)
Jason-3	48	97%	0.05	94%	-0.28
Sentinel-6a HR	48	97%	0.05	94%	-0.25
Sentinel-6a LR	48	96%	0.048	94%	-0.29
Jason-3 retracked	48	93%	0.074	87%	-0.38
Sentinel-6a HR retracked	48	97%	0.046	95%	-0.105
Sentinel-6a LR retracked	48	96%	0.054	93%	-0.35

From the table above, by analysing the performance parameters for Lake Huron, it can be seen that all six mission perform very well in the overlapping periods of operation. The RMSE values lie in the range of 4 to 8 cm and the correlation in all cases is above 90%. The absolute value of offsets with in-situ data lies in the range of 10 to 40 cm. Unlike, for Lake Michigan and Lake Erie, in this case, a good correlation is observed for Jason-3 retracked as well. Again, since the lake is very large in size, this analysis does not conclusively assess the advantages of Sentinel-6aHR mission over the classic LRM missions. In this case also, since the Improved Threshold retracker creates a multiple leading edge due to a slight change in slope, quality of the retracked data becomes a little less.

5.5. Lake Superior

Lake Superior is the largest fresh water lake in the world. To retrieve the satellite data from the OpenADB datasets for Lake Superior, the track number ‘143’ was used in the latitude range of 48 to 48.2 degrees north to obtain the water level time series for all hundred thresholds. The RMSE, R2, offset with in-situ data and the number of data points have been plotted below.

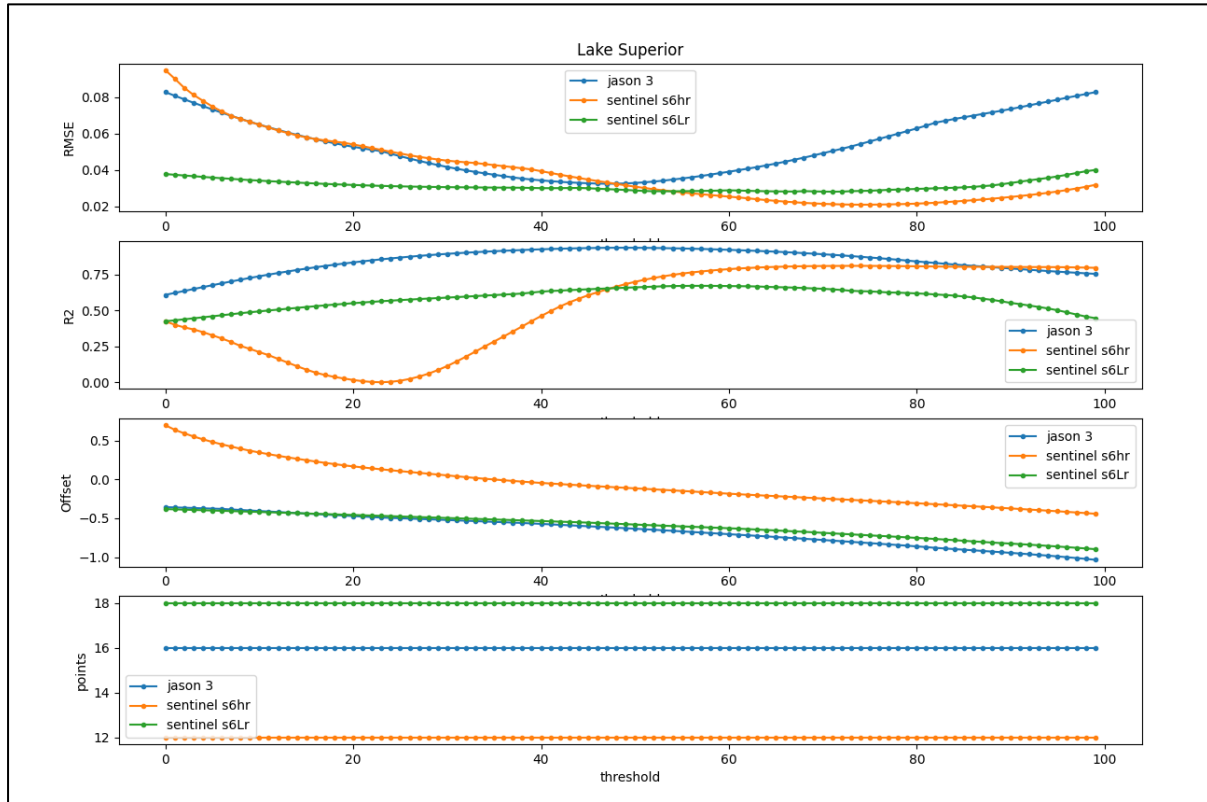


Figure 5.13: Plots for variation in RMSE, R2, offset and number of points for Lake Superior

For the outlier rejection algorithm for determination of the optimum threshold, as specified in the section 4.3, following upper and lower limits were used:

Number of minimum data points (N_{min}) = 30

Minimum standard deviation ($h_{std,min}$) = 0.05m

Tolerance ($r_{threshold}$) = 0.05m

For lake Superior, the trends in the variation of the RMSE and correlation values are similar to those in previous cases. The RMSE reduces gradually from 8.8cm to 2cm and then increases slightly with minimum values lying around the threshold of 83%. This could also mean a slight change in slope in the later bins in the leading edge of the waveform. Jason-3 shows similar behavior of decreasing and increasing nature of RMSE value varying between 4cm and 8cm. this could mean a slight change in slope in the leading edge of the waveform with location in the middle of the bins. Sentinel-6a LR mission seems somewhat constant with slight increasing nature along with the increasing thresholds. It is a little difficult analyse the minima for RMSE in this case, so we would rely on the threshold which give the maximum correlation. This value lies around the threshold of 55%.

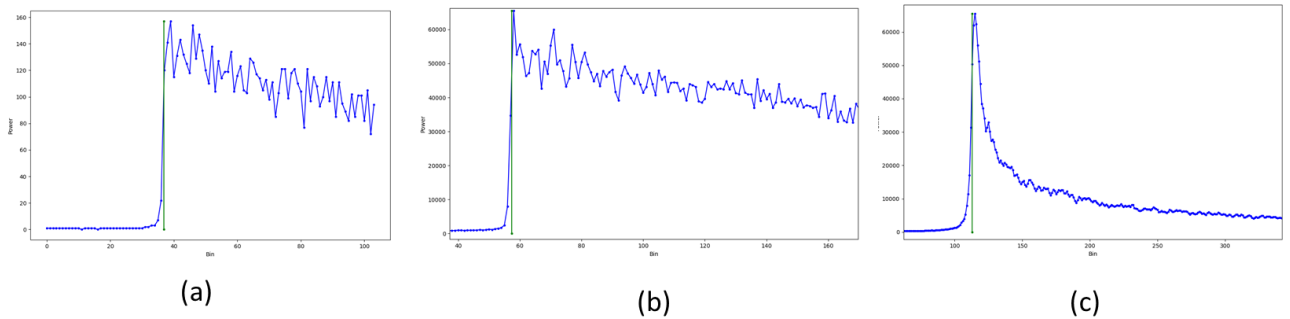


Figure 5.14: Return waveforms for Lake Superior and the position of the retracking gate. (a) Jason-3 mission with threshold of 45%, (b) Sentinel-6aLR mission with threshold of 55%, (c) Sentinel-6aHR mission with threshold of 83%

For Jason-3 waveform, there is a slight change in the slope observed in the leading edge due to a windy atmosphere of the lake. This results in multiple leading edge resulting in the decreasing increasing nature of the RMSE values along the thresholds as described in Figure 5.14. For the Sentinel-6aLR mission, the leading edge is longer and smoother resulting in the retracking bin being located around the middle point of the leading edge. This gives the optimum threshold value of 40% in the middle part of the spectrum. Sentinel-6HR as in earlier cases is very smooth and noise free and results in optimum threshold in the later part of the threshold spectrum.

So from observing the above waveforms, the result for the optimum thresholds for Lake Superior are:

Table 5.9: Optimum threshold values and number of points for Lake Superior

Mission	Optimum threshold	Number of Data Points
Jason-3	45	18
Sentinel-6aHR	83	12
Sentinel-6aLR	55	18

Based on the above derived thresholds, the water level time series for Lake Superior is generated in the overlapping period of operation for all six missions (Jason-3, Jason-3 retracked, Sentinel-6aLR, Sentinel-6LR retracked, Sentinel-6HR, Sentinel-6aHR retracked) along with the in-situ data.

For the outlier rejection algorithm for determination of the time series, as specified in the section 4.3, following upper and lower limits were used:

Number of minimum data points (N_{min}) = 30

Minimum standard deviation ($h_{std,min}$) = 0.5m

Tolerance ($r_{threshold}$) = 0.5m

So, using the outlier rejection for time series determination, the following water level time series for Lake Superior were obtained in the overlapping period of operation using the thresholds as mentioned in the table 5.9.

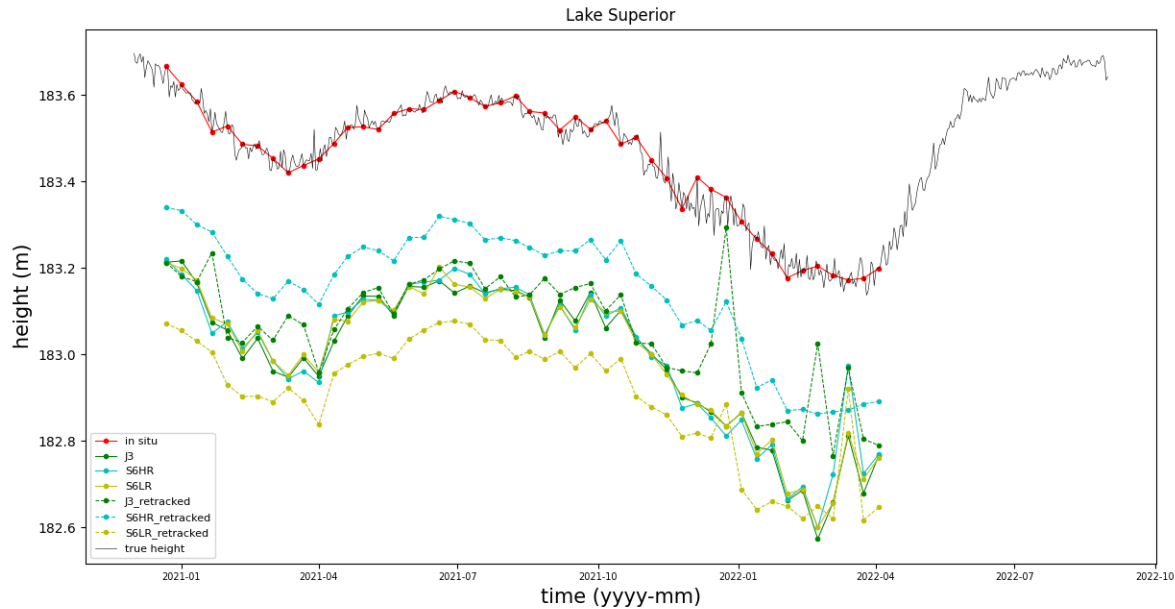


Figure 5.15: Water level time series for Lake Superior in the overlapping period of operation

Based on the water levels derived above, the following performance parameters were calculated:

Table 5.10: Performance analysis of Lake Superior

satellite	# data pts	corr coeff	RMSE (m)	R2	offset in situ (m)
Jason-3	45	96%	0.053	92%	-0.3
Sentinel-6a HR	45	96%	0.049	93%	-0.29
Sentinel-6a LR	45	97%	0.044	95%	-0.32
Jason-3 retracked	45	91%	0.078	84%	-0.38
Sentinel-6a HR retracked	45	95%	0.057	91%	-0.29
Sentinel-6a LR retracked	45	95%	0.059	91%	-0.54

So, just like the previous investigated larger lakes, Lake Superior shows great results for all six time series. The RMSE values lie in the range of 4 to 8cm and the correlation coefficient is greater than 90% in all cases. The absolute value of the offset from in-situ data remains in the range of 29 to 55 cm.

After investigating the water level time series over the Great Lakes, due to larger size of the lakes, both LRM and SAR mission performed quite well using both the on-board and the Improved Threshold Retracker. However, one might notice a very small decline in quality (by a few centimeters) when using the Improved Threshold retracker on Great Lakes. Since these lakes depict an “ocean-like” waveform, the on-board retracker works best for those as it ignores slight variations in the slope of the leading edge which the ITR does not and thus causing a small difference in RMSE.

However, this difference is very small to make such conclusion. For this, a more number of larger lakes must be investigated which is not the purpose of this thesis. The purpose of this thesis is to study the

difference in measurements from LRM and SAR data. So, for a conclusive analysis of the quality of the high resolution Sentinel-6a data, smaller lakes must be investigated.

5.6. Lake of Woods

Lake of Woods is the largest lake in North America after the five Great Lakes. The satellite data for this lake had been acquired using the tracking number '178' and the latitude range of 48.8 to 49.17 degrees north to obtain the water level time series for all hundred thresholds. The RMSE, R2, offset with in-situ data and the number of data points have been plotted below. The major problem for this lake is that freezes over winters resulting in multi peaked waveforms and corrupted the range estimation. So for proper analysis, only the values during the summer months are considered for evaluation of this particular lake.

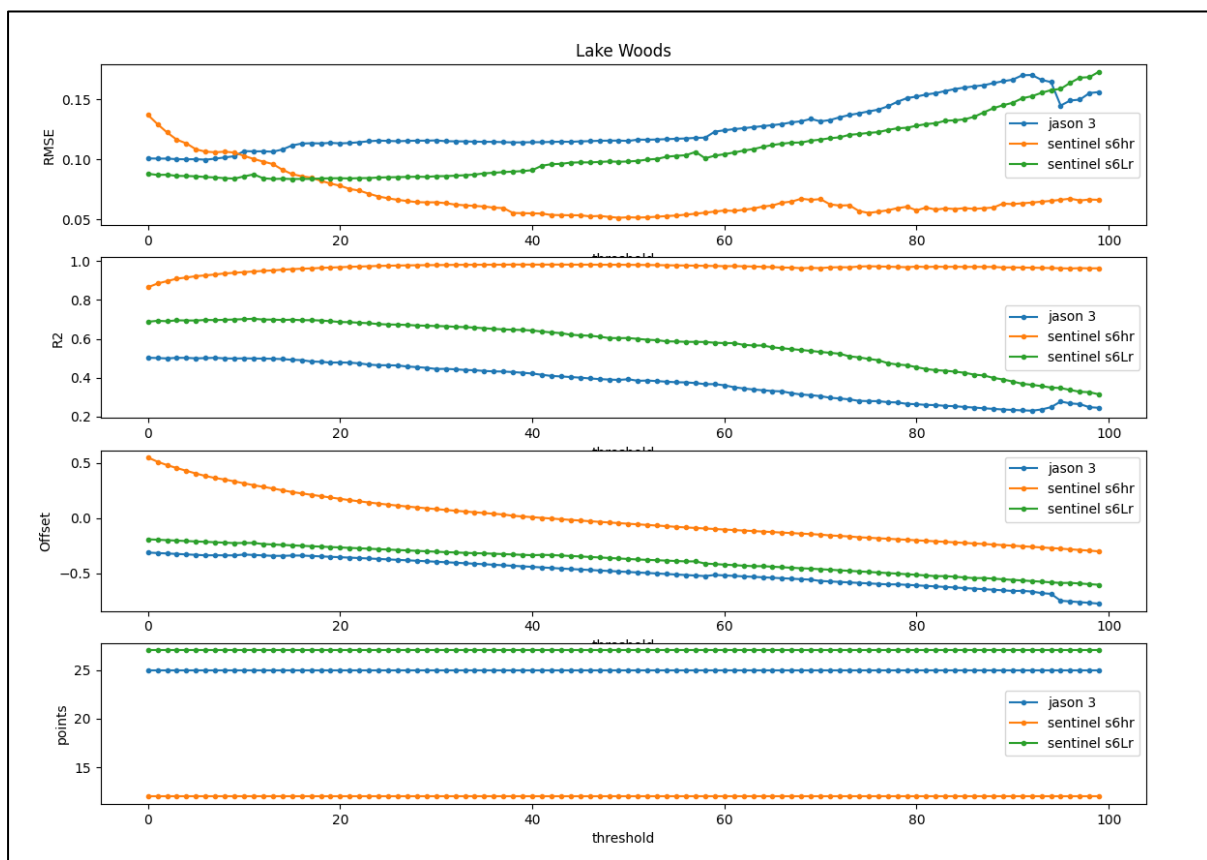


Figure 5.16: Plots for variation in RMSE, R2, offset and number of points for Lake Woods

Since it is a smaller lakes, the upper and lower limits for the outlier rejection algorithm were changed and the new values are:

Number of minimum data points (N_{min}) = 15

Minimum standard deviation ($h_{std,min}$) = 0.5m

Tolerance ($r_{threshold}$) = 0.5m

The period of operation considered is from March 2021 to October 2021 and March 2022 to September 2022 (only for the Sentinel-6aLR and Sentinel-6aHR missions as Jason-3 services were discontinued in April 2022).

CHAPTER 5: EXPERIMENTS AND RESULTS

Looking at the above Figure 5.16, apart from slight variations, the trend of movement of the RMSE and correlation value remains a little similar to that of the Great Lakes. However, there are certain differences which can be observed. For the high resolution SAR mission, the RMSE values vary from 13 cm to 5cm and then increase to 9cm. This could indicate the variation in the selection of the leading edge at a particular junction. For LRM missions of Jason-3 and Sentinel-6aLR, both missions show a similar trend of increasing RMSE values with threshold and minimum values lying in the early part of the threshold spectrum. This is an indication of shorter leading edges as detected by the Improved Threshold Retracker. Additionally, one can observe that the behavior for smaller lake has become a little noisier. To understand these trends in more depth, one needs to look at the waveforms returned from the lake surface.

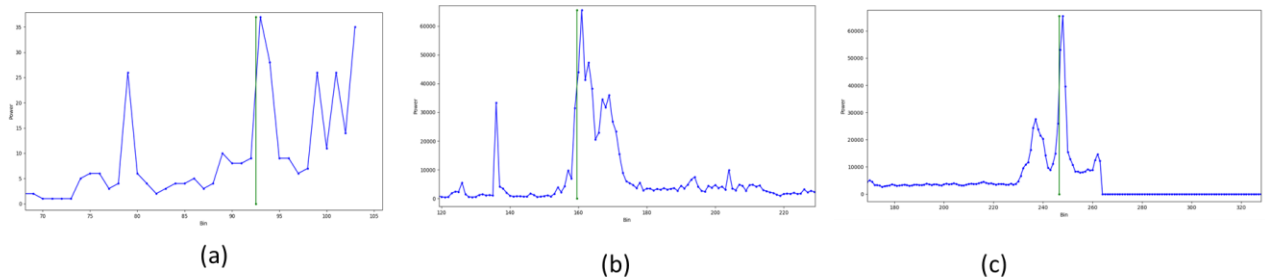


Figure 5.17: Return waveforms for Lake of Woods and the position of the retracking gate. (a) Jason-3 mission with threshold of 8%, (b) Sentinel-6aLR mission with threshold of 12%, (c) Sentinel-6aHR mission with threshold of 50%

Along the coastal lines, the waveforms were contaminated by land, so to understand their shape better, the waveform from the middle of the lake has been shown in the Figure 5.17. As expected, the returned waveforms from lake of woods are complex, peaky and very noisy. Although it can be observed that the noise level in the Sentinel-6aHR is comparatively less which helps to some extent determine the leading edge of the waveform. Due to multiple peaks around the selected leading edge in Figure 5.17 (c), the movement in Retracker bin in either left or right direction would result in increased errors in the range estimation. This explains the decreasing increasing behaviour of the RMSE values along the thresholds with minimum value occurring at the threshold of 50%. The presence of multiple peaks around the leading edge also describes the noise level observed in the RMSE plot. The LRM missions are much more complex when compared to the SAR mission because of lower along track resolution. The leading edge detected provides the middle point at a lower threshold value because of shorter lengths.

So from observing the above waveforms, the result for the optimum thresholds for Lake of Woods are:

Table 5.11: Optimum threshold values and number of points for Lake Woods

Mission	Optimum threshold	Number of Data Points
Jason-3	8	25
Sentinel-6aHR	50	12
Sentinel-6aLR	12	27

CHAPTER 5: EXPERIMENTS AND RESULTS

Based on the above derived thresholds, the water level time series for Lake Woods is generated in the overlapping period of operation for all six missions (Jason-3, Jason-3 retracked, Sentinel-6aLR, Sentinel-6LR retracked, Sentinel-6HR, Sentinel-6aHR retracked) along with the in-situ data.

For the outlier rejection algorithm for determination of the time series, as specified in the section 4.3, following upper and lower limits for the Sentinel-6aHR unretacked mission were used:

Number of minimum data points (N_{min}) = 15

Minimum standard deviation ($h_{std,min}$) = 0.75m

Tolerance ($r_{threshold}$) = 1m

For the other missions, the limits used were:

Number of minimum data points (N_{min}) = 15

Minimum standard deviation ($h_{std,min}$) = 0.5m

Tolerance ($r_{threshold}$) = 0.5m

So, using the outlier rejection for time series determination, the following water level time series for Lake of Woods were obtained in the overlapping period of operation using the thresholds as mentioned in the table 5.11.

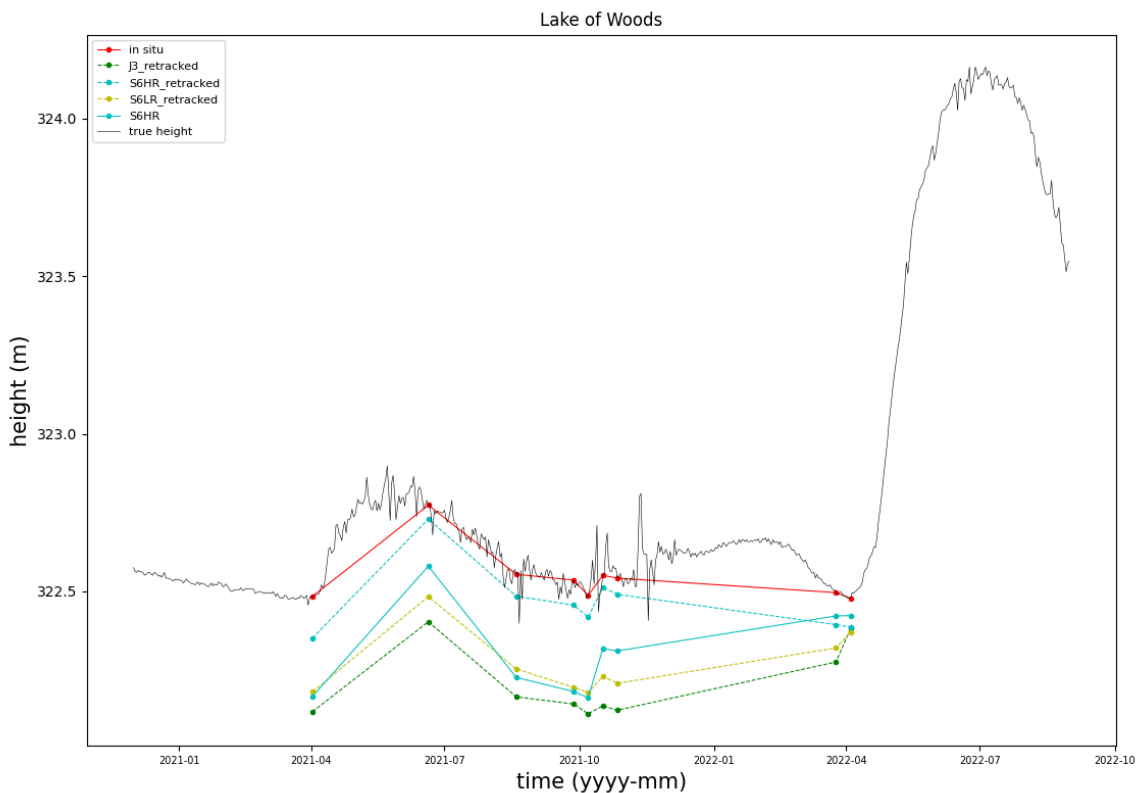


Figure 5.18: Water level time series for Lake Woods in the overlapping period of operation

CHAPTER 5: EXPERIMENTS AND RESULTS

As can be noticed from time series above, a data gap can be observed from 2021-11 to 2022-03 as these are the winter months and the height values will be corrupted due to ice sheet formation. Based on the water levels derived above in the common periods of operation, the following performance parameters were calculated:

Table 5.12: Performance analysis of Lake Woods

satellite	# data pts	corr coeff	RMSE (m)	R2	offset in situ (m)
Sentinel-6a HR	9	63%	0.104	40%	-0.224
Jason-3 retracked	9	47%	0.115	23%	-0.39
Sentinel-6a HR retracked	9	97%	0.028	95%	-0.08
Sentinel-6a LR retracked	9	63%	0.08	45%	-0.30

Since the periods of operation have been reduced in this as well only the dates when the data from all 4 missions along with the in-situ data is available have been used, as a result the number of data points are very less. This has impacted the correlation in the LRM missions as well as the Sentinel-6aHR retracked with on-board Retracker. However, the results provided by the Sentinel-6aHR mission retracked with the Improved Threshold Retracker at a threshold of 50% has provided great results of correlation of 97% and RMSE of 2.8 cm. However, the overall RMSE values for all missions lie in the range of 2cm to 11.5 cm which is still good given the smaller size of the lake.

5.7. Lake Winnebago

Out of all the lakes investigated till, Lake Winnebago is the largest lake which is completely situated within the state of Wisconsin in USA. The satellite data has been acquired using the track number ‘219’ and the latitude range of 43.97 to 44.1 degrees north to obtain the water level time series for all hundred thresholds. The RMSE, R2, offset with in-situ data and the number of data points have been plotted below. The major problem for this lake too is that freezes over winters resulting in multi peaked waveforms and corrupted the range estimation. So for proper analysis, only the values during the summer months are considered for evaluation of this particular lake.

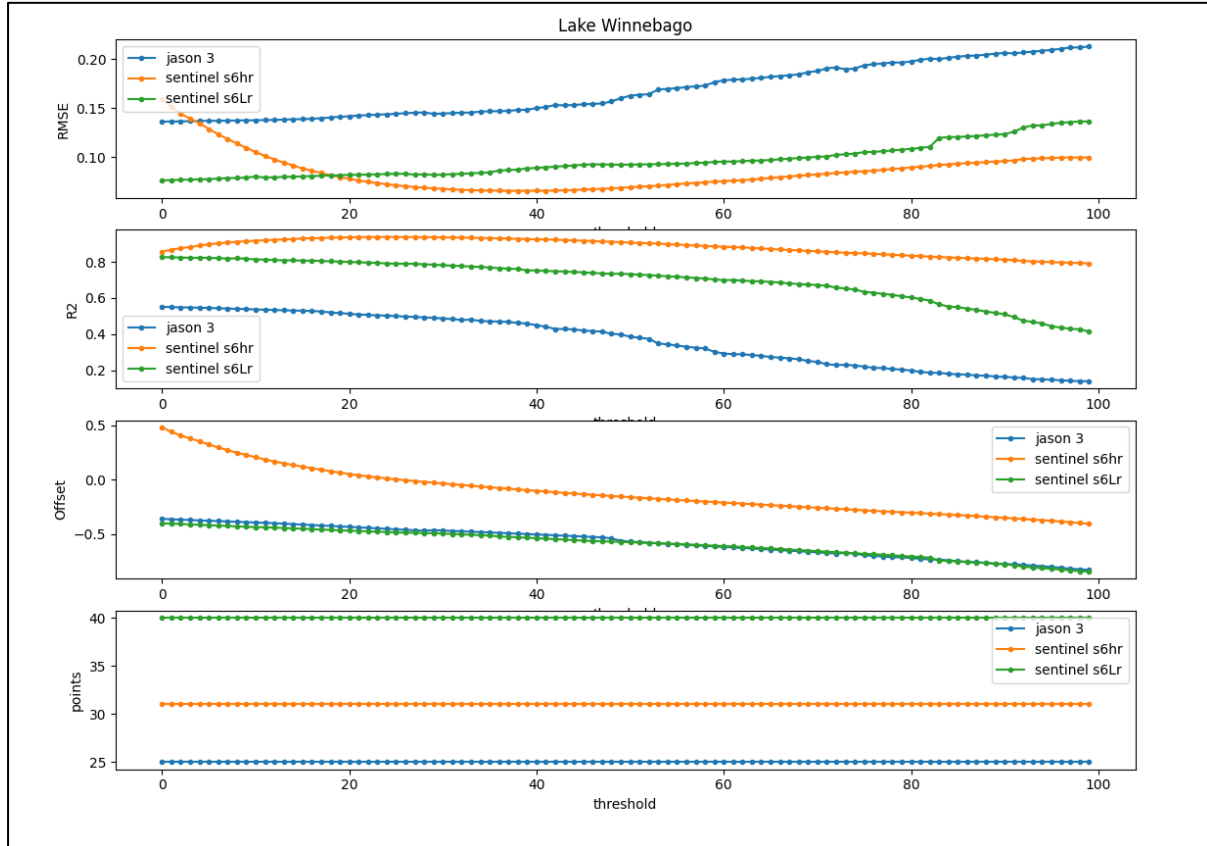


Figure 5.19: Plots for variation in RMSE, R2, offset and number of points for Lake Winnebago

Since it is a smaller lake, the upper and lower limits for the outlier rejection algorithm were changed and the new values are:

Number of minimum data points (N_{min}) = 15

Minimum standard deviation ($h_{std,min}$) = 0.5m

Tolerance ($r_{threshold}$) = 0.5m

The period of operation considered is from March 2021 to October 2021 and March 2022 to September 2022 (only for the Sentinel-6aLR and Sentinel-6aHR missions as Jason-3 services were discontinued in April 2022).

Looking at the above figure, a smoother variation in RMSE values can be observed with increasing thresholds as compared to the Lake of Woods although the overall trend remains similar to it. The RMSE values vary in a decreasing increasing mode with the minimum value lying around the threshold of 40% for the Sentinel-6aHR mission. This could be due to either presence of additional peaks around

the leading edge or more likely due the variation in the slope of the leading edge. On the other hand, the for the LRM missions, the RMSE values depict an increasing behavior with minimum value occurring in the earlier part of the threshold spectrum. The returned waveform could be slightly for these missions and the leading edge might be shorted in length. To understand this more details, one needs to check out the retracked waveforms for these missions.

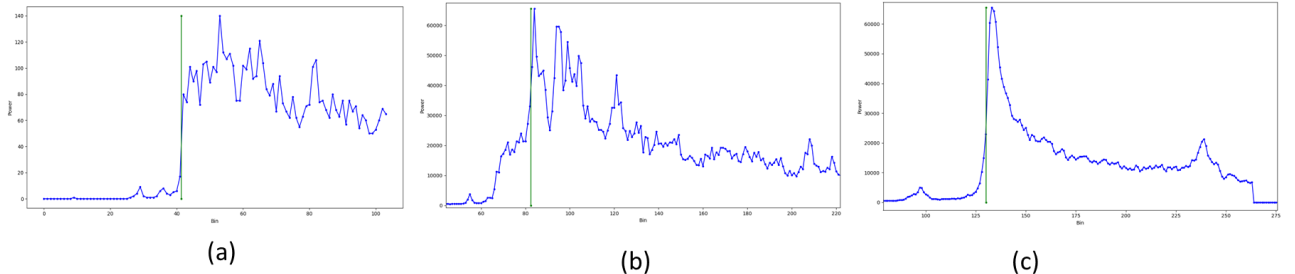


Figure 5.20: Return waveforms for Lake Winnebago and the position of the retracking gate. (a) Jason-3 mission with threshold of 15%, (b) Sentinel-6aLR mission with threshold of 10%, (c) Sentinel-6aHR mission with threshold of 40%

The waveforms for the Lake Winnebago depict “Quasi-Brown” waveform shape which is the typical “ocean-type” waveform with increased noise in the LRM mission. For the Sentinel-6aLR and Jason-3 mission, as predicted earlier, the leading edge as detected by the Improved Threshold Retracker is shorter in size and as a result provides a better two-way time measurement when the threshold values which are used are in the lower part of the threshold spectrum. And as can be observed from the Figure 5.19, with higher thresholds, the noise increases a bit. The high resolution SAR mission shows a much smoother waveform with reduced errors. However, when observed from Figure 5.20 (c), a small peak is present on the left side of the leading edge. This peak could be the reason for the decreasing increasing nature of the RMSE value with the increasing thresholds as shown in Figure 5.19.

So after observing the above waveforms, the result for the optimum thresholds for Lake Winnebago are:

Table 5.13: Optimum threshold values and number of points for Lake Winnebago

Mission	Optimum threshold	Number of Data Points
Jason-3	15	25
Sentinel-6aHR	40	31
Sentinel-6aLR	10	40

Based on the above derived thresholds, the water level time series for Lake Huron is generated in the overlapping period of operation for all six missions (Jason-3, Jason-3 retracked, Sentinel-6aLR, Sentinel-6aLR retracked, Sentinel-6HR, Sentinel-6aHR retracked) along with the in-situ data.

For the outlier rejection algorithm for determination of the time series for sentinel-6HR retracked with on-board retracker, as specified in the section 4.3, following upper and lower limits were used:

Number of minimum data points (N_{min}) = 15

Minimum standard deviation ($h_{std,min}$) = 0.75m

Tolerance ($r_{threshold}$) = 1m

CHAPTER 5: EXPERIMENTS AND RESULTS

And in case of getting the water time series for other missions retracked with the Improved Threshold Retracker, the following tolerance values:

Number of minimum data points (N_{min}) = 15

Minimum standard deviation ($h_{std,min}$) = 0.75m

Tolerance ($r_{threshold}$) = 0.5m

So, using the outlier rejection for time series determination, the following water level time series for Lake Winnebago were obtained in the overlapping period of operation using the thresholds as mentioned in the table 5.13.

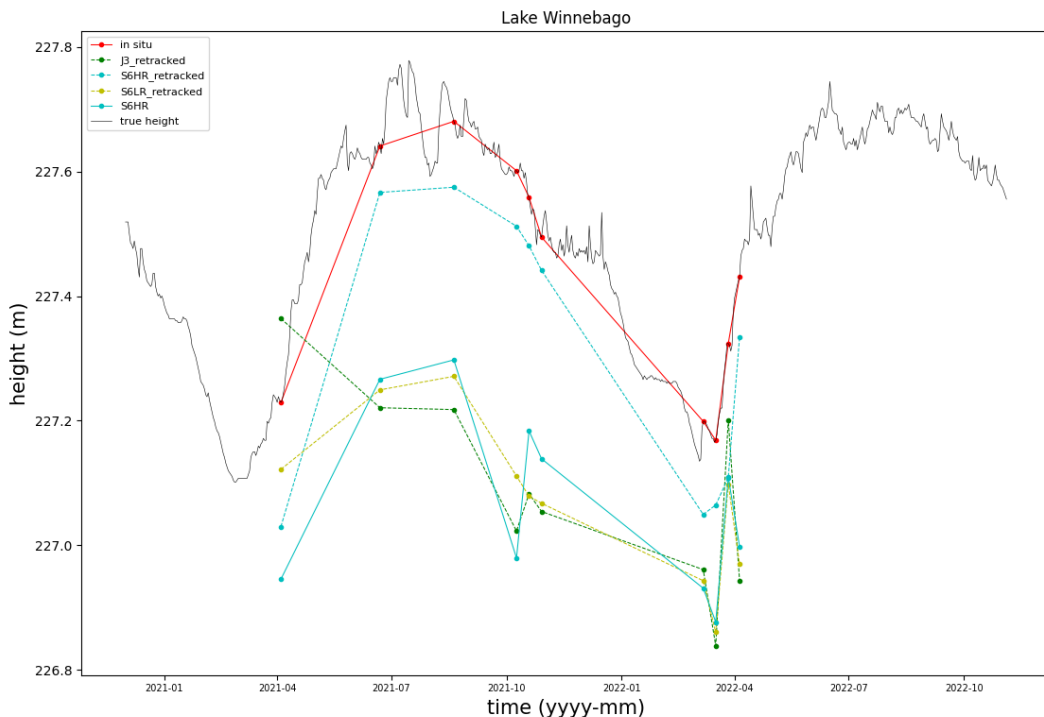


Figure 5.21: Water level time series for Lake Winnebago in the overlapping period of operation

Again, as can be observed from the time series above, a data gap can be observed from 2021-11 to 2022-03 as these are the winter months and they height values will be corrupted due to ice sheet formation. Based on the water levels derived above in the common periods of operation, the following performance parameters were calculated:

CHAPTER 5: EXPERIMENTS AND RESULTS

Table 5.14: Performance analysis of Lake Winnebago

satellite	# data pts	corr coeff	RMSE (m)	R2	offset with situ (m)
Sentinel-6a HR	10	80%	0.11	65%	-0.40
Jason-3 retracked	10	26%	0.20	7%	-0.39
Sentinel-6a HR retracked	10	98%	0.06	96%	-0.07
Sentinel-6a LR retracked	10	75%	0.12	57%	-0.37

As observed from the waveforms, the missions depict a slightly noisier version of the “Qausi-Brown” waveform. Therefore, expectedly, the performance of the missions in check must be good. But due to the smaller size of the lake and lower along track resolution combined with the reduced number of data points, the LRM missions did not perform well with the maximum correlation by Sentinel-6aLR mission being 75%. However, the results provided by the Sentinel-6aHR mission retracked with the Improved Threshold Retracker at a threshold of 40% has provided great results of correlation of 98% and RMSE of 6 cm. Overall, the RMSE values for all missions lie in the range of 2cm to 11.5 cm which is still good given the smaller size of the lake.

5.8. Lake Richland Chambers

Moving south, the state of Texas has a large number of lakes and rivers, combined with an extensive network gauges provided by the Texas Water Development Board, analysing the altimetry data for these lakes became easier. Bigger advantage is that these lakes do not freeze during winters, therefore will allow monitoring over a larger period of time. The satellite data for Lake Richland Chambers have acquired using the track number '052' along the latitudes of 31.93 to 32 degrees north to obtain the water level time series for all hundred thresholds. The RMSE, R2, offset with in-situ data and the number of data points have been plotted below.

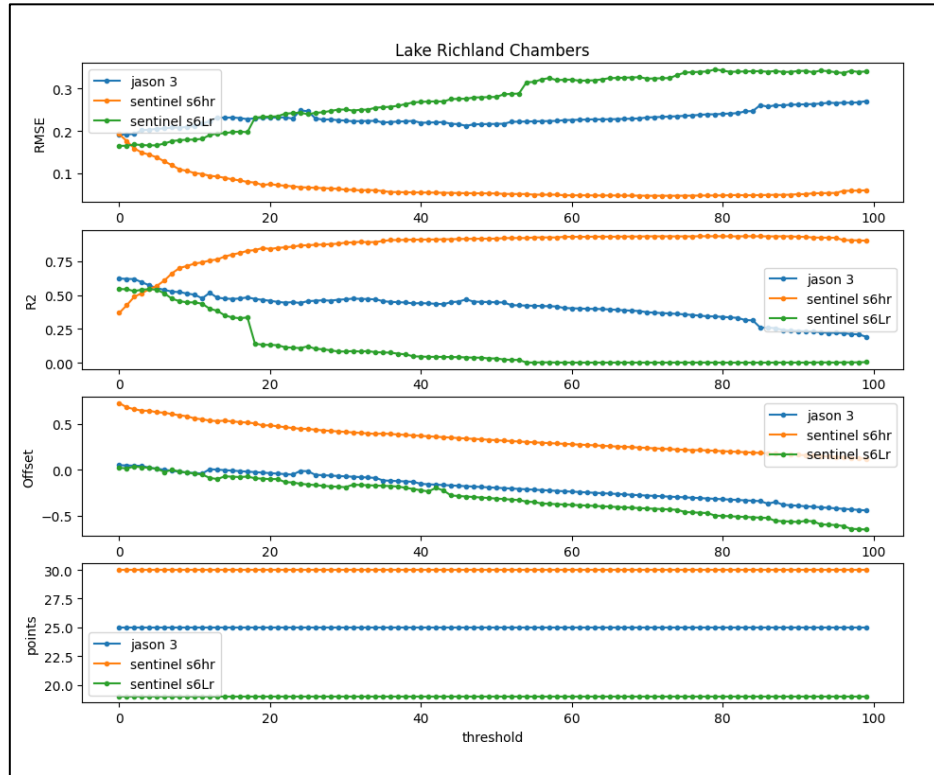


Figure 5.22: Plots for variation in RMSE, R2, offset and number of points for Lake Richland Chambers

The upper and lower limits for the outlier rejection algorithms are:

Number of minimum data points (N_{min}) = 15

Minimum standard deviation ($h_{std,min}$) = 0.5m

Tolerance ($r_{threshold}$) = 0.5m

The trend in the variation in the RMSE value for the Lake Richland Chambers is a little similar to what has been observed for the previous smaller lakes. The Sentinel-6aHR provides a smooth flow of the RMSE values in a very subtle decreasing increasing pattern. Extracting the threshold for the minimum value of RMSE seems a little difficult here because it becomes almost constant after a certain threshold and increases a bit in the later parts of the threshold spectrum. The LRM missions are also depicting the same behavior of reducing RMSE values with increasing thresholds but the noise levels in these cases are higher as compared to the previous smaller lakes investigated. To understand the behavior in detail, one needs to have a look at the waveforms.

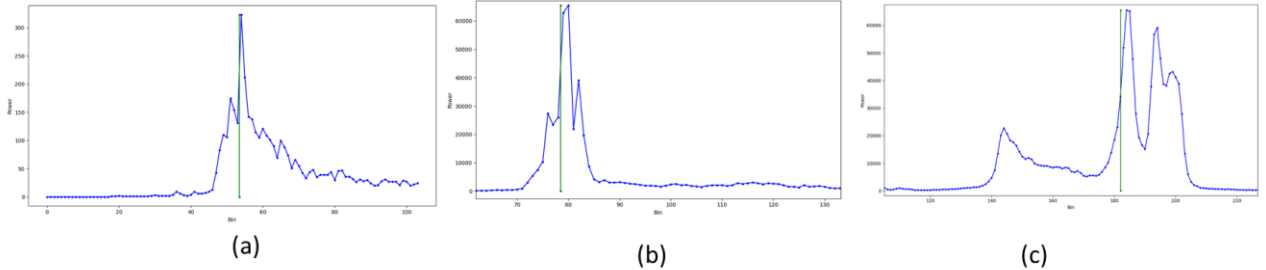


Figure 5.23: Return waveforms for Lake of Woods and the position of the retracking gate. (a) Jason-3 mission with threshold of 4%, (b) Sentinel-6aLR mission with threshold of 4%, (c) Sentinel-6aHR mission with threshold of 59%

The satellite coverage over the Richland Chambers lake along the width of the lake is around 5km. the along track resolution for LRM satellites is 30km. Naturally, many unwanted objects will be present in the altmetry footprint. As a result we observe, peaky and noisy echos in the Quasi specular waveforms for all the missions. For Sentinel-6aLR and Jason-3, the leading edge determined by the Improved Threshold Retracker is shorter in size, thereby it explains the lower threshold values for better estimation of the range. In case of Sentinel-6a HR, the waveform is peaky not that much noisy. As a result, the detection of the leading edge is comparitively easier with respect to the LRM missions. Additionally, specifically in this case, the higher resolution of 300m for SAR altimetry has allowed for some measurements which are not corrupted by the surroundings. The presence of a small peak on the left side of the leading edge in Figure 5.23 (c) could explain the behavior of the RMSE value which decreases till a certain threshold, remains almost constant due to smoother leading edge and then increase slightly as another peak is reached.

Based on the above observations of the waveforms, the optimum thresholds for the Richland Chambers lake are:

Table 5.15: Optimum threshold values and number of points for Lake Richland Chambers

Mission	Optimum threshold	Number of Data Points
Jason-3	4	25
Sentinel-6aHR	59	30
Sentinel-6aLR	4	18

For the generation of time series, the outlier rejection algorithm was applied on the missions, and for Sentinel-6aHR untracked mission, the limits used were:

Number of minimum data points (N_{min}) = 15
 Minimum standard deviation ($h_{std,min}$) = 0.75m
 Tolerance ($r_{threshold}$) = 1m

For other missions the limits used were:

Number of minimum data points (N_{min}) = 15
 Minimum standard deviation ($h_{std,min}$) = 0.75m
 Tolerance ($r_{threshold}$) = 1m

So, using the outlier rejection for time series determination, the following water level time series for Lake Richland Chambers were obtained in the overlapping period of operation using the thresholds as mentioned in the table 5.15.

CHAPTER 5: EXPERIMENTS AND RESULTS

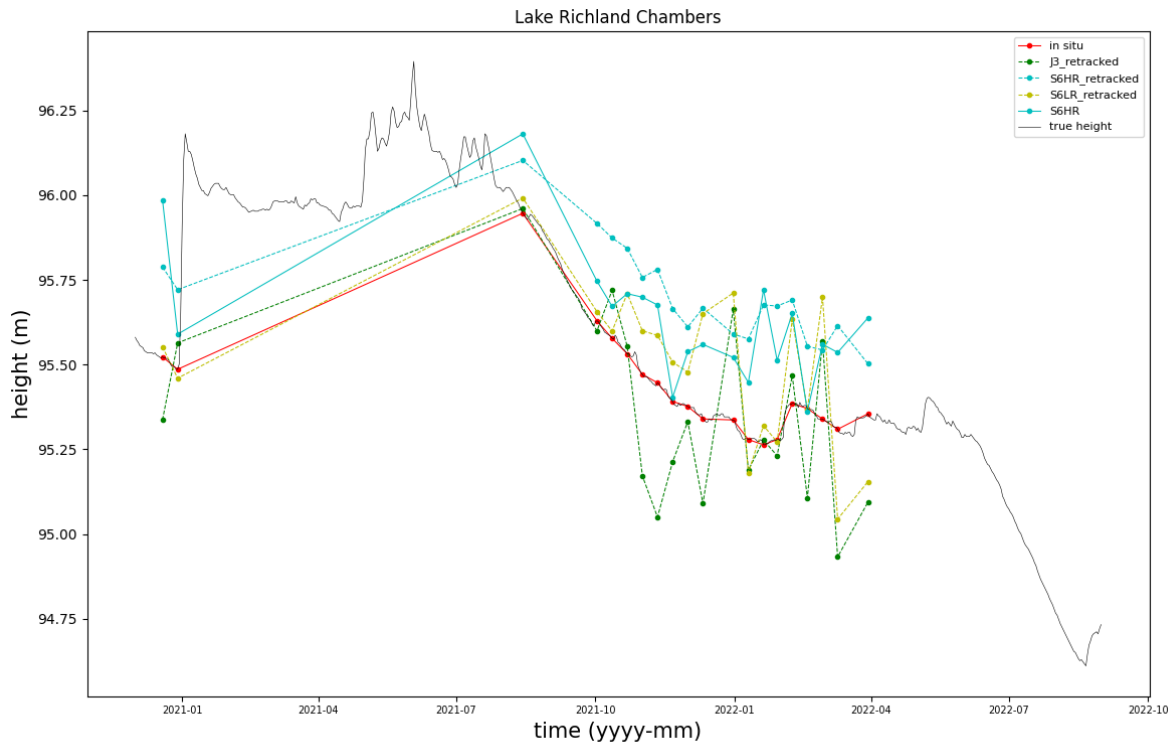


Figure 5.24: Water level time series for Lake Richland Chambers in the overlapping period of operation

Based on the water levels derived above in the common periods of operation, the following performance parameters were calculated:

Table 5.16: Performance analysis of Lake Richland Chambers

satellite	# data pts	corr coeff	RMSE (m)	R2	offset in situ (m)
Sentinel-6a HR	20	78%	0.11	61%	0.23
Jason-3 retracked	20	68%	0.19	46%	-0.07
Sentinel-6a HR retracked	20	90%	0.07	81%	0.29
Sentinel-6a LR retracked	20	68%	0.19	47%	0.18

The retracked data from Sentinel-6aHR again shows much better performance out of all the missions in the overlapping period of operations with correlation of 90% and RMSE of 7cm. The water levels from the LRM missions are corrupted due to a larger footprint of the antenna. This could explain the higher variation and noise in the estimated height when compared to the in-situ data. Because of this lower correlations are observed for these missions. However, the overall RMSE varies from 7 cm to 19 cm which, given the size of lake, seems fine.

5.9. Lake Toledo Bend

Toledo Bend is a reservoir located in Texas. The satellite data for the lake can be acquired from the satellite track '041' in the latitude range of 31.77 to 31.84 degrees north to obtain the water level time series for all hundred thresholds. The RMSE, R2, offset with in-situ data and the number of data points have been plotted below.

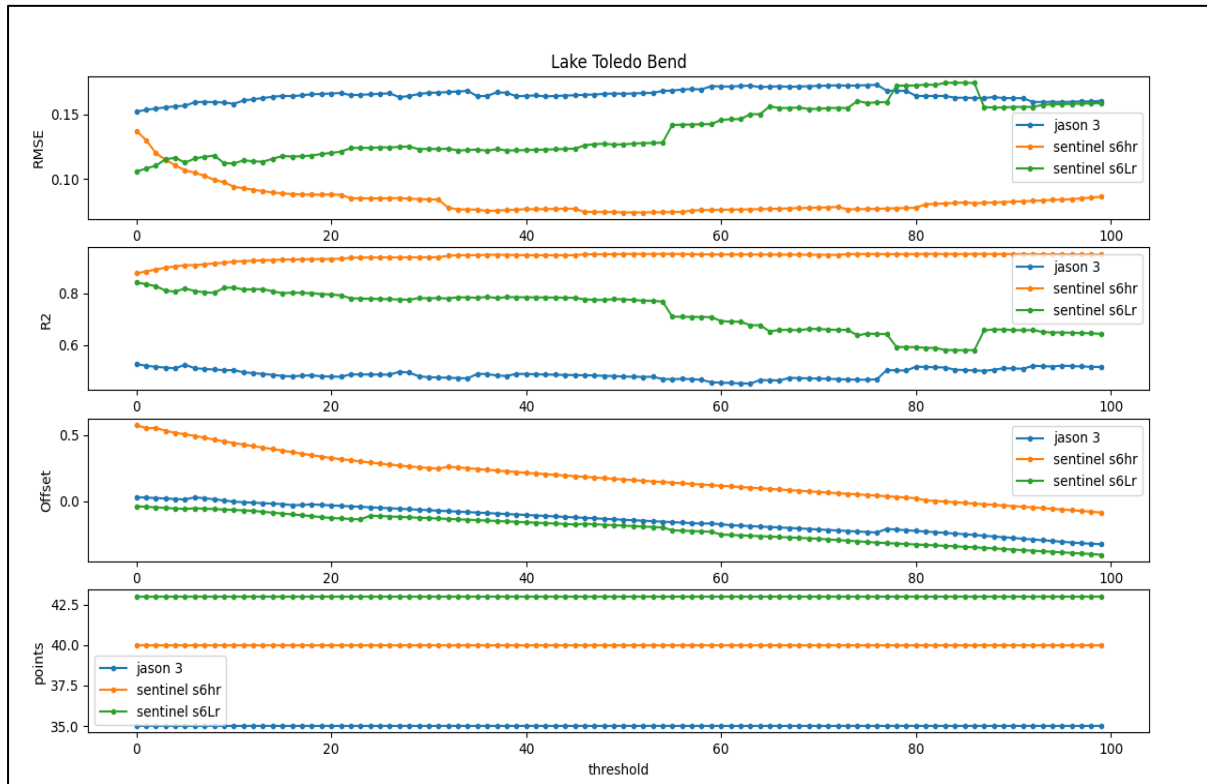


Figure 5.25: Plots for variation in RMSE, R2, offset and number of points for Toledo Bend Reservoir

The upper and lower limits for the outlier rejection algorithms are:

Number of minimum data points (N_{min}) = 15

Minimum standard deviation ($h_{std,min}$) = 0.5m

Tolerance ($r_{threshold}$) = 0.5m

A noisier variation in the RMSE and the correlations of the Toledo Bend lake can be observed in the above figure. Although the trend of the variation remains quite similar to the previous lakes. The decreasing increasing behavior of the RMSE values for the high resolution SAR data and the increasing trend for the both LRM data. The increased noise in all three missions is an indication of a waveform which is noisy and peaky. Similar to previous cases, the high resolution waveform must have a peak before the leading edge resulting in the said behavior. And similar as previous cases for LRM mission, the leading edge must be shorter in length. These hypothesis can be confirmed by looking at the waveforms of the respective missions over the lake.

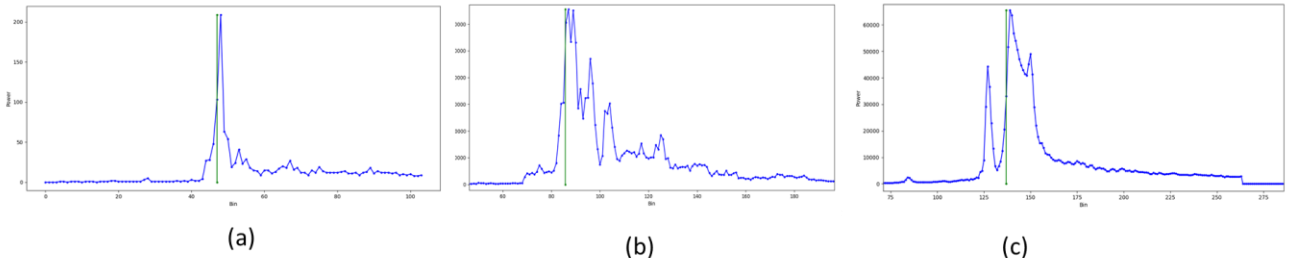


Figure 5.26: Return waveforms for Lake Toledo Bend and the position of the retracking gate. (a) Jason-3 mission with threshold of 10%, (b) Sentinel-6aLR mission with threshold of 10%, (c) Sentinel-6aHR mission with threshold of 50%

The satellites pass over the Toledo Bend lake covering only width of the lake which is only 5.5 kms. Naturally for a LRM mission whose along track resolution is 30km will have a lot of unwanted objects like land and vegetation in its footprint. As expected, we observe that the waveforms are very complex in all three missions, which could explain the noisy variations in the RMSE values in the Figure 5.25. as to the explanation regarding the behavior of the variation in RMSE for all three missions is considered, the hypothesis presented earlier is true. For the high resolution SAR mission, there is a peak which is, although, bigger in size as compared to the Richland Chambers lake and could be the reason for the noisy variation of the RMSE data for that mission.

Based on the analysis of the above waveforms, the optimum threshold for each mission for Lake Toledo Bend are:

Table 5.17: Optimum threshold values and number of points for Toledo Bend Reservoir

Mission	Optimum threshold	Number of Data Points
Jason-3	10	43
Sentinel-6aHR	50	40
Sentinel-6aLR	10	35

For the generation of time series, the outlier rejection algorithm was applied on the missions, and for Sentinel-6aHR untracked mission, the limits used were:

Number of minimum data points (N_{min}) = 15

Minimum standard deviation ($h_{std,min}$) = 0.75m

Tolerance ($r_{threshold}$) = 1m

For other missions the limits used were:

Number of minimum data points (N_{min}) = 15

Minimum standard deviation ($h_{std,min}$) = 0.5m

Tolerance ($r_{threshold}$) = 0.5m

So, using the outlier rejection for time series determination, the following water level time series for Lake Toledo Bend were obtained in the overlapping period of operation using the thresholds as mentioned in the table 5.17.

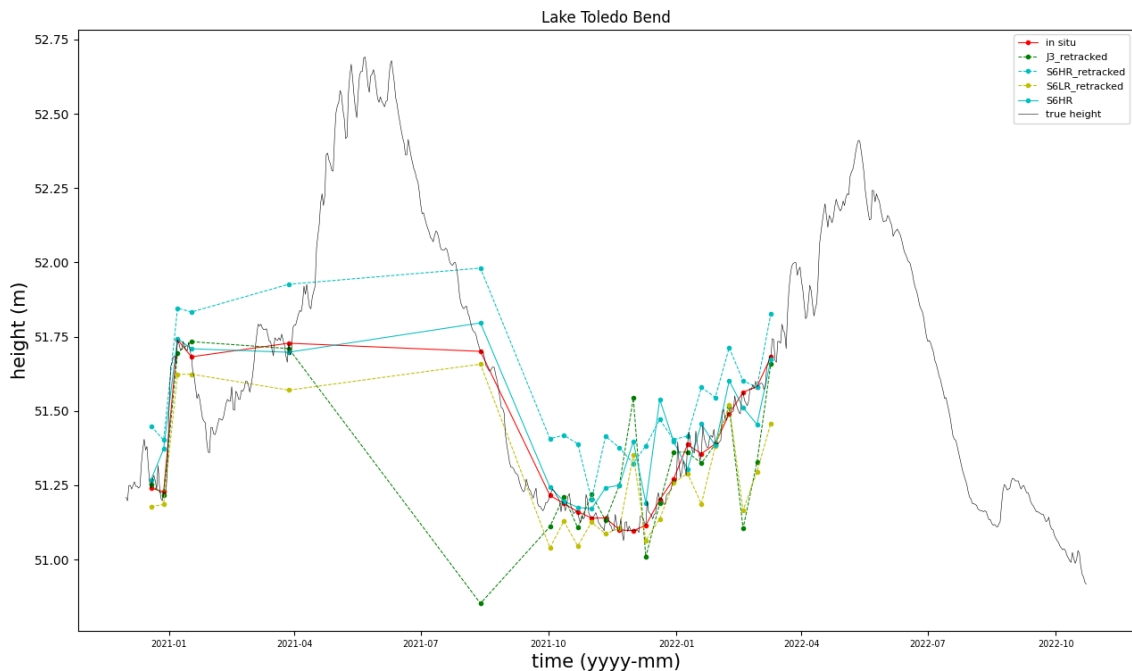


Figure 5.27: Water level time series for Toledo Bend Reservoir in the overlapping period of operation

Because of the application of the outlier rejection algorithm with a tolerance of 50cm for the retracked missions, there are some data gaps observed in the time periods of 2021-04 to 2021-08. Noticing, many series were generated based on different tolerance values, it was noticed that as the tolerance value increases, the number of “bad” values also increase which ultimately results in wrong values of the performance parameters. Therefore, in this case the tolerance value of 50cm may cause some data gaps but it returns better quality heights. Based on the retrieved height values, the performance parameters were analysed below:

Table 5.18: Performance analysis of Toledo Bend Reservoir

satellite	# data pts	corr coeff	RMSE (m)	R2	offset in situ (m)
Sentinel-6a HR	23	88%	0.12	77%	0.12
Jason-3 retracked	23	49%	0.23	24%	-0.018
Sentinel-6a HR retracked	23	93%	0.08	86%	0.17
Sentinel-6a LR retracked	23	84%	0.12	70%	-0.083

Sentinel-6HR data again provided high quality data over the smaller lakes with a good correlation of 93% and the RSME of 8cm. Interestingly, looking at the complex waveform in the Figure 5.26 (b) for Sentinel-6aLR mission, the use of appropriate threshold has allowed Sentienl-6 mission to provide a very good correlation of 84% along with the RMSE of 12cm. Jason-3 data has not performed well although the RMSE is around 23cm. Additionally, we can observe a very quality provided by the Sentinel-6aHR data retracked using the on-board retracker. The smaller footprint size of the mission has allowed to measure the height in error range of 12 cm without using any external retracking algorithm. This shows the quality of measurements the SAR mission with interleaved mode provides.

5.10. Lake O.H. Ivie

Lake O.H. Ivie is another lake in Texas USA. The satellite missions in this study pass through the lake along the track number of '143' and latitude range of 31.48 and 31.55 degrees north. It covers a width of 6.5 kms along the track but after looking at the map, it can be seen that there are a couple of small islands along the track which cause errors in the range estimation.

So for the aforementioned latitude range and pass numbers, the RMSE and correlation for all 100 thresholds is determined and plotted to understand the behaviour with increasing threshold.

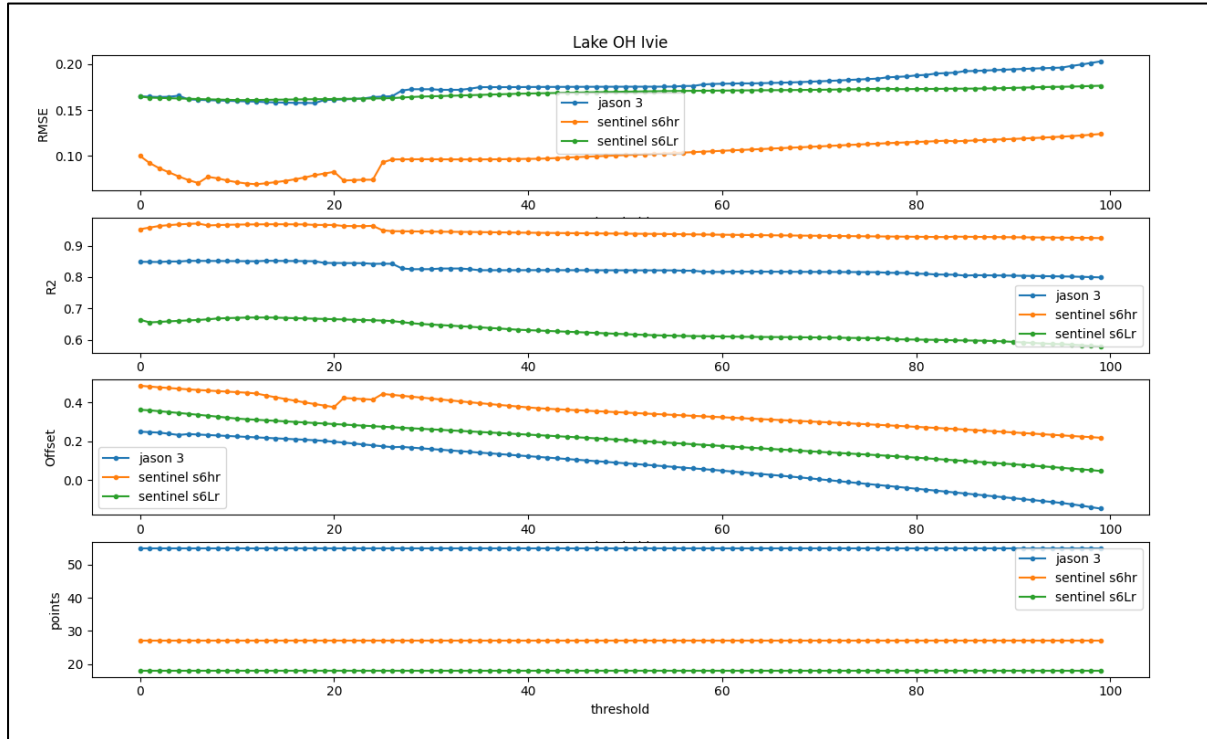


Figure 5.28: Plots for variation in RMSE, R2, offset and number of points for Lake O.H. Ivie

The outlier rejection algorithm used for this uses the following limits:

The upper and lower limits for the outlier rejection algorithms are:

Number of minimum data points (N_{min}) = 15

Minimum standard deviation ($h_{std,min}$) = 0.5m

Tolerance ($r_{threshold}$) = 0.5m

Unlike the previous cases, the RMSE and correlation show a slightly different behavior in this case. The difference is the shift of the optimum threshold from the middle part of the threshold spectrum to the earlier part. Also the shift near the optimum threshold is also not smooth as one might expect based on earlier cases. The reason might be due to the noisy leading edge. The LRM missions show a similar behavior as before although the minimum threshold has also shifted for them. But still the waveforms will noisy for this case too. For more clarity of these plots, analysis of the waveforms are required.

CHAPTER 5: EXPERIMENTS AND RESULTS

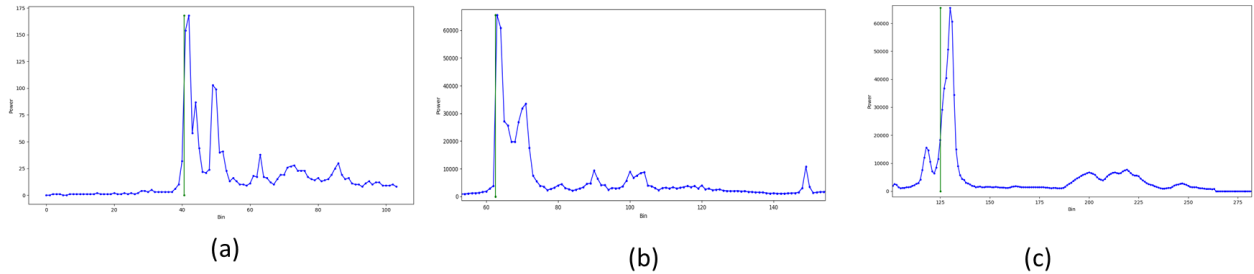


Figure 5.29: Return waveforms for Lake O.H. Ivie and the position of the retracking gate. (a) Jason-3 mission with threshold of 18%, (b) Sentinel-6aLR mission with threshold of 18%, (c) Sentinel-6aHR mission with threshold of 15%

As explained earlier, the waveforms for all three missions are complex with many peaks and noise. In this case, the waveforms are slightly different than the smaller lakes discussed before. The LRM missions have the similar waveforms as before because of the large footprint size. The only difference in this case is the slight shift of the optimum threshold towards a higher value because of less noise on the leading edge. However, in case of Sentinel-6a HR mission, the leading is noisy and has a small peak towards its left. This could explain the variation of the RMSE values along increasing threshold in Figure 5.28. Expectedly, this noise could have been caused due to the presence of small islands (as shown in Figure 5.30) along the track of the satellite, which added their own reflections and consequently noise along the leading edge. Because of that, the retracker positions the retracking bin on the smaller leading edge leading to an optimum threshold value in the earlier part of the threshold spectrum.

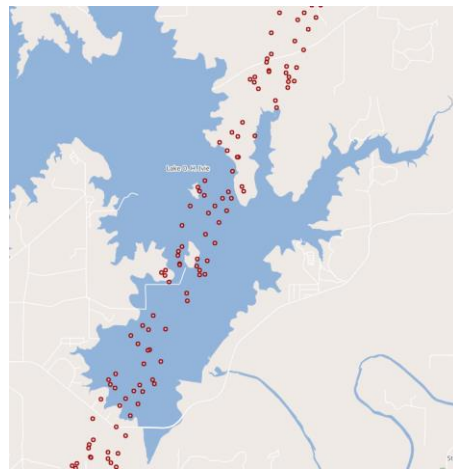


Figure 5.30: Presence of small islands along the satellite track leading to errors in the range estimation

So, based on the analysis of the above waveforms, the optimum threshold for each mission for Lake O.H. Ivie are:

Table 5.19: Optimum threshold values and number of points for Lake O.H. Ivie

Mission	Optimum threshold	Number of Data Points
Jason-3	18	53
Sentinel-6aHR	15	26
Sentinel-6aLR	18	17

For the generation of time series, the outlier rejection algorithm was applied on the missions, and for Sentinel-6aHR untracked mission, the limits used were:

Number of minimum data points (N_{min}) = 15

Minimum standard deviation ($h_{std,min}$) = 0.75m

Tolerance ($r_{threshold}$) = 1.5m

For other missions the limits used were:

Number of minimum data points (N_{min}) = 15

Minimum standard deviation ($h_{std,min}$) = 0.5m

Tolerance ($r_{threshold}$) = 2m for LRM missions

Tolerance ($r_{threshold}$) = 1m for SAR mission

So, using the outlier rejection for time series determination, the following water level time series for Lake O.H. Ivie were obtained in the overlapping period of operation using the thresholds as mentioned in the table 5.19.

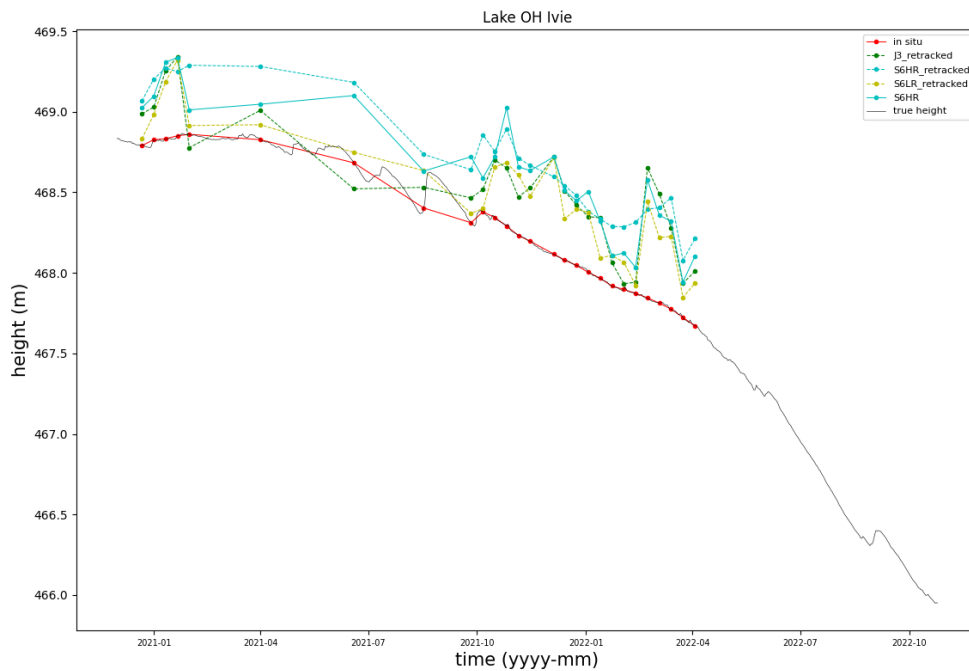


Figure 5.31: Water level time series for Lake O.H. Ivie in the overlapping period of operation

For this lake, due to presence of a few islands along the track, the tolerance value for the outlier rejection algorithms were increased to avoid any loss of “good data”. Also looking at the variation of the in-situ data with time, many values which would have matched the behaviour of the in-situ data

CHAPTER 5: EXPERIMENTS AND RESULTS

would have been removed if the tolerances were reduced to around 50 cm for example. So based on the derived water levels, the performance parameters have been analysed as follows:

Table 5.20: Performance analysis of Lake O.H. Ivie

satellite	# data pts	corr coeff	RMSE (m)	R2	offset in situ (m)
Sentinel-6a HR	27	91%	0.16	83%	0.43
Jason-3 retracked	27	84%	0.21	70%	0.32
Sentinel-6a HR retracked	27	97%	0.09	94%	0.44
Sentinel-6a LR retracked	27	90%	0.16	83%	0.24

Looking at the figures in the table above, one might say that the altimetry data from all 4 missions provide amazing results for Lake O.H. Ivie based on the higher correlation. But in this case, a thing which should be noted is that the number of data points for this lake is higher than the ones available for the previous small lakes. Also, looking at the figure 5.31, the annual variation in the height values for the lake quite prominent, so if the data points move along the same direction, naturally the correlation would increase. So to analyse the results by fair means, one must look at the RMSE values which are very similar and close to one's calculated for the previous areas of investigation. They vary in the similar range of 9 cm to 21 cm for all smaller lakes till now. The presence of the smaller island along the track also did not affect the estimation of height values.

5.11. Lake Sam Rayburn

The Sam Rayburn Reservoir is located in Texas USA and the satellite track ‘041’ passing through it. The analysis for the water level height will be conducted in the latitude range of 31.1 to 31.19 degrees north to determine and plot the RMSE and correlation for all 100 thresholds on the Improved Threshold Retracker.

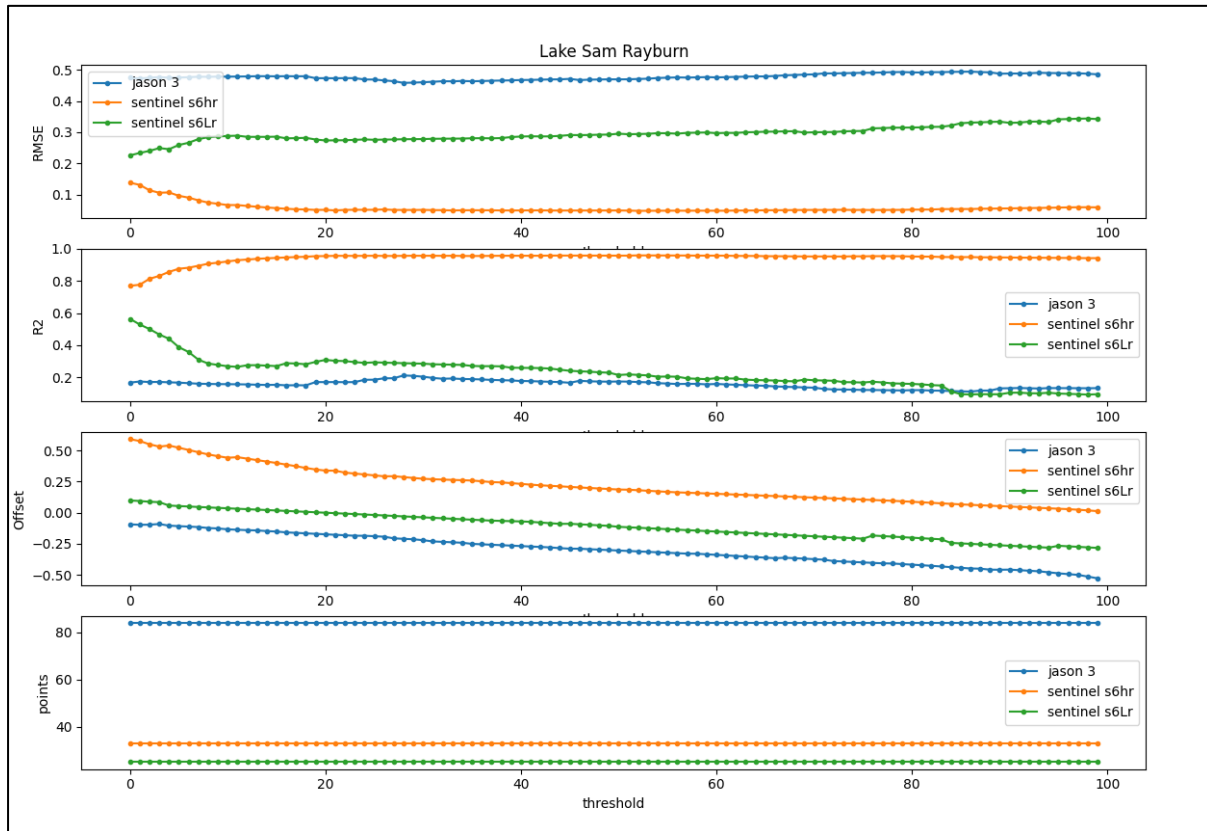


Figure 5.32: Plots for variation in RMSE, R2, offset and number of points for Sam Rayburn Reservoir

The outlier rejection algorithm used for this uses the following limits:

The upper and lower limits for the outlier rejection algorithms are:

Number of minimum data points (N_{min}) = 15

Minimum standard deviation ($h_{std,min}$) = 0.5m

Tolerance ($r_{threshold}$) = 0.5m

The Sam Rayburn reservoir shows somewhat similar results as those of the earlier smaller lakes. The only difference in this is that variation in the RMSE value is more subtle after a certain threshold, thereby making it a little difficult to understand where does the minimum value lies. Expectedly, the waveform will depict a very small peak in the power followed a very smooth leading edge. For the LRM missions, the behavior is also similar to the previous missions. To understand the trend in more detail, lets have a look at the returned waveforms for the lake.

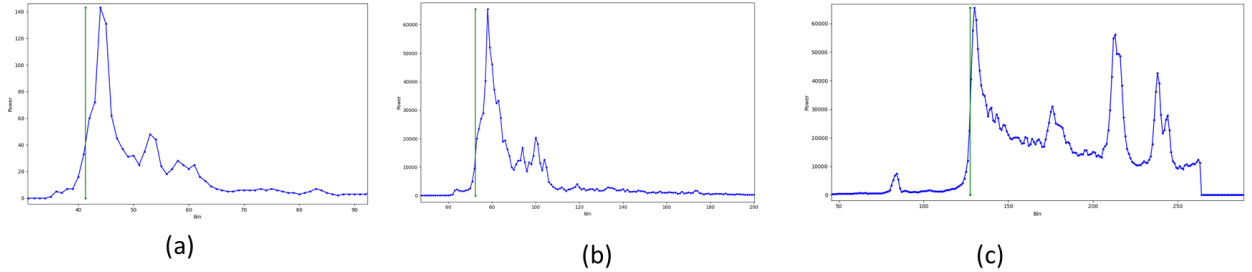


Figure 5.33: Return waveforms for Lake Sam Rayburn and the position of the retracking gate. (a) Jason-3 mission with threshold of 5%, (b) Sentinel-6aLR mission with threshold of 5%, (c) Sentinel-6aHR mission with threshold of 45%

Both LRM missions return very similar waveforms which is complex and noisy. The leading edge detected by the retracker is short thus requiring the optimum range to be in the earlier part of the spectrum. For the SAR mission, the waveform has multiple peaks but the leading edge from the first return of the signal is very smooth and noise free. So, as predicted earlier, there is a small peak in the power before the leading edge which may originate from the residual delay doppler power from the previous measurement. This results in the slightly higher RMSE in the earlier part of the threshold spectrum. The smoothness of the leading edge retrieved a very good quality range estimation for all thresholds over a certain optimum value which is also described in the Figure 5.32.

Based on the analysis of the subwaveforms, following thresholds are considered as optimum thresholds for Sam Rayburn Reservoir.

Table 5.21: Optimum threshold values and number of points for Sam Rayburn Reservoir

Mission	Optimum threshold	Number of Data Points
Jason-3	5	82
Sentinel-6aHR	45	33
Sentinel-6aLR	5	22

For the generation of time series, the outlier rejection algorithm was applied on the missions, and for Sentinel-6aHR untracked mission, the limits used were:

Number of minimum data points (N_{min}) = 15
 Minimum standard deviation ($h_{std,min}$) = 0.75m
 Tolerance ($r_{threshold}$) = 1.5m

For other missions the limits used were:

Number of minimum data points (N_{min}) = 15
 Minimum standard deviation ($h_{std,min}$) = 0.5m
 Tolerance ($r_{threshold}$) = 2m for LRM missions
 Tolerance ($r_{threshold}$) = 1m for SAR mission

So, using the outlier rejection for time series determination, the following water level time series for the Sam Rayburn Reservoir were obtained in the overlapping period of operation using the thresholds as mentioned in the table 5.21.

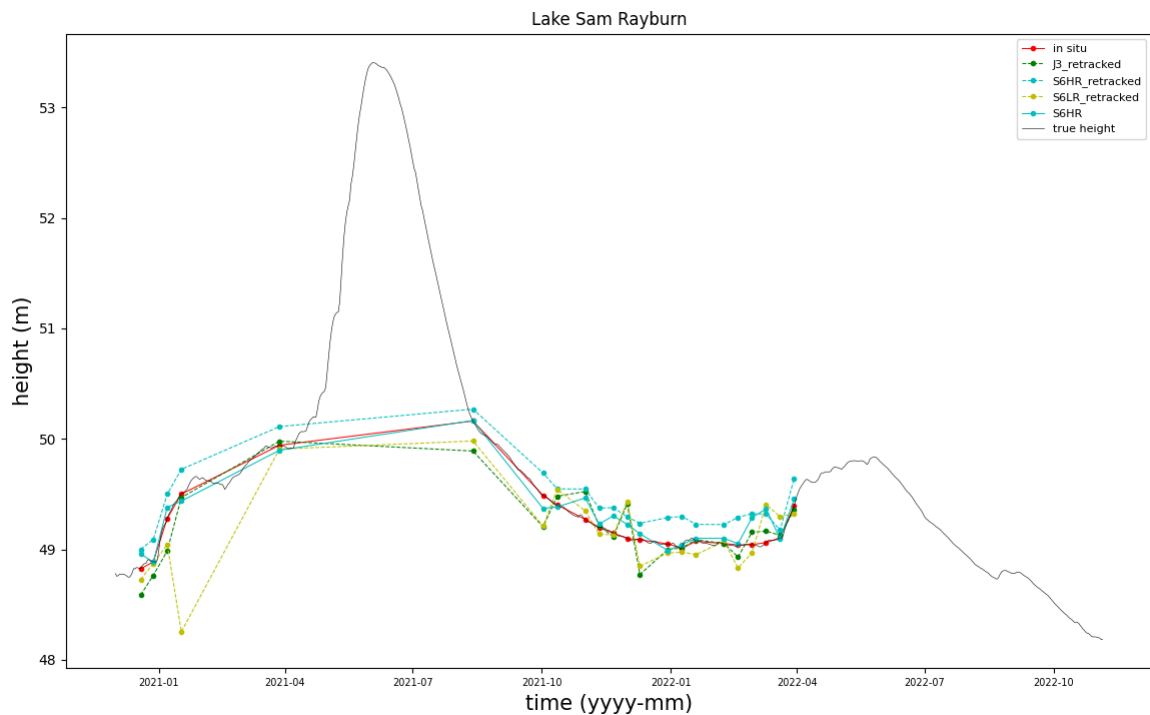


Figure 5.34: Water level time series for Sam Rayburn Reservoir in the overlapping period of operation

As can be observed in the above time series, a data gap is present in the time periods of 2021-04 to 2021-08. The most likely reason is due the rejection of those values during the outlier rejection. To understand whether increasing the tolerance for outlier rejection would improve the performance of the time series or not, experimentation with the tolerance values were done. The tolerance values which are already 1m and 2m for SAR and LRM data respectively were increased to a higher value, although the number of data points were added but many “bad” values were added too and the quality of the time series reduced.

So based on the outlier limits as mentioned before, the performance parameters were analyzed for Lake Sam Rayburn:

Table 5.22: Performance analysis of Sam Rayburn Reservoir

satellite	# data pts	corr coeff	RMSE (m)	R2	offset in situ (m)
Sentinel-6a HR	22	94%	0.14	89%	0.15
Jason-3 retracked	22	87%	0.18	76%	0.04
Sentinel-6a HR retracked	22	98%	0.05	96%	0.22
Sentinel-6a LR retracked	22	62%	0.31	39%	0.001

So, except the Sentinel-6aLR data, other missions perform really well especially the SAR data both retracked and un-retracked. The RMSE values lie in the similar range (5cm to 18cm) as before except the value of Sentinel-6LR retracked.

5.12. Lake Sidney Lanier

Lake Sidney Lanier is a reservoir located in the US state of Georgia. The satellite track that passes through the lake has the track number ‘015’ along the latitudes of 34.15 and 34.3 degrees north. Analysis will be carried out to determine and plot the RMSE and correlation for all 100 thresholds on the Improved Threshold Retracker.

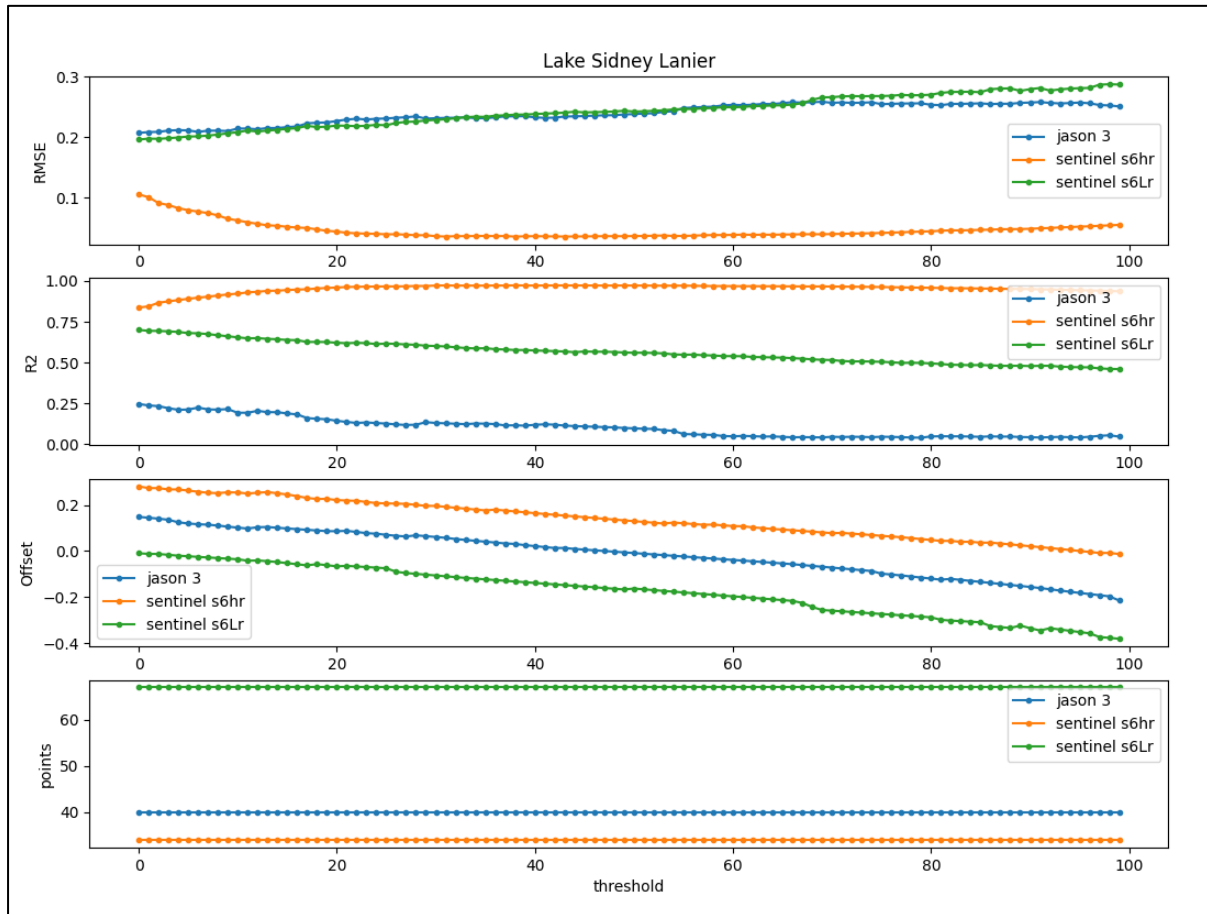


Figure 5.35: Plots for variation in RMSE, R2, offset and number of points for Lake Sidney Lanier

The outlier rejection algorithm used for this uses the following limits:

The upper and lower limits for the outlier rejection algorithms are:

Number of minimum data points (N_{min}) = 15

Minimum standard deviation ($h_{std,min}$) = 0.5m

Tolerance ($r_{threshold}$) = 0.5m

The lake shows somewhat a similar behavior as observed in previous lakes like Sam Rayburn. The variation in RMSE for Sentinel-6aHR data is less subtle in this case and has the decreasing increasing nature. For LRM missions, the trend also is similar to cases before. The reasons are also most likely same. The returned waveforms for these missions will provide a much better understanding.

CHAPTER 5: EXPERIMENTS AND RESULTS

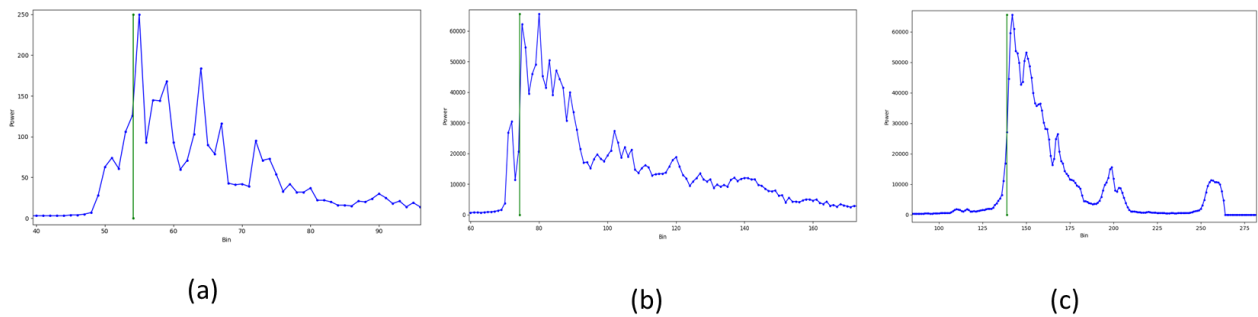


Figure 5.36: Return waveforms for Lake Sidney Lanier and the position of the retracking gate. (a) Jason-3 mission with threshold of 5%, (b) Sentinel-6aLR mission with threshold of 5%, (c) Sentinel-6aHR mission with threshold of 45%

Just like in the case of Sam Rayburn Reservoir, the waveforms are complex, multipeaked and noisy. The leading edge detected for LRM missions is shorter in length hence the smaller value of the threshold. For SAR mission, the leading is smooth and has a very short peak before it. Thus explaining the variation in RMSE values along the threshold.

The optimum thresholds are:

Table 5.23: Optimum threshold values and number of points for Lake Sidney Lanier

Mission	Optimum threshold	Number of Data Points
Jason-3	5	63
Sentinel-6aHR	45	33
Sentinel-6aLR	5	39

For the generation of time series, the outlier rejection algorithm was applied on the missions, and for Sentinel-6aHR untracked mission, the limits used were:

Number of minimum data points (N_{min}) = 15
 Minimum standard deviation ($h_{std,min}$) = 0.75m
 Tolerance ($r_{threshold}$) = 1.5m

For other missions the limits used were:

Number of minimum data points (N_{min}) = 15
 Minimum standard deviation ($h_{std,min}$) = 0.5m
 Tolerance ($r_{threshold}$) = 2m for LRM missions
 Tolerance ($r_{threshold}$) = 1m for SAR mission

So, using the outlier rejection for time series determination, the following water level time series for the Lake Sidney Lanier were obtained in the overlapping period of operation using the thresholds as mentioned in the table 5.23.

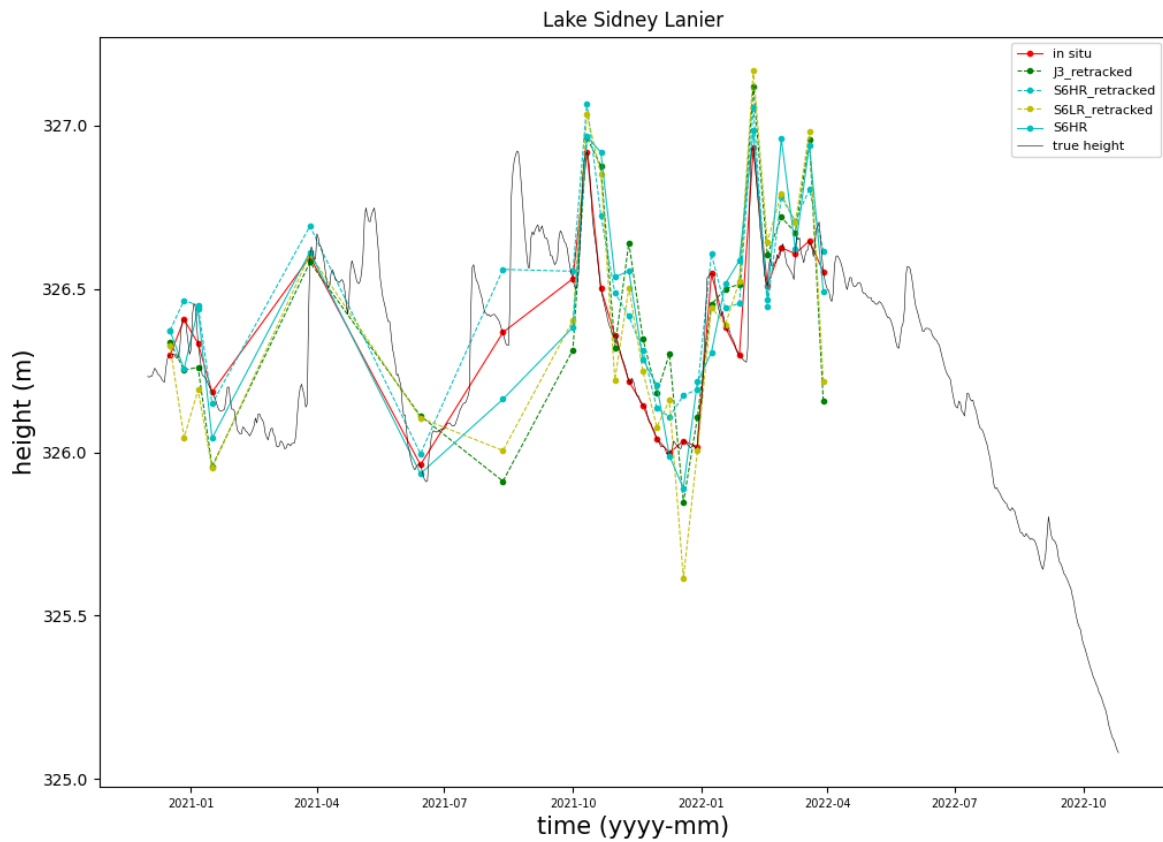


Figure 5.37: Water level time series for Lake Sidney Lanier in the overlapping period of operation

Based on the derived water level heights, the performance parameters are as below:

Table 5.24: Performance analysis of Lake Sidney Lanier

satellite	# data pts	corr coeff	RMSE (m)	R2	offset in situ (m)
Sentinel-6a HR	26	82%	0.17	68%	0.07
Jason-3 retracked	26	75%	0.22	56%	-0.03
Sentinel-6a HR retracked	26	96%	0.07	93%	0.08
Sentinel-6a LR retracked	26	81%	0.21	67%	-0.016

The altimetry datasets perform very well for Lake Sidney Lanier with RMSE values lying in the range of 7cm to 22cm. Sentinel-6aHR retracked data provides the best quality as compared to the classic LRM missions.

5.13. Lake Ray Roberts

Lake Ray Roberts is another lake located in the US state of Texas and the satellite track number '052' passes through it along the latitudes of 33.43 and 33.445 degrees north. To evaluate the behaviour of RMSE and correlation values for its water level time series, the water level time series for all 100 thresholds need to be analysed.

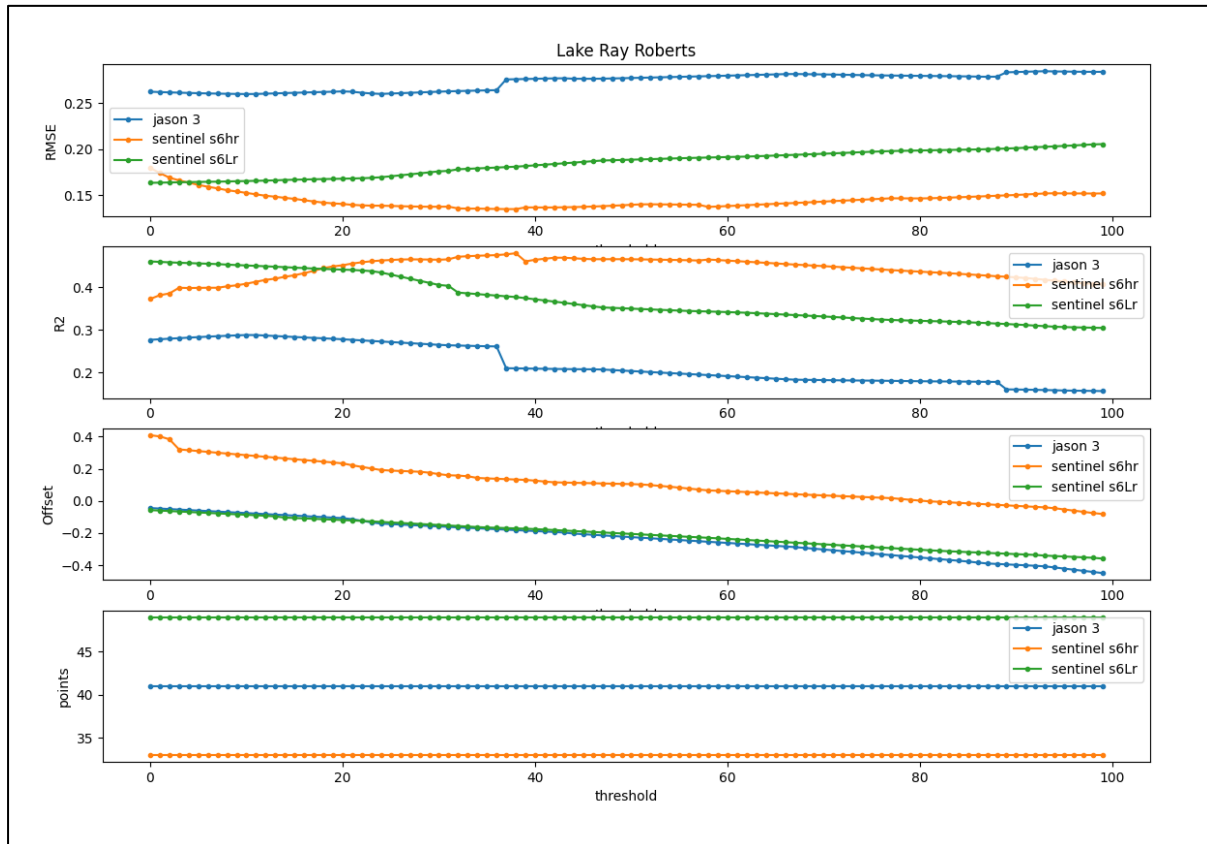


Figure 5.38: Plots for variation in RMSE, R2, offset and number of points for Lake Ray Roberts

The outlier rejection algorithm used for this uses the following limits:

The upper and lower limits for the outlier rejection algorithms are:

Number of minimum data points (N_{min}) = 15

Minimum standard deviation ($h_{std,min}$) = 0.5m

Tolerance ($r_{threshold}$) = 0.5m

The SAR mission and the LRM mission both depict similar behavior they have been depicting for previous target area. However a small noise can be observed in the middle part of the threshold spectrum which also happens to be around the optimum threshold value for SAR mission. This might happen due to slight noise in the leading edge of the waveform. To understand this better, one needs to have a look at the waveforms for all the missions.

CHAPTER 5: EXPERIMENTS AND RESULTS

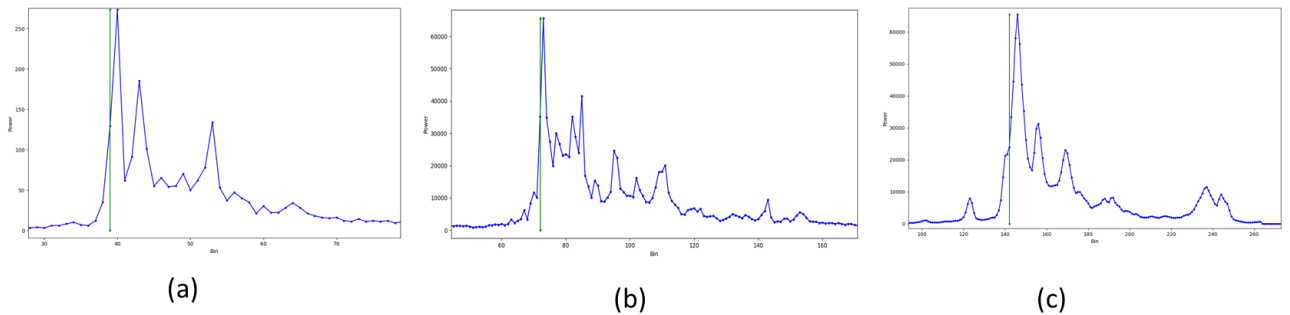


Figure 5.39: Return waveforms for Lake Sidney Lanier and the position of the retracking gate. (a) Jason-3 mission with threshold of 10%, (b) Sentinel-6aLR mission with threshold of 5%, (c) Sentinel-6aHR mission with threshold of 40%

The waveforms are noisy and peaky for all three missions. For LRM the leading edge is shorter so the optimum threshold is in the earlier spectrum of threshold. For SAR mission, as predicted earlier, the leading edge is a little noisy thus causing the slight noise in the variation of RMSE along the thresholds.

The optimum threshold values are:

Table 5.25: Optimum threshold values and number of points for Lake Ray Roberts

Mission	Optimum threshold	Number of Data Points
Jason-3	10	48
Sentinel-6aHR	40	32
Sentinel-6aLR	5	40

For the generation of time series, the outlier rejection algorithm was applied on the missions, and for Sentinel-6aHR untracked mission, the limits used were:

Number of minimum data points (N_{min}) = 15
 Minimum standard deviation ($h_{std,min}$) = 0.75m
 Tolerance ($r_{threshold}$) = 1.5m

For other missions the limits used were:

Number of minimum data points (N_{min}) = 15
 Minimum standard deviation ($h_{std,min}$) = 0.5m
 Tolerance ($r_{threshold}$) = 2 m for LRM missions
 Tolerance ($r_{threshold}$) = 1 m for SAR mission

So, using the outlier rejection for time series determination, the following water level time series for the Lake Ray Roberts were obtained in the overlapping period of operation using the thresholds as mentioned in the table 5.23.

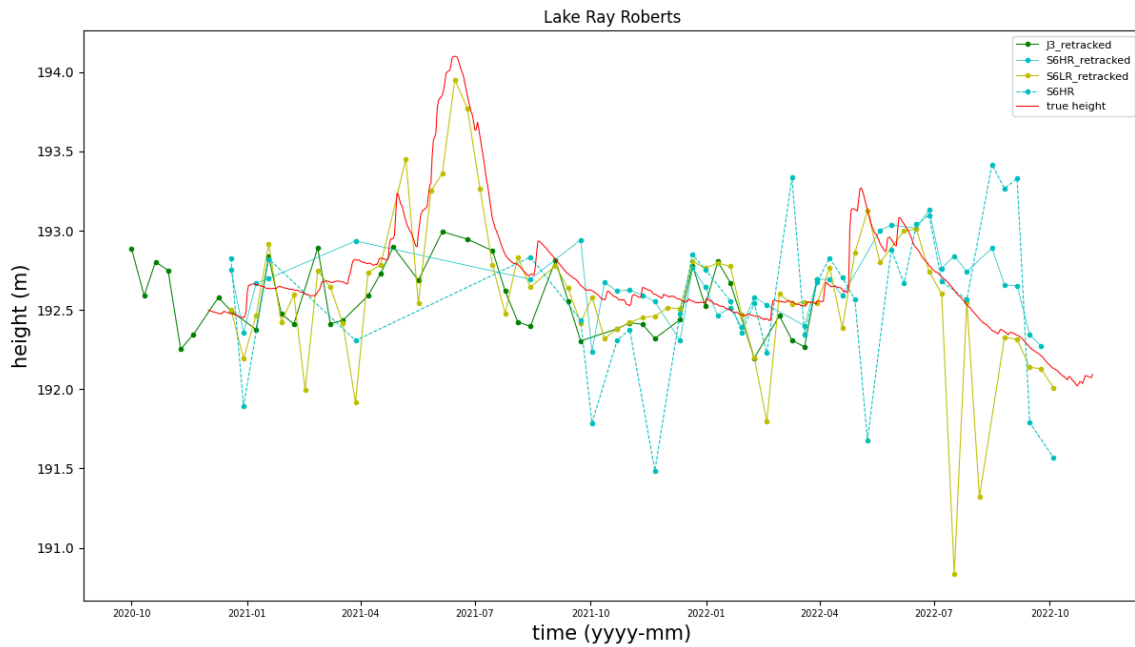


Figure 5.40: Water level time series for Lake Ray Roberts in the overlapping period of operation

For earlier cases, the time series was plotted at points where all four mission values are available. But after many experimentation with the tolerance values, the performance of the altimeters have been very poor. So it get an overview of the quality of measurements provided by each mission, the time series have been plotted for individual mission with its overlapping date in the in-situ data. Following quality parameters were assessed:

Table 5.26: Performance analysis of Lake Ray Roberts

satellite	# data pts	corr coeff	RMSE (m)	R2	offset in situ (m)
Sentinel-6a HR	35	5.5%	0.53	0.3%	0.012
Jason-3 retracked	42	54%	0.25	29%	-0.07
Sentinel-6a HR retracked	37	65%	0.167	42%	0.11
Sentinel-6a LR retracked	63	72%	0.33	53%	-0.06

As can been seen from the above plots and table figures, the altimetry data for Lake Ray Roberts perform poorly. The minimum RMSE is of the Sentinel-6HR retracked data with a value of 16.7 cm. more investigation in the quality assessment and the selection of outlier rejection algorithm is required.

5.14. Lake Tawakoni

For Lake Tawakoni, the ground track of '219' was chosen along the latitudes of 32.8460 to 32.93 degrees north for estimation of optimum thresholds based on height values determined for all 100 thresholds. After computing the RMSE, R2, offset with in-situ values as well number of available data points along the whole threshold spectrum, the following plot was obtained:

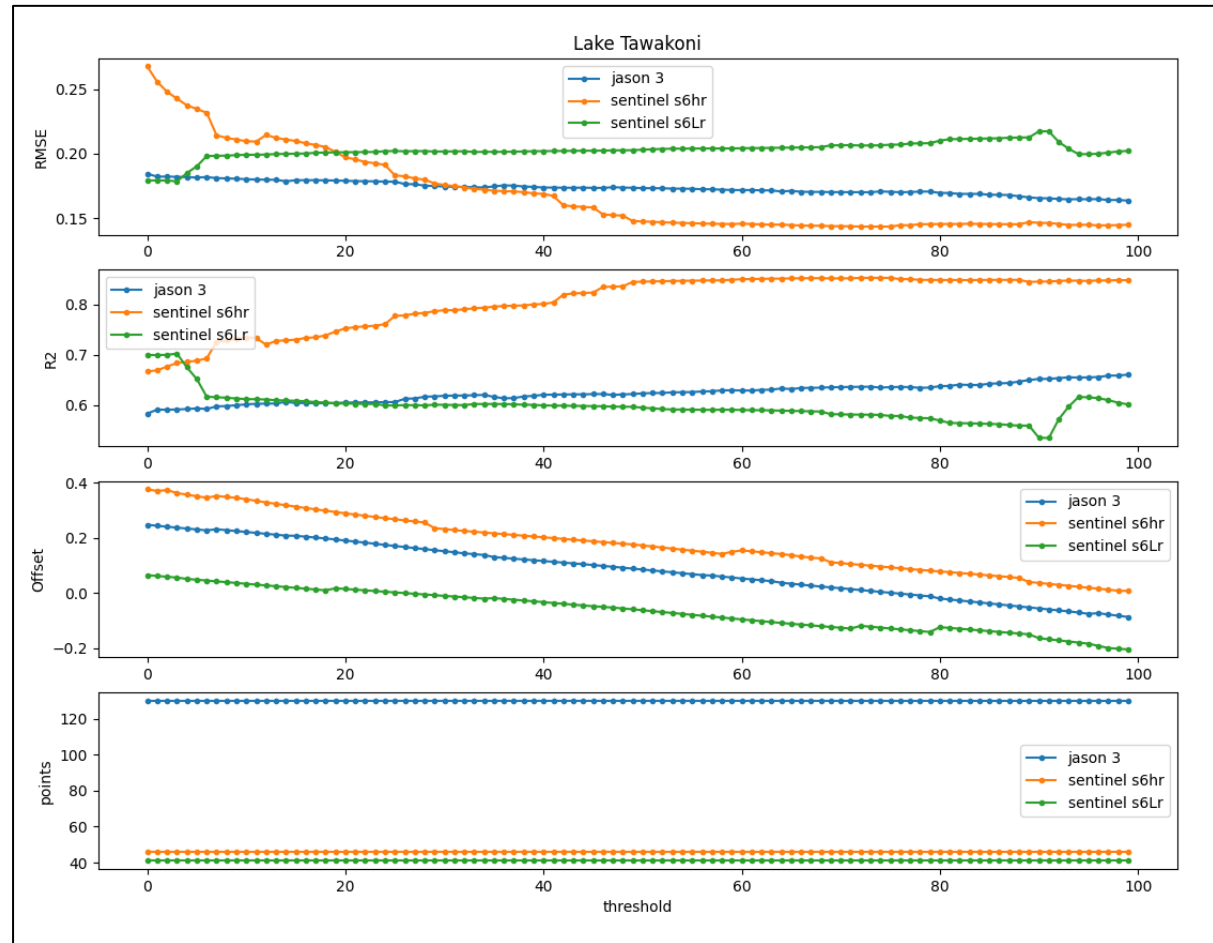


Figure 5.41: Plots for variation in RMSE, R2, offset and number of points for Lake Tawakoni

The outlier rejection algorithm used for this uses the following limits:

The upper and lower limits for the outlier rejection algorithms are:

Number of minimum data points (N_{min}) = 15

Minimum standard deviation ($h_{std,min}$) = 0.5m

Tolerance ($r_{threshold}$) = 0.5m

The behavior of the lake is not similar to the one's analysed before. The RMSE for SAR mission reduces with increasing threshold and is noisy during that. The minima occurs around the threshold of 45%. The waveform for SAR could be peaky before the determination of the leading edge and then becomes smooth once the threshold is reached. The LRM missions somehow shows constant behavior throughout with subtle changes in the RMSE values. Looking at the map of the lake, there is a huge piece of land between the water surface along the track of the satellite. This could result in a complex waveforms.

The analysis can be done in more detail by checking their waveforms.

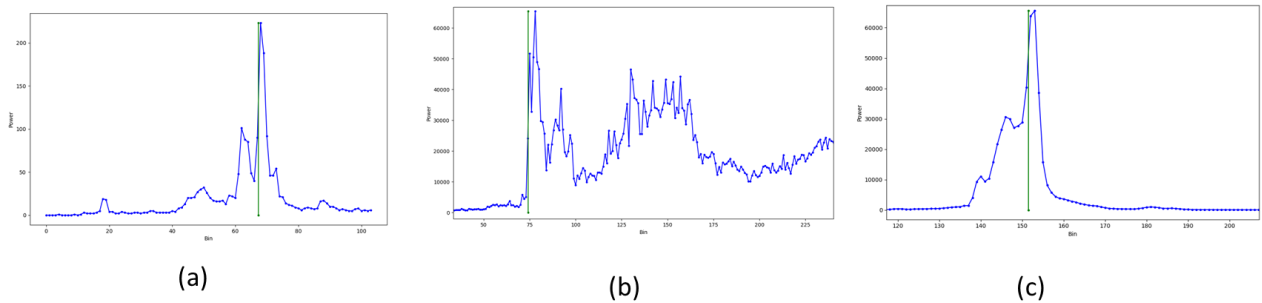


Figure 5.42: Return waveforms for Lake Tawakoni and the position of the retracking gate. (a) Jason-3 mission with threshold of 20%, (b) Sentinel-6aLR mission with threshold of 5%, (c) Sentinel-6aHR mission with threshold of 45%

Majority of the waveforms returned for all three missions are from the water surface are Quasi-specular in nature due to presence of land in its proximity and calmer waters. The Figure 5.42 above depicts the one of the few waveforms which can yeild a good result. As it can be seen that waveforms are complex in nature and are very noisy and peaky. For the SAR waveform as predicted, the leading edge is noisier than the trailing edge. This results in the behavior in the RMSE values in Figure 5.41. The LRM missions provide the best retracked range when the threshold is in the earlier part of the spectrum because of the shorter leading edges.

The optimum thresholds are:

Table 5.27: Optimum threshold values and number of points for Lake Tawakoni

Mission	Optimum threshold	Number of Data Points
Jason-3	20	130
Sentinel-6aHR	45	44
Sentinel-6aLR	5	38

For the generation of time series, the outlier rejection algorithm was applied on the missions, and for Sentinel-6aHR unretacked mission, the limits used were:

Number of minimum data points (N_{min}) = 15
 Minimum standard deviation ($h_{std,min}$) = 0.75m
 Tolerance ($r_{threshold}$) = 1.5m

For other missions the limits used were:

Number of minimum data points (N_{min}) = 15
 Minimum standard deviation ($h_{std,min}$) = 0.5m
 Tolerance ($r_{threshold}$) = 2 m for LRM missions
 Tolerance ($r_{threshold}$) = 1 m for SAR mission

So, using the outlier rejection for time series determination, the following water level time series for the Lake Tawakoni were obtained in the overlapping period of operation using the thresholds as mentioned in the table 5.27.

CHAPTER 5: EXPERIMENTS AND RESULTS

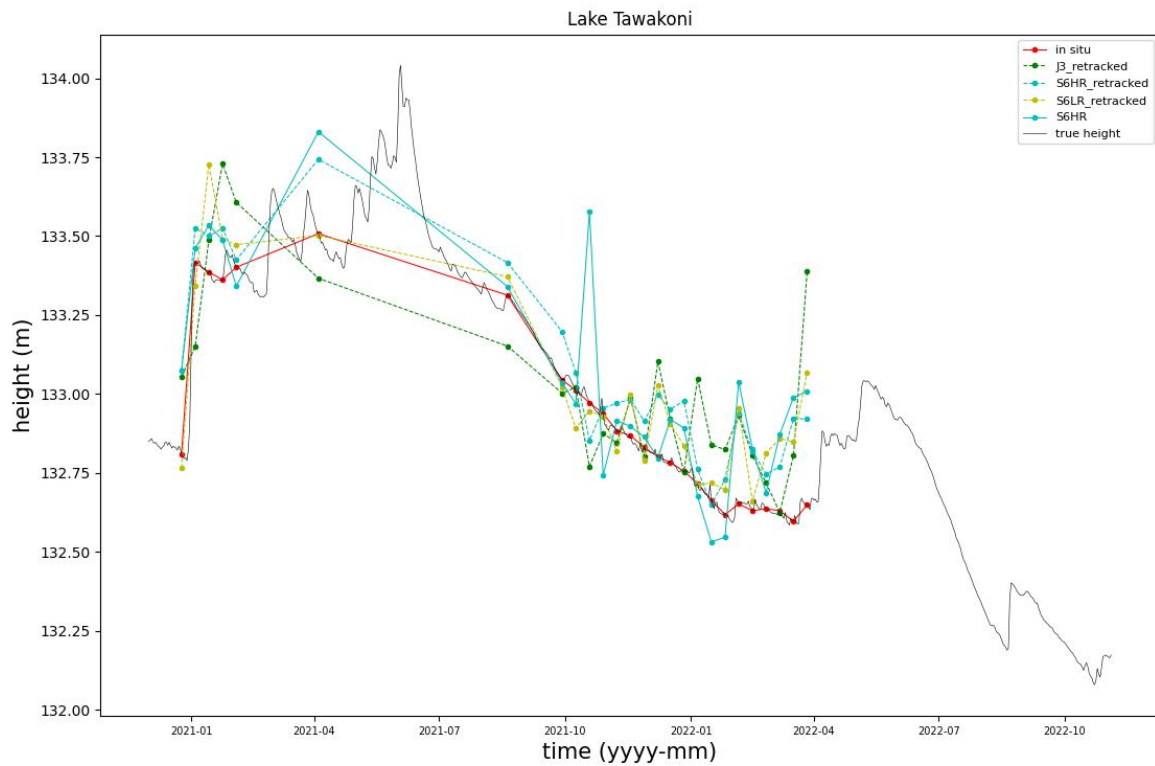


Figure 5.43: Water level time series for Lake Tawakoni in the overlapping period of operation

Table 5.28: Performance analysis of Lake Tawakoni

satellite	# data pts	corr coeff	RMSE (m)	R2	offset in situ (m)
Sentinel-6a HR	26	83%	0.18	68%	0.123
Jason-3 retracked	26	73%	0.21	53%	0.13
Sentinel-6a HR retracked	26	94%	0.10	88%	0.09
Sentinel-6a LR retracked	26	88%	0.13	78%	0.097

The altimetry datasets perform very well for Lake Tawakoni with RMSE values lying in the range of 10cm to 21cm. Sentinel-6aHR retracted data provides the best quality as compared to the classic LRM missions.

5.15. Lake Champlain

Lake Champlain is a lake located in North America, bordering Canada. The satellite track number 126 passes over it in the latitude range of 44.22 to 44.246 degrees north. The lake also freezes over during winters so the analysis will be conducted only for the summer months. The plots for RMSE and correlation with respect to 100 thresholds are shown below:

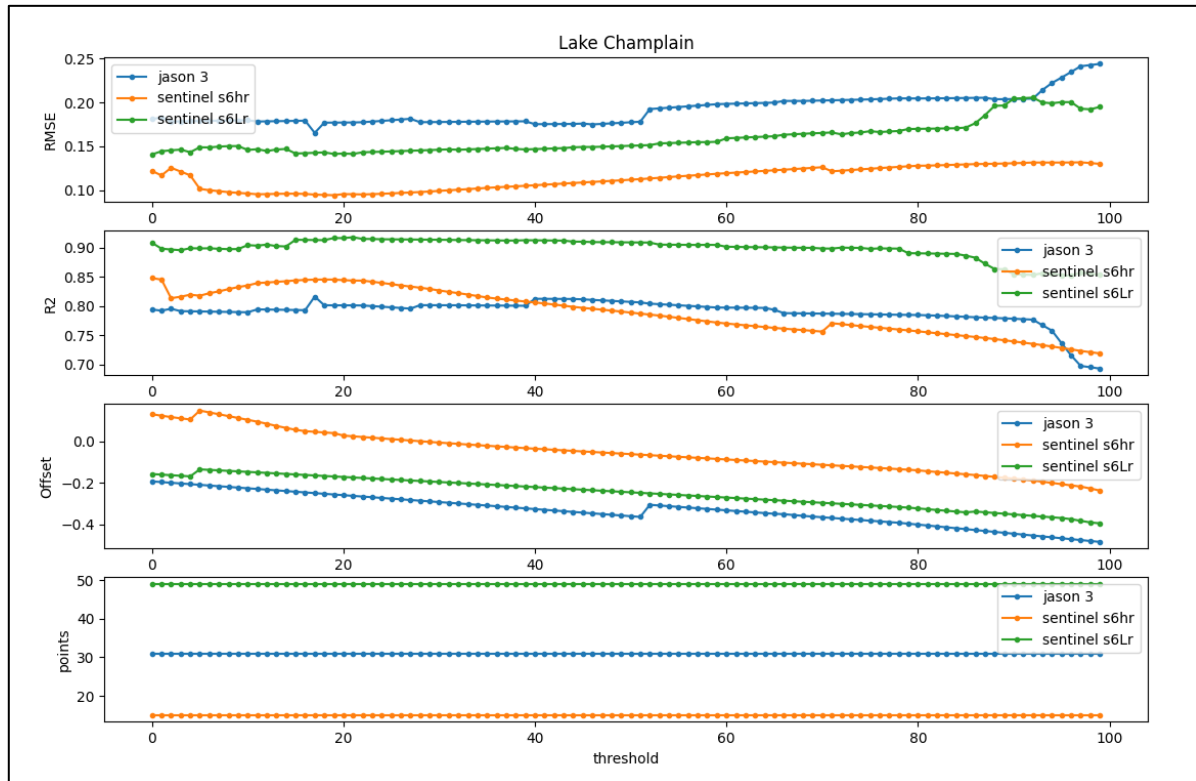


Figure 5.44: Plots for variation in RMSE, R2, offset and number of points for Lake Champlain

The outlier rejection algorithm used for this uses the following limits:

The upper and lower limits for the outlier rejection algorithms are:

Number of minimum data points (N_{min}) = 15

Minimum standard deviation ($h_{std,min}$) = 0.5m

Tolerance ($r_{threshold}$) = 0.5m

The SAR mission and the LRM mission both depict the similar behavior they have been depicting for previous target area. However for the SAR mission the optimum threshold lies in the earlier part of the spectrum which could be indication of a short leading edge with a short peak before it in the waveform. The LRM mission although a little noisy depict the similar increasing behavior. To understand this better, one needs to have a look at the waveforms for all the missions.

CHAPTER 5: EXPERIMENTS AND RESULTS

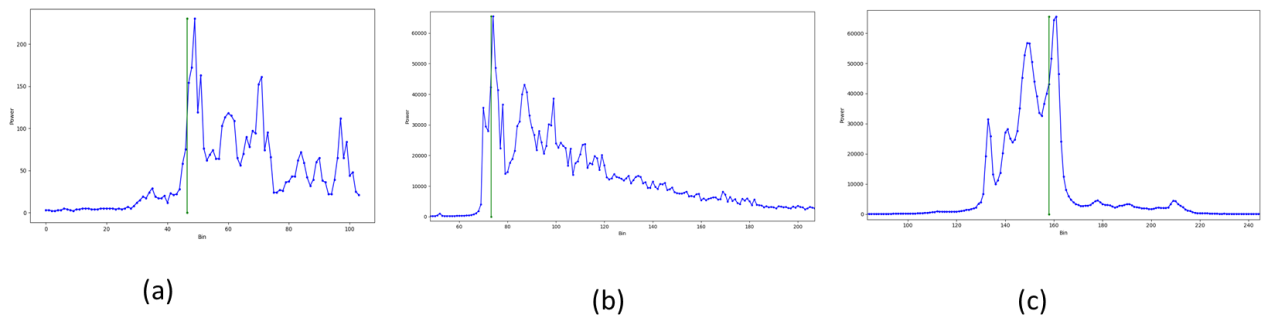


Figure 5.45: Return waveforms for Lake Champlain and the position of the retracking gate. (a) Jason-3 mission with threshold of 17%, (b) Sentinel-6aLR mission with threshold of 18%, (c) Sentinel-6aHHR mission with threshold of 15%

Just like in Lake Sidney Lanier, most of the waveforms were Quasi-specular as well as flat patch in nature. But to understand the behavior in the RMSE variation, waveforms from the middle of the lakes were picked for better understanding. The waveforms from the LRM missions show similar behavior and consequences as in earlier cases. However, in case of SAR mission, the waveform is multipeaked but with low noise. These peaks are present before the derived leading edge which explains the noise in the RMSE variation in the earlier spectrum of the threshold. And the shorter length of the leading edge also results in a smaller optimum threshold value.

The optimum threshold values are:

Table 5.29: Optimum threshold values and number of points for Lake Champlain

Mission	Optimum threshold	Number of Data Points
Jason-3	17	30
Sentinel-6aHHR	18	14
Sentinel-6aLR	15	48

For the generation of time series, the outlier rejection algorithm was applied on the missions, and for Sentinel-6aHHR untracked mission, the limits used were:

Number of minimum data points (N_{min}) = 15
 Minimum standard deviation ($h_{std,min}$) = 0.75m
 Tolerance ($r_{threshold}$) = 1.5m

For other missions the limits used were:

Number of minimum data points (N_{min}) = 15
 Minimum standard deviation ($h_{std,min}$) = 0.5m
 Tolerance ($r_{threshold}$) = 2 m for LRM missions

Tolerance ($r_{threshold}$) = 1 m for SAR mission

So, using the outlier rejection for time series determination, the following water level time series for the Lake Champlain were obtained in the overlapping period of operation using the thresholds as mentioned in the table 5.29.

CHAPTER 5: EXPERIMENTS AND RESULTS

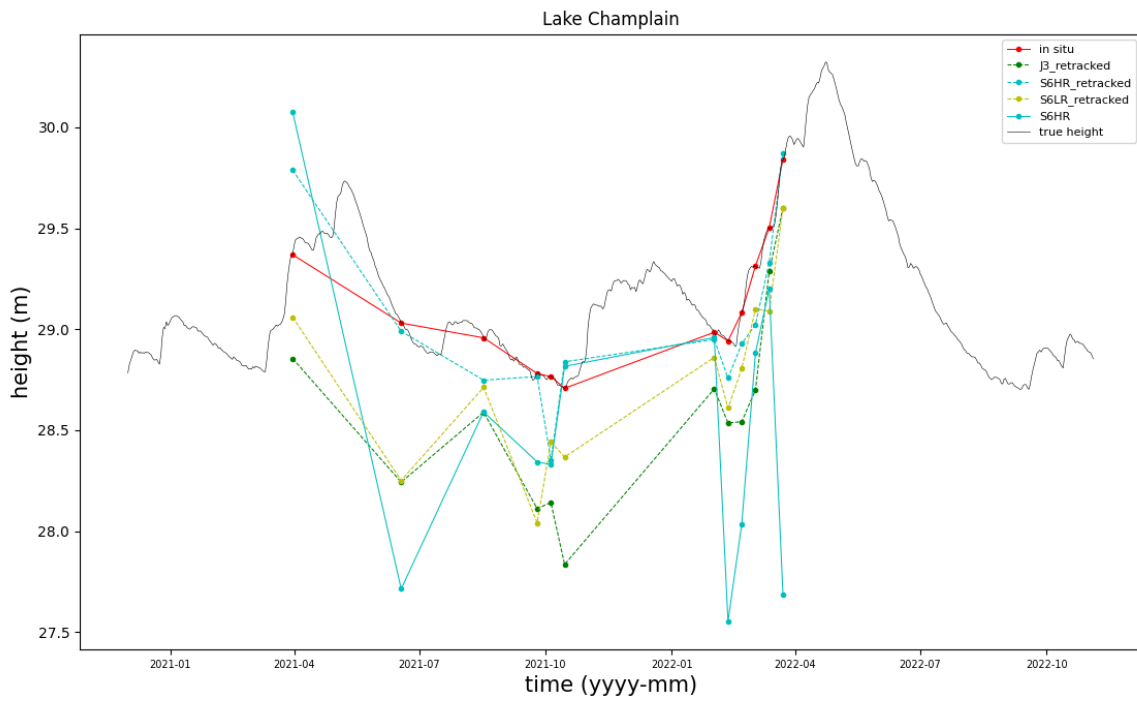


Figure 5.46: Water level time series for Lake Champlain in the overlapping period of operation

The time series have been generated in the summer months only since the lake freezes during winters. The performance of these height values have been analysed:

Table 5.30: Performance analysis of Lake Champlain

satellite	# data pts	corr coeff	RMSE (m)	R2	offset in situ (m)
Sentinel-6a HR	12	11%	0.73	1.3%	-0.54
Jason-3 retracked	12	94%	0.21	88%	-0.44
Sentinel-6a HR retracked	12	87%	0.20	76%	-0.07
Sentinel-6a LR retracked	12	89%	0.22	80%	-0.25

As can be seen from the above plots and table figures, the altimetry data for Lake Champlain perform poorly. The minimum RMSE is of the Sentinel-6HR retracked data with a value of 20 cm. More investigation in the quality assessment and the selection of outlier rejection algorithm is required.

5.16. Optimum threshold distribution

Based on the values derived from the plots from the previous sections from each lake, the following histograms were created to analyse the best threshold for each mission based on the least RMSE and highest correlation. The histograms measures the number of occurrences of a particular threshold value which is best for that particular lake.

The analysis for the optimum threshold for the Jason-3 mission is shown below:

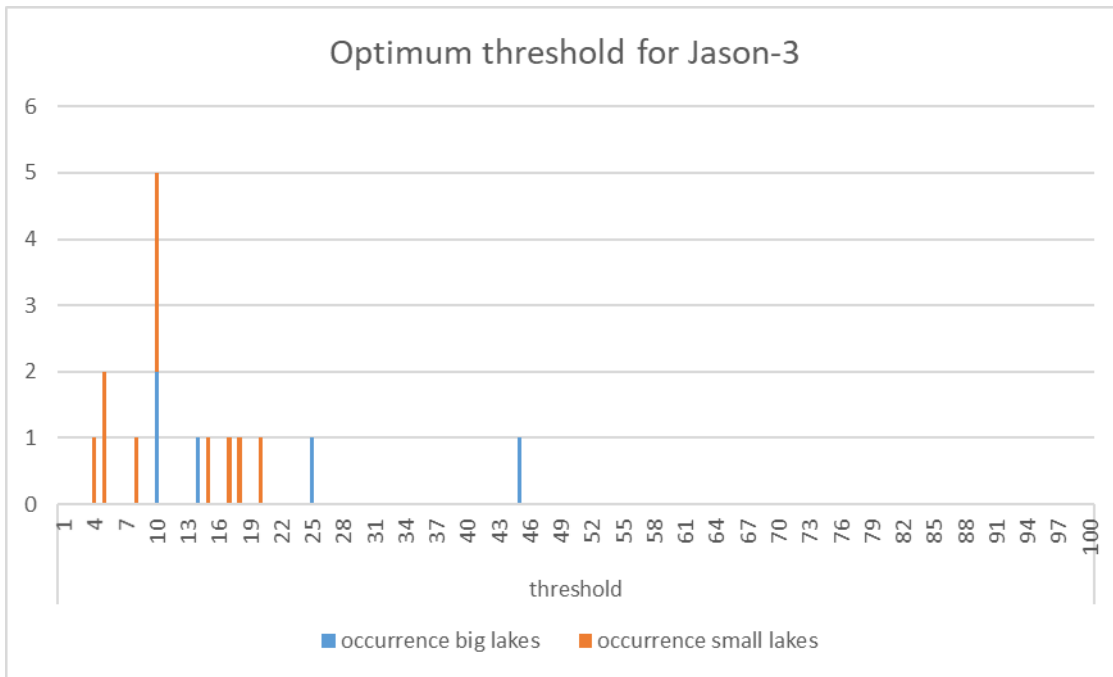


Figure 5.47: Histogram to find the optimum threshold for retracking using the Jason-3 mission

Apart from a few variations, it can be observed that for the Jason-3 mission, the optimum threshold lies in the earlier part of the threshold spectrum for both big and smaller lakes. The threshold value lying in the middle part of the spectrum is from Lake Superior which is the largest lake by surface area in the world. Due to its larger size, the lake depicts “ocean-lake” waveforms. That means due to a windy weather over the lake, waves form over the water surface which yields to rapid change in the slope of the leading edge. The change in this slope results in multiple leading edges which provide the best range values when the retracking bin is in the middle of them. Other than that, the next highest threshold lies on 25% for Lake Huron which also has a rougher surface and high waves. According to the NOAA website for Great Lakes, the daily wave height in both Lake Superior and Huron vary from 0.5 m to 1 m. Since, the Great Lakes depict Quasi-Brown like waveforms, retracking the heights using the onboard retracker seems like a better option which can also be seen from the performance analysis of these lakes. So when the smaller lakes are considered, the threshold values seem to be more clustered around the earlier part of the thresholds. So for them, the smaller threshold value of optimally 10% should agree since they are calmer surfaces. However, with an increase in the number of areas investigation, we would have more data regarding the occurrences and therefore the histograms would become more clear and distinct.

CHAPTER 5: EXPERIMENTS AND RESULTS

For Sentinel-6a LR mission, based on the derived thresholds, the histogram for the occurrence is

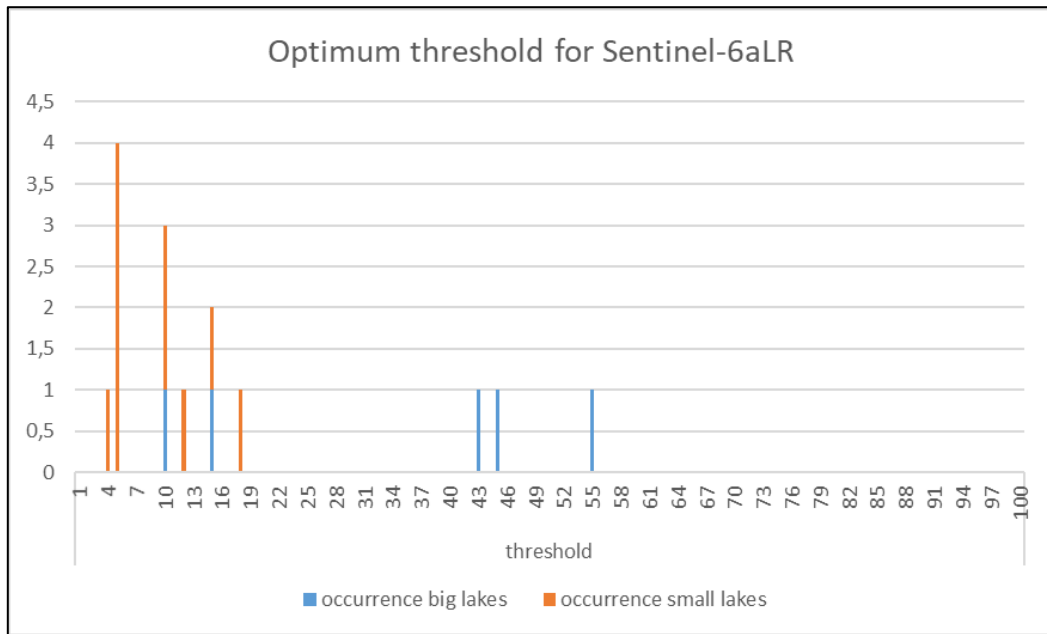


Figure 5.48: Histogram to find the optimum threshold for retracking using the Sentinel-6aLR mission

Just like in the case of Jason-3 satellite, the Sentinel-6aLR mission has noisier leading edges in the waveform depending upon the surface roughness of the lake. This results in the variation of the optimal threshold along the threshold axis. Again the quality results for the Great Lakes show a slight decline in quality (by a few centimeters) when using the Improved threshold retracker over the on-board retracker which is more compatible with ocean-like waveforms. So if considering only the smaller lakes to use the ITR retracker over them, the more calmer water surfaces with of course the complex waveforms, the ITR works quite well in retracking range from that. Also the optimum range lies in a particular earlier part of the threshold spectrum with optimum value of 5%. However, again, with an increase in the number of areas investigation, we would have more data regarding the occurrences and therefore the histograms would become more clear and distinct.

For Sentinel-6a HR mission, based on the derived thresholds, the histogram for the occurrence is

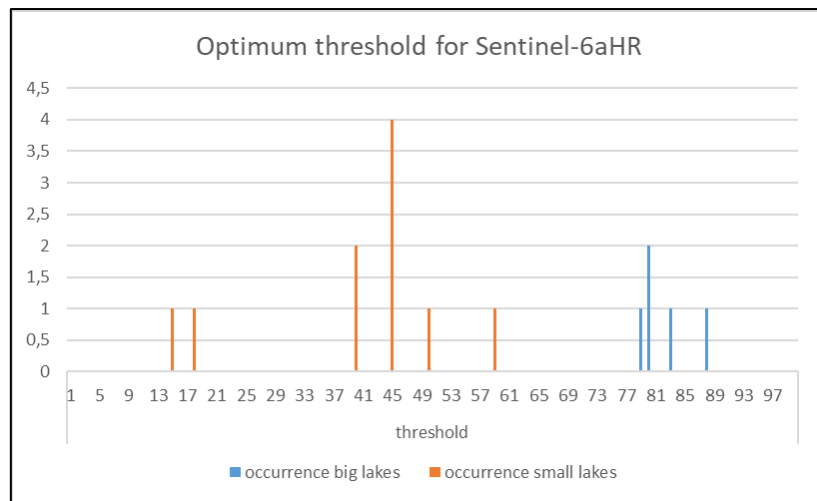


Figure 5.49: Histogram to find the optimum threshold for retracking using the Sentinel-6aHR mission

CHAPTER 5: EXPERIMENTS AND RESULTS

For Sentinel-6aHR, the difference in the distribution of occurrences for both smaller and larger lakes are more distinct and clear. For smaller lakes, the occurrences are much more densely located around 45%. For larger lakes, the occurrences are more densely located around 80%. The major reason behind this could be the reduction in the noise in the leading edges of waveform for both Great Lakes and smaller lakes. The smoother leading edge gives a constant threshold values throughout the areas of investigation. In case of small lakes, two instances have given a threshold values slightly different than the others in the same category. Those two values are from Lake O.H. Ivie and Lake Champlain. For O.H. Ivie, as mentioned before, there are a few islands present along the satellite track which causes slight errors in the determination of the leading edge of the SAR waveform, resulting in multiple leading edges and thus an optimum threshold in the earlier part of the spectrum. For Lake Champlain, the number of measurement available are very less due to a smaller length along the river width covered by the satellite pass, the waveform is multi peaked before the estimation of the leading edge by the Retracker which results in a shorter length of the leading edge and thus the optimum threshold in the earlier part of the threshold spectrum.

Therefore, from the above analysis of the variation in the optimum thresholds based on the missions, one can notice that these values depend heavily on the waveforms returned which in turn depend upon the characteristics of the water surface and its surroundings. The noisier and more complex the waveform is, the higher are the chances of a shorter or a noisier detected leading edge. As a result, the investigation show a smaller value for the optimum thresholds in this case. For LRM missions, the optimum threshold lie in the earlier part of the threshold spectrum because of noisy waveforms returned from the antenna. On the other hand, due to high along track resolutions and the increased number of measurements due to the open burst mode of Sentinel-6aHR mission, the waveforms returned are much smoother which allows the retracker to position the retracking bin with a higher accuracy thus allowing a higher thresholds for both smaller and larger lakes. However, in case of very smaller lakes, in which land areas are included even in the along track footprint of the SAR antenna, multiple peaks are formed in the waveform before the leading edge which cannot be avoided. Therefore, other processing techniques like land-water mask or establishing virtual stations etc, could help with the improvement of the results

5.17. Offset validation

The purpose of the Sentinel-6a satellite was to continue the decade long services provided by the Jason series of satellites. To understand the potential of the mission, one needs to analyse the water levels provided by both missions in the overlapping period of operation when they started flying in tandem in the orbit.

Based on the water level time series generated for each lake in the previous sections, the intermission wise offsets are calculated to understand the differences in the measured heights.

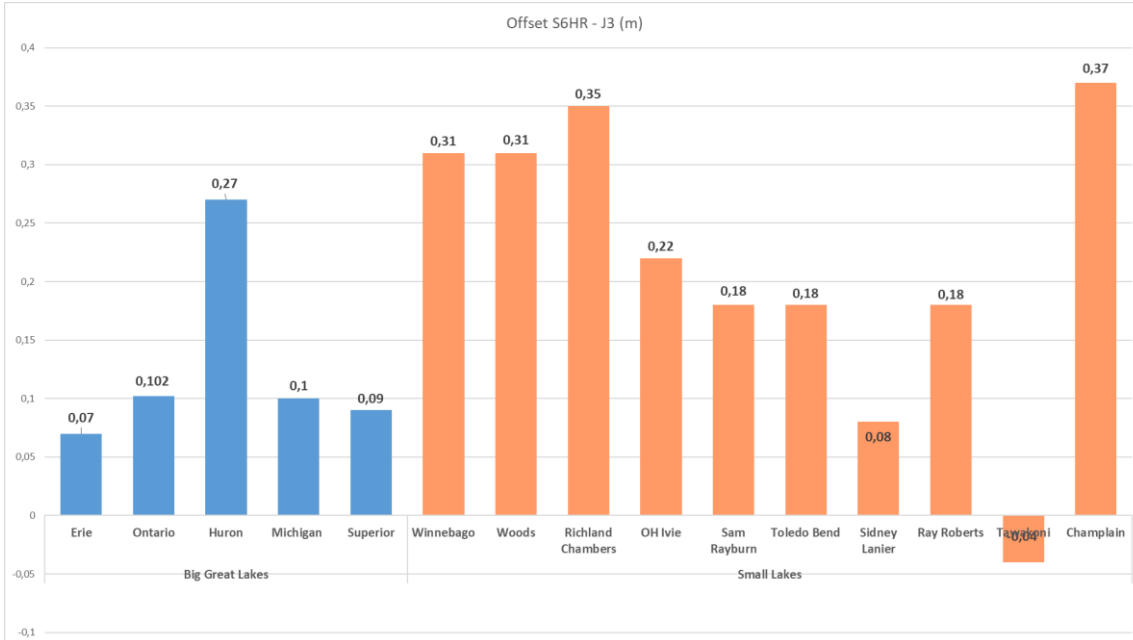


Figure 5.50: Histogram to validate offset for Sentinel-6aHR retracked and Jason-3 retracked missions

The absolute values of offsets between the median values of the height between Sentinel-6aHR and Jason-3 LRM missions lies in the range of 7cm to 27 cm for the great lakes and 4 cm to 37 cm for smaller lakes. In Great Lakes, the offset remains almost similar in the range of 7 to 10 cm except in Lake Huron where the offset reaches 27cm. This increase in the differences in the respective height values could be explained an error during retracking procedure because after looking at Table 5.8, the offsets between the unretacked Jason 3 and Sentinel-6HR data is around 3cm which almost same as the other great lakes too. By looking at the smaller lakes, one can notice that the offsets between the LRM and SAR data has increased because of increased errors in the Jason-3 LRM data.

Checking out the differences in the LRM missions of Jason-3 and Sentinel-6aLR missions. After looking at the Figure 5.51, as expected these offsets are very less in values ranging from 2cm to 17cm in Great Lakes and 1 cm to 19cm in smaller lakes. Although, both missions have the LRM mode of acquisition with same orbit and same along track resolution. The difference arises in this is because of the presence of the interleaved mode in LRM data. This ensures the backwards compatibility of the LRM data with historic reference values to mitigate any bias that might occur in the water level measurements. Therefore we see differences in these values ideally large in Great Lakes. Because the Great Lakes have been easily monitored by the LRM missions in the past with high accuracy, therefore the interleaved mode has mitigated any biases that might occur. For smaller lakes, the previous and current LRM missions do not provide data with a high accuracy, therefore, we see many small values

CHAPTER 5: EXPERIMENTS AND RESULTS

within 10cms. The smaller offset in lake Huron will become more clear once we investigate the sentinel-6a HR and LR height differences.

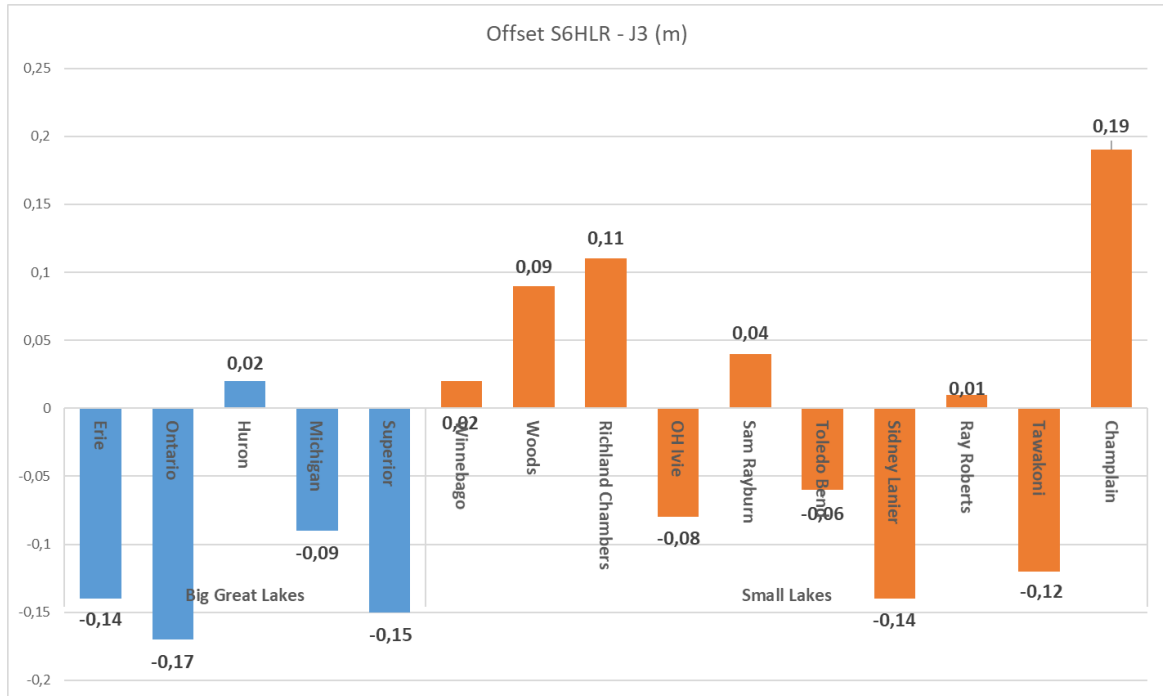


Figure 5.51: Histogram to validate offset for Sentinel-6aLR retracked and Jason-3 retracked missions

So the differences in the height values between Sentinel-6a SAR and LRM data should provide a clear picture on how well the SAR data operates as compared to the LRM data operating in parallel on the same satellite. As can be observed from the Figure 5.52, the offset values are more or less constant for both Great Lakes and smaller lakes with values varying the range of 20 cm to 27 cm for Great Lakes and a slightly larger range of 10 to 29 cm. This shows that roughly for every measurement derived by the LRM mission, the SAR mode adds around 23 cm to those measurements which improved the quality of the data to a huge extent. The mean value of offset for smaller lakes also lies around the value of 20cm which again helps in getting better quality time series.

Therefore, with a high quality SAR mode of acquisition and a backward compatible LRM mode of measurements on board the Sentinel-6a mission provide great measurements to a very high quality and thus would operate very in providing a long term water level time series for not just the oceans but also the small rivers and lakes.

CHAPTER 5: EXPERIMENTS AND RESULTS

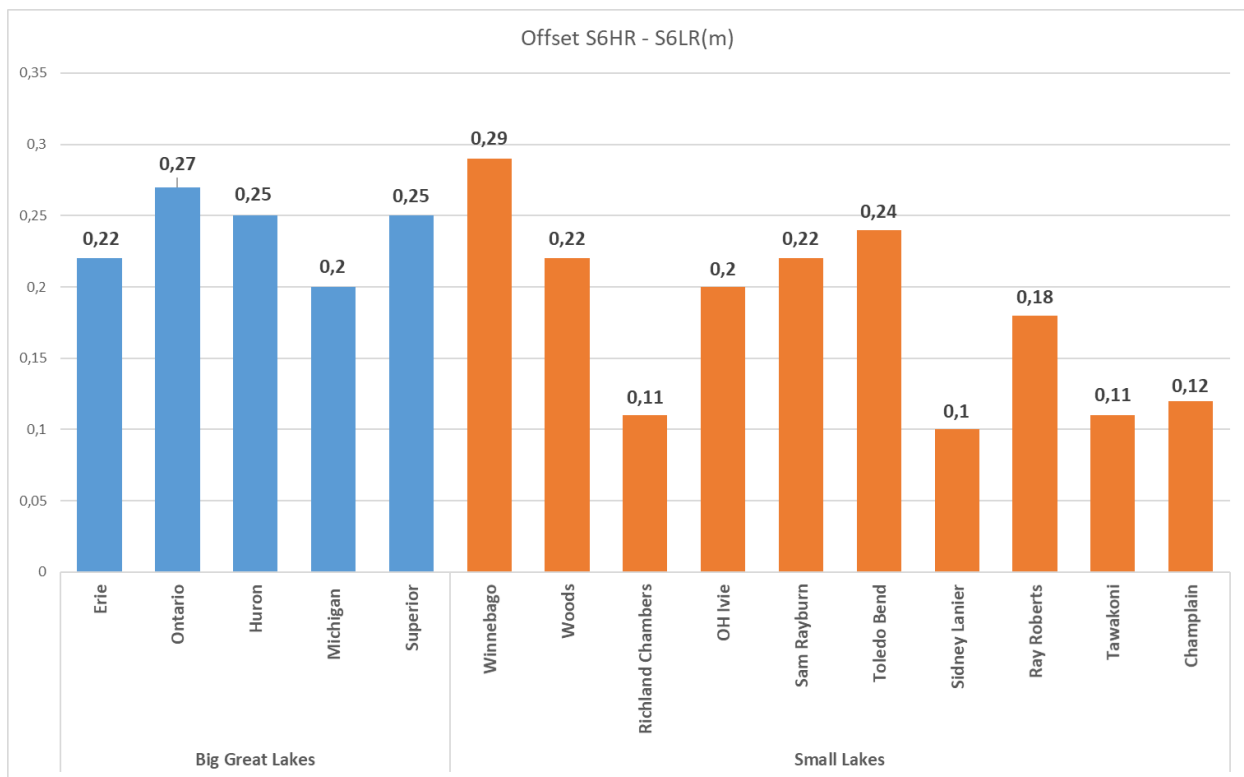


Figure 5.52: Histogram to validate offset for Sentinel-6aHR retracked and Sentinel-6aLR retracked missions

5. Summary, Conclusion and future work

5.1. Summary and Conclusion

The accurate and near-real time monitoring of terrestrial water bodies is very necessary for maintaining the hydrological balance as well as support human life. For this many satellite altimetry missions are actively working in providing regular, high quality measurements of our ocean surfaces as well as the inland water bodies. One such mission is the Jason series of satellites which have provided services in providing altimetry measurements for over a decade. The recently launched Sentinel-6 MF satellite is a part of the European Commission's Copernicus programme. The aim of the mission is to continue the services provided by the Jason-3 satellites globally. The new satellite works on open burst interleaved mode which provides measurements in SAR and LRM parallelly. Although, the Jason-3 services have provenly provided high quality altimetry data globally, its potential over small and complex inland water bodies is still constrained largely due to big footprint size of the antenna. The motivation behind this thesis was to evaluate the potential of Sentinel-6/Jason-CS mission over the inland water bodies and validate its objective of continuity of the services provided by the Jason series of satellites.

We started the procedure by investigating the water level time series over major smaller and bigger lakes in the USA using both the heights retracked by both the on-board retracker and the Improved Threshold Retracker. To get the best out of the Improved Threshold Retracker, the water level series were generated for all 0-100% threshold values to obtain the optimum threshold for each mission and area of investigation. Using this optimum threshold, water level time series for all the target areas was generated and consequently the quality of results was analysed with respect to the in-situ data in the overlapping period of operations for all the missions. Consequently, investigation on the intermission offsets as well as an estimation of an optimal threshold based on the target size was also carried out.

After conducting those investigations, following conclusions could be determined:

- The open burst interleaved mode of the Sentinel-6a satellite has huge advantages when studying the smaller and the larger lakes. Due to the open-burst SAR mode, the number of measurement increased by manifold resulting in the returned waveforms to be noise free. This allowed the Improved Threshold Retracker to effectively detect the leading edges and provide high quality data. Moreover, due to the backward compatibility of the LRM data with historical reference data for inter-calibration with current data has allowed to mitigate any bias that might occur which was shown in better quality measurements provided by the LRM of Sentinel-6 as compared to Jason-3 in a few cases.
- During our investigation of the optimum thresholds to be used for the Improved Threshold Retracker, it showed that the selection of the optimum threshold varied highly on the returned waveform from the signal which in turn depended on the characteristics and surroundings of the water body. So for Great Lakes, the waveforms are more Quasi-Brown shaped and thus they work the best with the on-board Retracker which it is designed for. So for the LRM missions, the investigation did not yield any conclusive trend due to noisy leading edge caused due to rough lake surfaces. But for SAR mission, since the leading edges got

smoothened, the Retracker was able to conclusively suggest that best threshold for the Sentinel-6aHR mission is around 80%. However for the smaller lakes, the waveforms were already noisy and complex and the leading edges were short due to which a lower threshold was selected to be optimum one. For SAR, the smooth leading edges allowed the retracked to position itself at a more effective bin. So for the LRM missions, the best threshold lies in the earlier part of the spectrum (5% to 10%) and for SAR missions, it lies in the middle around 40% to 50%. For this study over 15 lakes were investigated, but if more lakes and river would be added, one might be able to understand the threshold distribution in more deterministic manner.

- After using the separate optimum thresholds determined for each mission and area of investigation, the water level time series were generated for each lake. After analysing the performance of the missions over different sizes and location of the water bodies, Sentinel-6aHR retracked height values performed the best over the smaller lakes with RMSE lying in the range of 3cm to 10cm as compared to the LRM missions which had RMSE in the range of 10 cm to 30 cm. During the investigation it got pointed out that in these situations in which the lakes are monitored only in the overlapping periods of operation, the number of points reduced and because of which the correlation reduced too. Since it is very seasonal too, the correlation cannot be considered as a reliable quality measurement for this thesis. However, the best quality of results were provided by the Sentinel-6aHR retracked data and it thus proves how well the mission can be used for continuous monitoring of water level data for smaller lakes too.
- During the investigation of the intermission offset validation, the differences in the height values estimated for all three missions was calculated. It was found that the offset values between Jason3 and Sentinel-6aHR varied more especially in the smaller lakes region because of high error in the Jason-3 measurement over those regions. However, after computing the differences in the height values of Sentinel-6aHR and Sentinel-6aLR, the offset remains almost constant for both Great Lakes and smaller lakes. This validates the backward compatibility of the Sentinel-6 LRM data with the historical references. This shows that the Sentinel-6a mission is more than compatible to continue the providing the regular water level time series globally, not just for oceans and large water bodies but smaller lakes and rivers as well.

During the thesis certain problems were faced:

- Selection of a more robust and automatic outlier rejection algorithm
- Lower number of data points available due because the overlap period of operation were limited within December 2020 to March 2022
- Rejection of more data points due to ice-sheet formations over the lakes bordering Canada
- Higher distances between the satellite track and the location of gauge stations.

5.2. Future Work

SAR altimetry data has proven to be very effective in monitoring small lakes and rivers. Many SAR mission like Sentinel-3 and CryoSat-2 cannot regularly monitor the global water bodies due to lower temporal resolution. Sentinel-6a mission has the capability regularly provide altimetry services at a temporal gap of 10 days. Moreover the interleaved open burst SAR mode of acquisition has proven to provide higher accuracy data over many smaller lakes and rivers. However, due to a higher inclination and higher ground track distance, many inland water bodies are missed due to the unavailability of the ground track over the body location. Therefore multi-mission collaboration could be investigated to monitor more water bodies for a more effective understanding of its performance.

Consequently, only 15 lakes were monitored in the thesis. Inclusion of more lakes and reservoirs in this study would help in evaluating the optimum thresholds more distinctly for the future studies.

Even though the along track resolution of SAR altimetry is 300 m which is way better than the LRM missions, in many smaller bodies land and vegetation are still included due to their presence along the track. In this case, many techniques like land-water mask or establishing virtual stations might help.

Furthermore, various other retracking methods could be employed to help fix the noise and improve range estimation. An advanced outlier rejection algorithm might be able to improve the performance too.

References

Altimetry.info URL: <http://altimetry.info/>

Aviso Altimetry (CNES & CLS) (2014) URL:

https://www.aviso.altimetry.fr/gallery/entry_21_altimetry_principle_topex_poseidon_satellite_.html

Berry P. (2006) Two decades of inland water monitoring using satellite radar altimetry. 614

Berry P., Garlick J., Freeman J. & Mathers E. (2005) Global inland water monitoring from multi-mission altimetry, *Geophysical Research Letters*. 32(16).

Bertiger W., Desai S., Dorsey A., Haines B., Harvey N., Kuang, D. & Sibores, A (2008) Jason-2 Precision orbit determination status. In OSTST workshop.

Biancamaria S., Andreadis K. M., Durand M., Clark E. A., Rodriguez E., Mognard N. M., Alsdorf D. E., Lettenmaier D. P., and Oudin Y. (2010). Preliminary Characterization of SWOT Hydrology Error Budget and Global Capabilities. *IEEE Journal of Selected Topics in Applied Earth Observations and Remote Sensing*. 3 (1): 6–19.

Boergens E., Dettmering D., Schwatke C. & Seitz F. (2016) Treating the hooking effect in satellite altimetry data: A case study along the mekong river and its tributaries. *Remote Sensing* 8(2): 91.

Brown G. (1977). The average impulse response of a rough surface and its applications. *IEEE Transactions on Antennas and Propagation*. 25 (1): 67–74.

Calmant S. & Seyler F. (2006) Continental surface waters from satellite altimetry. *Comptes Rendus Geoscience*. 338(14-15): 1113–1122.

Chander S., Ganguly D., Dubey A.K., Gupta P.K., Singh R.P. & Chauhan P. (2014) Inland Water Bodies Monitoring using Satellite Altimetry over Indian Region. *The International Archives of the Photogrammetry, Remote Sensing and Spatial Information Sciences*. XL-8

Chelton D. B., Ries J. C., Haines B. J., Fu L.-L., and Callahan P. S. (2001). Chapter 1 Satellite Altimetry. *International Geophysics*, 69. Ed. by L.-L. Fu and A. Cazenave: 1 –ii.

Coe M.T., Birkett C.M. (2004) Calculation of river discharge and prediction of lake height from satellite radar altimetry: Example for the Lake Chad basin. *Water Resources Research*. 40(10). DOI:

Cooley H. (2006) *Floods and droughts*. Island Press: Washington, DC, USA.

Crétaux J.-F. & Birkett C. (2006) Lake studies from satellite radar altimetry. *Comptes Rendus Geoscience* 338(14-15): 1098–1112.

Deng X. (2003). Improvement of Geodetic Parameter Estimation in Coastal Regions from Satellite Radar Altimetry. PhD thesis. Curtin University of Technology.

Deng X. and FeatherstoneW. E. (2006). A coastal retracking system for satellite radar altimeter waveforms: Application to ERS-2 around Australia. *Journal of Geophysical Research: Oceans*, 111 (C6).

DGFI Pass locator, URL: <https://openadb.dgfi.tum.de/en/passlocator/>

DGFI-TUM Open Altimeter Database (2022) URL: <https://openadb.dgfi.tum.de/en/missions/>

Dingman S. (2001) Physical Hydrology, 2nd edn. Prentice-Hall Inc., Englewood Cliffs, New Jersey, USA.

Donlon C. J., Cullen R., Giulicchi L., Vuilleumier P., Francis C. R., Kuschnerus M., & Tavernier, G. (2021) The Copernicus Sentinel-6 mission: Enhanced continuity of satellite sea level measurements from space. *Remote Sensing of Environment*. 258: 112395.

Eakins B. & Sharman G. (2010) 'Volumes of the world's oceans from etopo1', NOAA National Geophysical Data Center, Boulder, CO 7.

Eymard L& Obligis E (2006) The altimetric Wet Tropospheric Correction : Progress since the ERS-1 mission.

Fekete B., Vörösmarty C. (2007) The current status of global river discharge monitoring and potential new technologies complementing traditional discharge measurements. *Proceedings of the PUB Kick-off Meeting*. 309: 20-22.

Frappart F., Blarel F., Fayad I., Bergé-Nguyen M., Crétaux J. F., Shu S. & Baghdadi N. (2021) Evaluation of the performances of radar and lidar altimetry missions for water level retrievals in mountainous environment: The case of the Swiss lakes. *Remote Sensing*, 13(11): 2196.

Gleick P.H. (1993) Water and Conflict – Fresh Water Resources and International Security. *International Security*. 18(1): 79-112.

Hagemann S. & Dümenil L. (1998) A parameterization of the lateral waterflow for the global scale. *Climate Dyn.* 14: 17–31.

Halicki M. & Niedzielski T. (2022) The accuracy of the Sentinel-3A altimetry over Polish rivers. *Journal of Hydrology*, 606:127355.

Harvey K. D. and Grabs W. (2003) WMO Report of the GCOS/GTOS/HWRP expert meeting on hydrological data for global studies. Tech. rep. No. 1156. Toronto, Canada: Report COS 84, Report GTOS 32, World Meteorological Organization (WMO)/TD.

Hwang C., Jinyun G., Deng X., Hsu H-Y, Liu Y. (2006) Coastal Gravity Anomalies from Retracked Geosat/GM Altimetry: Improvement, Limitation and the Role of Airborne Gravity Data. *Journal of Geodesy*. (80): 204-216.

Kim Y., Schmid T., Charbiwala Z.M., Friedman J. & Srivastava M.B. (2008) Nawms: nonintrusive autonomous water monitoring system, in 'Proceedings of the 6th ACM conference on Embedded network sensor systems', ACM, pp. 309–322.

Lan Vu P., Frappart F., Darrozes J., Ramillen G., Marieu V., Blarel F., Bonnefond P. (2018) Jason-3 and Sentinel-3A Altimeter Validation Along the French Atlantic Coast in the Southern Bay of Biscay. *IGARSS 2018-2018 IEEE International Geoscience and Remote Sensing Symposium*. IEEE 3793-3796

Lanfear K.J. & Hirsch R.M. (1999) USGS Study reveals a decline in long-record streamgages. *Eos, Transactions American Geophysical Union*. 80(50): 605-607

Maillard P., Bercher N.; Calmant S (2015) New processing approaches on the retrieval of water levels in ENVISAT and SARAL radar altimetry over rivers: A case study of the São Francisco River, Brazil. *Remote Sens. Environ.* (156): 226–241.

Martin-Puig C., Ruffini G., Marquez J., Cotton D., Srokosz M., Challenor P., & rome Benveniste J. (2008) Theoretical model of SAR altimeter over water surfaces. In IGARSS 2008-2008 IEEE International Geoscience and Remote Sensing Symposium (Vol. 3, pp. III-242). IEEE.

Nielsen K., Stenseng L., Andersen O. B., Villadsen H. & Knudsen P. (2015) Validation of CryoSat-2 SAR mode based lake levels. *Remote Sensing of Environment.* 171: 162-170.

NOAA Tides and Currents, URL: <https://tidesandcurrents.noaa.gov/>

Peterson T. C., Anderson D., Cohen S., Cortez-Vázquez M., Murnane R., Parmesan C., Phillips D., Pulwarty R. & Stone J (2008) Why weather and climate extremes matter. *Weather and Climate Extremes in a Changing Climate. Regions of Focus: North America, Hawaii, Caribbean, and US Pacific Islands.* 11–33.

Quarley G. D., Srokosz M. A., & McMillan A.C. (2001) : Analyzing Altimeter Artifacts: Statistical Properties of Ocean Waveforms. *Journal of Atmospheric and Oceanic Technology.* 18: 2074–2091

R.K. Raney, John Hopkins University Applied Physics Laboratory URL:

<https://www.aviso.altimetry.fr/en/techniques/altimetry/principle/delay-doppler-/sar-altimetry.html>

Raney R. K. (1998) The delay/Doppler radar altimeter. *IEEE Transactions on Geoscience and Remote Sensing,* 36(5): 1578-1588.

Rapley C. G, Laboratory M. S. S., and Agency E. S. (1987) An exploratory study of inland water and land altimetry using Seasat data : Final report. European Space Agency.

Rosmorduc V., Benveniste J., Bronner E., Dinardo S., Lucas B. M., Niejmeier S. & Earith D. (2010) Basic radar altimetry toolbox & tutorial. In proceedings of ‘ESA living planet symposium’, Bergen, Norway.

Schwatke C., Dettmering D., Bosch W. & Seitz F. (2015) DAHITI – an innovative approach for estimating water level time series over inland waters using multi-mission. *Hydrology and Earth System Sciences.* 19(10): 4345-4364.

Sentinel Online, URL: <https://sentinels.copernicus.eu/web/sentinel/home>

Shiklomanov A. I., Lammers R. B., and Vörösmarty C. J. (2011) Widespread decline in hydrological monitoring threatens Pan-Arctic Research. *Eos, Transactions American Geophysical Union.* 83 (2): 13–17.

Texas Water Development Board, URL: <https://www.twdb.texas.gov/mapping/>

Tourian M. J., Elmi O., Mohammadnejad A. & Sneeuw N. (2017) Estimating river depth from swot-type observables obtained by satellite altimetry and imagery. *Water.* 9(10): 753.

Tourian, M. J. (2012), Controls on satellite altimetry over inland water surfaces for hydrological purposes, Master’s thesis.

Tseng K.-H., Shum C., Yi Y., Fok H. S., Kuo C., Lee H., Cheng X., & Wang X. (2013). Envisat Altimetry Radar Waveform Retracking of Quasi-Specular Echoes over the Ice-Covered Qinghai Lake. *Terrestrial Atmospheric and Oceanic Sciences*. 24: 615–627.

USGS National Water Dashboard, URL:

<https://dashboard.waterdata.usgs.gov/app/nwd/en/?aoi=default>

Vignudelli S., Kostianoy A.G., Cipollini P., & Benveniste, J. (Eds.). (2011). *Coastal altimetry*. Springer Science & Business Media.

Wahr J.M. (1985). Deformation induced by polar motion. *Journal of Geophysical Research: Solid Earth*. 90 (B11): 9363–9368

Wang B. (2019) Monitoring inland surface water level from Sentinel-3 data, Master's thesis.

Williams W.D. (2002) Community participation in conserving and managing inland waters. *Aquatic Conserv: Mar. Freshw. Ecosyst.* 12: 315-326.

Wu Y. (2021) Exploring the performances of SAR altimetry and improvements offered by fully focused SAR, Master's Thesis.

Zhao D. (2018) Generating water level time series from satellite altimetry measurements for inland applications. Master's thesis.